



Characterization of Long SiAlON Ceramic Tubes for Gun Barrel Applications

by Andrew K. Woodruff and John Hellmann

ARL-CR-573

June 2006

prepared by

The Pennsylvania State University
College of Earth and Mineral Sciences
Department of Materials Science and Engineering
University Park, PA 16802

under contract

W911QX-05-P-0026

NOTICES

Disclaimers

The findings in this report are not to be construed as an official Department of the Army position unless so designated by other authorized documents.

Citation of manufacturer's or trade names does not constitute an official endorsement or approval of the use thereof.

Destroy this report when it is no longer needed. Do not return it to the originator.

Army Research Laboratory

Aberdeen Proving Ground, MD 21005-5069

ARL-CR-573**June 2006**

Characterization of Long SiAlON Ceramic Tubes for Gun Barrel Applications

Andrew K. Woodruff and John Hellmann

prepared by

The Pennsylvania State University
College of Earth and Mineral Sciences
Department of Materials Science and Engineering
University Park, PA 16802

under contract

W911QX-05-P-0026

REPORT DOCUMENTATION PAGE				Form Approved OMB No. 0704-0188	
Public reporting burden for this collection of information is estimated to average 1 hour per response, including the time for reviewing instructions, searching existing data sources, gathering and maintaining the data needed, and completing and reviewing the collection information. Send comments regarding this burden estimate or any other aspect of this collection of information, including suggestions for reducing the burden, to Department of Defense, Washington Headquarters Services, Directorate for Information Operations and Reports (0704-0188), 1215 Jefferson Davis Highway, Suite 1204, Arlington, VA 22202-4302. Respondents should be aware that notwithstanding any other provision of law, no person shall be subject to any penalty for failing to comply with a collection of information if it does not display a currently valid OMB control number. PLEASE DO NOT RETURN YOUR FORM TO THE ABOVE ADDRESS.					
1. REPORT DATE (DD-MM-YYYY) June 2006		2. REPORT TYPE Final		3. DATES COVERED (From - To) September 2004–April 2005	
4. TITLE AND SUBTITLE Characterization of Long SiAlON Ceramic Tubes for Gun Barrel Applications				5a. CONTRACT NUMBER W911QX-05-P-0026	
				5b. GRANT NUMBER	
				5c. PROGRAM ELEMENT NUMBER	
6. AUTHOR(S) Andrew K. Woodruff and John Hellmann				5d. PROJECT NUMBER 622618.H80	
				5e. TASK NUMBER	
				5f. WORK UNIT NUMBER	
7. PERFORMING ORGANIZATION NAME(S) AND ADDRESS(ES) The Pennsylvania State University College of Earth and Mineral Sciences Department of Materials Science and Engineering University Park, PA 16802				8. PERFORMING ORGANIZATION REPORT NUMBER	
9. SPONSORING/MONITORING AGENCY NAME(S) AND ADDRESS(ES) U.S. Army Research Laboratory ATTN: AMRSD-ARL-WM-MB Aberdeen Proving Ground, MD 21005-5069				10. SPONSOR/MONITOR'S ACRONYM(S)	
				11. SPONSOR/MONITOR'S REPORT NUMBER(S) ARL-CR-573	
12. DISTRIBUTION/AVAILABILITY STATEMENT Approved for public release; distribution is unlimited.					
13. SUPPLEMENTARY NOTES					
14. ABSTRACT <p>The extent of density gradients, dimensional fidelity, and strength was examined on several different lots of Kennametal TK4 SiAlON proposed for use as gun-tube liners. The formal U.S. Army Research Laboratory designation for this material is ITK4. Five different tubes of material were received, ITK4-4 (200 mm in length), ITK4-6 (100 mm in length), ITK4-7 (100 mm in length), ITK4-8 (100 mm in length), and ITK4-14 (200 mm in length). Immersion density, roundness based on measurements of inner and outer diameters, and strength via diametral compression of rings sectioned from tubes was characterized.</p> <p>The densities of all specimens tested were similar with few exceptions. The longer tubes exhibited a slightly more pronounced density gradient along the tube axes relative to the shorter tubes. However, none of the tubes showed greater than a 1% difference in density along their lengths. All tubes were within 1% out-of-roundness, with the majority of samples less than 0.5% out-of-round.</p> <p>The shorter tubes (ITK4-6, -7, and -8) had characteristic strengths approximately 50–65% higher than the longer tubes (ITK4-4 and -14); longer tubes exhibited a significantly higher extent of strength uniformity (22–39% difference in strength along the length) than the shorter tubes (nominally 5%). Higher densities correlated with higher strengths.</p>					
15. SUBJECT TERMS SiAlON, ceramic gun barrels, strength, fractography, long ceramic tubes					
16. SECURITY CLASSIFICATION OF:			17. LIMITATION OF ABSTRACT UL	18. NUMBER OF PAGES 118	19a. NAME OF RESPONSIBLE PERSON Jeffrey J. Swab
a. REPORT UNCLASSIFIED	b. ABSTRACT UNCLASSIFIED	c. THIS PAGE UNCLASSIFIED			19b. TELEPHONE NUMBER (Include area code) 410-306-0753

Contents

List of Figures	v
List of Tables	ix
1. Introduction	1
2. Literature Survey	2
3. Statement of Work	5
4. Experimental Procedure	6
4.1 Materials Studied.....	6
4.2 Density Determination.....	6
4.3 Roundness Testing.....	7
4.4 Strength Testing.....	7
5. Results and Discussion	12
5.1 Density Determination.....	12
5.2 Roundness Testing.....	19
5.3 Strength Testing.....	22
5.4 Strength/Density Comparisons.....	29
5.5 Fractography.....	33
6. Conclusions	36
7. Future Work	36
8. References	39
Appendix A. Immersion Density Measurements	41
Appendix B. Roundness Measurements	51
Appendix C. Diametral Compression Results	55

Appendix D. Fractography	60
Distribution List	94

List of Figures

Figure 1. Microstructure of Kennametal TK4 SiAlON (STK4) with 60% alpha phase and 40% beta phase. Sample was etched in molten KOH (3).	4
Figure 2. Schematic representation of the tangential stress field existing in a diametrically compressed O-ring specimen.	8
Figure 3. O-ring markings for specimens from ITK4-6 and ITK4-7.....	9
Figure 4. O-ring markings for specimens from ITK4-4, ITK4-8, and ITK4-14.....	9
Figure 5. Typical load-vs.-time graph for specimens tested in diametral compression with Grafoil at contacts.	10
Figure 6. Typical load-vs.-time graph for specimens tested in diametral compression with manila folder paper at contacts instead of Grafoil.	10
Figure 7. O-ring measurement schematic.	11
Figure 8. Density vs. temperature of calibrated kerosene used for immersion density measurements.....	12
Figure 9. Plot showing immersion density results for specimens from ITK4-4. Bars represent one standard deviation of three measurements for the sample. ITK4-4 was initially a 200-mm-long tube. Specimen no. 14 was unavailable for analysis.	13
Figure 10. Plot showing immersion density results for specimens from ITK4-6. Bars represent one standard deviation of three measurements for the sample. ITK4-6 was initially a 100-mm-long tube.	13
Figure 11. Plot showing immersion density results for specimens from ITK4-7. Bars represent one standard deviation of three measurements for the sample. ITK4-7 was initially a 100-mm-long tube.	14
Figure 12. Plot showing immersion density results for specimens from ITK4-8. Bars represent one standard deviation of three measurements for the sample. ITK4-8 was initially a 100-mm-long tube.	14
Figure 13. Plot showing immersion density results for specimens from ITK4-14. Bars represent one standard deviation of three measurements for the sample. ITK4-14 was initially a 200-mm-long tube. Specimen no. 3 was unavailable for analysis.	15
Figure 14. ITK4-4 diametral compression results. Average is shown as dark horizontal line.	23
Figure 15. ITK4-4 Weibull analysis of maximum stress using Weib Par and maximum likelihood.	23
Figure 16. ITK4-6 diametral compression results. Average is shown as dark horizontal line.	24
Figure 17. ITK4-6 Weibull analysis of maximum stress using Weib Par and maximum likelihood.	24
Figure 18. ITK4-7 diametral compression results. Average is shown as dark horizontal line.	25

Figure 19. ITK4-7 Weibull analysis of maximum stress using Weib Par and maximum likelihood.	25
Figure 20. ITK4-8 diametral compression results. Average is shown as dark horizontal line.	26
Figure 21. ITK4-8 Weibull analysis of maximum stress using Weib Par and maximum likelihood.	26
Figure 22. ITK4-14 diametral compression results. Average is shown as dark horizontal line.....	27
Figure 23. ITK4-14 Weibull analysis of maximum stress using Weib Par and maximum likelihood.	27
Figure 24. Weibull plots of strength data from specimens from ITK4-X sorted by tube of origin.	28
Figure 25. Comparison of strength and density values for specimens from ITK4-4. ITK4-4 was initially a 200-mm-long tube. Specimen 14 was not available for analysis. The solid lines represent the averages of the data while the dotted lines represent one standard deviation.....	30
Figure 26. Comparison of strength and density values for specimens from ITK4-6. ITK4-6 was initially a 100-mm-long tube. The solid lines represent the averages of the data while the dotted lines represent one standard deviation.	30
Figure 27. Comparison of strength and density values for specimens from ITK4-7. ITK4-7 was initially a 100-mm-long tube. The solid lines represent the averages of the data while the dotted lines represent one standard deviation.	31
Figure 28. Comparison of strength and density values for specimens from ITK4-8. ITK4-8 was initially a 100-mm-long tube. The solid lines represent the averages of the data while the dotted lines represent one standard deviation.	31
Figure 29. Comparison of strength and density values for specimens from ITK4-14. ITK4-14 was initially a 100-mm-long tube. Specimen 3 was not available for testing. Specimen 11 was broken during preloading and no data was available for strength analysis. The solid lines represent the averages of the data while the dotted lines represent one standard deviation.....	32
Figure 30. Typical micrograph of failure origin for O-rings tested under diametral compression.	34
Figure 31. Typical EDS spectrum in and around failure origins of ITK4-X specimens.	34
Figure 32. Fracture origin of specimen 5 from ITK4-4, side 1. Failure appears to have been caused by an agglomerate or inclusion of some sort.	35
Figure 33. Fracture origin of specimen 5 from ITK4-4, side 2. Failure appears to have been caused by an agglomerate or inclusion of some sort.	35
Figure D-1. ITK4-4 specimen 1.....	60
Figure D-2. ITK4-4 specimen 2.....	60
Figure D-3. ITK4-4 specimen 3.....	61
Figure D-4. ITK4-4 specimen 4.....	61

Figure D-5. ITK4-4 specimen 5.....	62
Figure D-6. ITK4-4 specimen 6.....	62
Figure D-7. ITK4-4 specimen 7.....	63
Figure D-8. ITK4-4 specimen 8.....	63
Figure D-9. ITK4-4 specimen 9.....	64
Figure D-10. ITK4-4 specimen 10.....	64
Figure D-11. ITK4-4 specimen 11.....	65
Figure D-12. ITK4-4 specimen 12.....	65
Figure D-13. ITK4-4 specimen 13.....	66
Figure D-14. ITK4-4 specimen 15.....	66
Figure D-15. ITK4-4 specimen 16.....	67
Figure D-16. ITK4-4 specimen 17.....	67
Figure D-17. ITK4-4 specimen 18.....	68
Figure D-18. ITK4-4 specimen 19.....	68
Figure D-19. ITK4-6 specimen 1.....	69
Figure D-20. ITK4-6 specimen 2.....	69
Figure D-21. ITK4-6 specimen 3.....	70
Figure D-22. ITK4-6 specimen 4.....	70
Figure D-23. ITK4-6 specimen 5.....	71
Figure D-24. ITK4-6 specimen 6.....	71
Figure D-25. ITK4-6 specimen 7.....	72
Figure D-26. ITK4-6 specimen 8.....	72
Figure D-27. ITK4-6 specimen 9.....	73
Figure D-28. ITK4-6 specimen 10.....	73
Figure D-29. ITK4-7 specimen 1.....	74
Figure D-30. ITK4-7 specimen 2.....	74
Figure D-31. ITK4-7 specimen 3.....	75
Figure D-32. ITK4-7 specimen 4.....	75
Figure D-33. ITK4-7 specimen 5.....	76
Figure D-34. ITK4-7 specimen 6.....	76
Figure D-35. ITK4-7 specimen 7.....	77
Figure D-36. ITK4-7 specimen 8.....	77
Figure D-37. ITK4-7 specimen 9.....	78
Figure D-38. ITK4-7 specimen 10.....	78

Figure D-39. ITK4-8 specimen 1.....	79
Figure D-40. ITK4-8 specimen 2.....	79
Figure D-41. ITK4-8 specimen 3.....	80
Figure D-42. ITK4-8 specimen 4.....	80
Figure D-43. ITK4-8 specimen 5.....	81
Figure D-44. ITK4-8 specimen 6.....	81
Figure D-45. ITK4-8 specimen 7.....	82
Figure D-46. ITK4-8 specimen 8.....	82
Figure D-47. ITK4-8 specimen 9.....	83
Figure D-48. ITK4-8 specimen 10.....	83
Figure D-49. ITK4-14 specimen 1.....	84
Figure D-50. ITK4-14 specimen 2.....	84
Figure D-51. ITK4-14 specimen 4.....	85
Figure D-52. ITK4-14 specimen 5.....	85
Figure D-53. ITK4-14 specimen 6.....	86
Figure D-54. ITK4-14 specimen 7.....	86
Figure D-55. ITK4-14 specimen 8.....	87
Figure D-56. ITK4-14 specimen 9.....	87
Figure D-57. ITK4-14 specimen 10.....	88
Figure D-58. ITK4-14 specimen 11.....	88
Figure D-59. ITK4-14 specimen 12.....	89
Figure D-60. ITK4-14 specimen 13.....	89
Figure D-61. ITK4-14 specimen 14.....	90
Figure D-62. ITK4-14 specimen 15.....	90
Figure D-63. ITK4-14 specimen 16.....	91
Figure D-64. ITK4-14 specimen 17.....	91
Figure D-65. ITK4-14 specimen 18.....	92
Figure D-66. ITK4-14 specimen 19.....	92
Figure D-67. ITK4-14 specimen 20.....	93

List of Tables

Table 1. Composition of microstructure of STK4 SiAlON.	3
Table 2. Statistical analysis of immersion density measurements for specimens from ITK4-4. Highlighted values denote dissimilar values based on the criteria.	16
Table 3. Statistical analysis of immersion density measurements for specimens from ITK4-6. Highlighted values denote dissimilar values based on the criteria.	17
Table 4. Statistical analysis of immersion density measurements for specimens from ITK4-7. Highlighted values denote dissimilar values based on the criteria.	17
Table 5. Statistical analysis of immersion density measurements for specimens from ITK4-8. Highlighted values denote dissimilar values based on the criteria.	18
Table 6. Statistical analysis of immersion density measurements for specimens from ITK4- 14. Highlighted values denote dissimilar values based on the criteria.	19
Table 7. ITK4-4 roundness test results.	20
Table 8. ITK4-6 roundness test results.	20
Table 9. ITK4-7 roundness test results.	21
Table 10. ITK4-8 roundness test results.	21
Table 11. ITK4-14 roundness test results.	22
Table 12. Comparison of overall strength data for ITK4-X tubes.....	29
Table A-1. ITK4-4 immersion density run no. 1.	41
Table A-2. ITK4-4 immersion density run no. 2.	42
Table A-3. ITK4-4 immersion density run no. 3.	42
Table A-4. ITK4-4 immersion density summary.....	43
Table A-5. ITK4-6 immersion density run no. 1.	43
Table A-6. ITK4-6 immersion density run no. 2.	44
Table A-7. ITK4-6 immersion density run no. 3.	44
Table A-8. ITK4-6 immersion density summary.....	44
Table A-9. ITK4-7 immersion density run no. 1.	45
Table A-10. ITK4-7 immersion density run no. 2.	45
Table A-11. ITK4-7 immersion density run no. 3.	45
Table A-12. ITK4-7 immersion density summary.....	46
Table A-13. ITK4-8 immersion density run no. 1.	46
Table A-14. ITK4-8 immersion density run no. 2.	46
Table A-15. ITK4-8 immersion density run no. 3.	47

Table A-16. ITK4-8 immersion density summary.....	47
Table A-17. ITK4-14 immersion density run no. 1.	48
Table A-18. ITK4-14 immersion density run no. 2.	48
Table A-19. ITK4-14 immersion density run no. 3.	49
Table A-20. ITK4-14 immersion density summary.....	49
Table B-1. Arbitrary measurements: made at a randomly chosen diameter and the diameter perpendicular to it.	51
Table B-2. Specific measurements: made based on orientation for strength testing.	51
Table B-3. Arbitrary measurements: made at a randomly chosen diameter and the diameter perpendicular to it.	52
Table B-4. Specific measurements: made based on orientation for strength testing.	52
Table B-5. Arbitrary measurements: made at a randomly chosen diameter and the diameter perpendicular to it.	52
Table B-6. Specific measurements: made based on orientation for strength testing.	53
Table B-7. Arbitrary measurements: made at a randomly chosen diameter and the diameter perpendicular to it.	53
Table B-8. Specific measurements: made based on orientation for strength testing.	53
Table B-9. Arbitrary measurements: made at a randomly chosen diameter and the diameter perpendicular to it.	54
Table B-10. Specific measurements: made based on orientation for strength testing.	54
Table C-1. ITK4-4 diametral compression results.....	55
Table C-2. ITK4-6 diametral compression results.....	56
Table C-3. ITK4-7 diametral compression results.....	57
Table C-4. ITK4-8 diametral compression results.....	58
Table C-5. ITK4-14 diametral compression results.....	59

1. Introduction

The application of engineered ceramics has long been recognized as a potential quantum improvement for gun barrels by allowing for greater control of temperature, reducing weight, increasing rates of fire, and controlling barrel wear and erosion (1). The greater erosion and thermochemical corrosion resistance of ceramics are expected to allow for the use of propellants that burn at a higher temperature and therefore give the projectile a much faster velocity. Typically, the faster a projectile is moving, the greater the range of the projectile and the more energy it will have upon impact with its target. All in all, this leads to a much better ballistics system.

One major motivation for building a better gun-barrel liner is political deterrence. Typically, it seems to be that whoever has the most powerful weapons has the power to enforce whatever policies they deem necessary. In today's world, the threat of violence is often more powerful than the actual act (2). This means that disputes between peoples of different political ideologies could be contained without the actual use of violence. If conflicts can be avoided by deterrence, then many peoples' lives (both civilians' and soldiers') would be saved. In addition, developing weapons with greater range and accuracy can significantly add to the safety of the soldiers utilizing these weapons on the battlefield. Also, substitution of more thermochemically robust ceramics for the chrome-plated steel that is conventionally used in gun tubes can enhance both environmental safety and health effects by eliminating the emission of toxic compounds that contain chrome during propellant combustion.

Recently, studies and tests have shown that ceramic gun barrels can potentially be used for limited time periods in standard ballistics applications without showing signs of wear or cracking (2). The initial problem here is to find a ceramic that has the properties necessary to be used for extended periods of time in the hazardous environment that is created from the firing of a ballistic weapon.

The temperatures and pressures that are generated from the firing of the propellant can lead to cracking and spallation within gun tubes because of the differences in thermal expansion, yield behavior, and modulus of elasticity between the liner and the gun barrel. In addition, corrosion and phase transitions can occur from the reactions between the propellant and the ceramic liner (2). All of these issues must be addressed to enable candidate materials selection and to ensure sustainability of the technology when fielded in a weapons system.

In addition, the steel gun barrels currently used by the U.S. Army have a short lifecycle. It is anticipated that ceramic gun-barrel liners will provide a 50% increase in barrel life with sustained accuracy for direct and indirect fire. The extended life of ceramic gun liners will lead to a reduction in maintenance costs for weapons that are capable of utilizing the technology (3).

The U.S. Army Research Laboratory (ARL), Aberdeen Proving Ground (APG), MD, originally chose eight materials that might be suitable for this purpose (3). These materials were tested by Van Akin to assess their relative performance in thermochemically aggressive environments simulating propellant combustion (2). The results of this testing showed that the Kennametal* TK4 SiAlON (STK4 per ARL nomenclature) had some of the best properties of all the tested materials. SiAlON gun-barrel liners have already been shown to be capable of surviving at least 1000 rounds in single-shot mode and 100 rounds in burst-firing mode of conventional ammunition in a .50-cal machine gun using M2 propellant (4).

Another consideration, however, in finding a suitable ceramic for gun-barrel liners is to determine if long tubes of a material can be manufactured with satisfactory fidelity in dimensions, composition, and strength. In order to evaluate the robustness of the tube, it will be necessary to determine the density and strength profile along the length of the tube. Strength and density are properties closely linked in ceramics, which means that a deviation of one will likely lead to a change in the other. Development of density gradients, deformation during handling of green compacts, and deformation induced by differential sintering kinetics during the sintering of regions with different starting densities can all lead to the production of tubes with gradients in strength and variations of dimensions. These gradients and deviations from anticipated dimensions all detract from the ability of the manufactured product to be used in gun-barrel applications.

Development of methods for quantifying density gradients, dimensional fidelity of tubes, and strength gradients are necessary. These methodologies can then be employed to enhance manufacturability and to help demonstrate the sustainability of ceramic gun tube liner technology.

2. Literature Survey

SiAlONs are solid solutions that consist of a silicon nitride (Si_3N_4) base with alumina and rare earth oxides which are added to promote liquid phase sintering and ultimately form the SiAlON composition. SiAlON combines excellent strength, hardness, fracture toughness and low thermal expansion with high corrosion resistance, high temperature strength, and oxidation resistance which are required for reliable performance, both thermochemically and thermomechanically, in aggressive applications.

Kennametal produces a SiAlON labeled as TK4 which the ARL has referred to as STK4 in their initial evaluation. Samples of this material in tube form had been supplied to ARL for examination for use as a gun tube liner material. However, early fracture analysis of STK4

* Kennametal Inc., Latrobe, PA (<http://www.kennametal.com>).

material revealed that many specimens were failing due to the presence of stainless-steel inclusions that were present due to the stainless-steel sieves used for the powders during processing. Once this was discovered, the use of stainless steel as a sieve material was eliminated and a different sieve material was used in its place. All material received after this point was given the ARL designation of ITK4 where the ‘I’ stands for improved. Aside from the material used for sieving, STK4 and ITK4 are exactly the same material (5).

The STK4, based on previous calculations and data, has a Young’s modulus of 336 GPa, a fracture toughness of $6.5 \text{ MPa}\cdot\text{m}^{1/2}$, and a density of 3.349 g/cm^3 (3). In most cases, the outcome of these tests would be influenced by the atmosphere in which the tests were conducted. However, silicon-nitride-based ceramics, such as SiAlONs, have been known to show very little change in fracture toughness or crack propagation behavior when exposed to various levels of moisture in the surrounding environment (6).

The purpose of this project is to determine if tubes of ITK4 SiAlON can be manufactured such that the integrity and properties of the tube are maintained along its entire length.

The material was manufactured by cold isostatic pressing, and then sintered in a pressureless process using a nitrogen overpressure to suppress decomposition. By using this sintering technique in lieu of the more commonly used hot-pressing techniques, the monetary and energy costs of manufacture are kept to a minimum. The ITK4 SiAlON was also subjected to a post-sintering, hot isostatic pressing process to achieve full densification (3). Small additions of sintering aids are added to the SiAlON to improve the densification kinetics which promotes densification via liquid phase sintering (7). In this case, ytterbium has been added as the sintering aid. The resultant SiAlON ceramic has the following phase assemblage (table 1), and a typical microstructure is shown in figure 1.

Table 1. Composition of microstructure of STK4 SiAlON.

60% Alpha SiAlON	$\text{Yb}_x\text{Si}_{12-(m+n)}\text{Al}_{m+n}\text{O}_n\text{N}_{16-n}$	$x \sim 0.29$ $m = 3x$ n - cannot be estimated from lattice parameter measurements
40% Beta SiAlON	$\text{Si}_{6-z}\text{Al}_z\text{O}_z\text{N}_{8-z}$	$z \sim 0.44$

In order to determine how well these tubes can be manufactured, it will be necessary to examine the different properties of the tubes themselves as well as the ceramic in the tubular configuration. Variability in both dimensional and density characteristics of the tubes can be introduced at various steps in the production process. When the powder is initially loaded to be cold-isostatically pressed, it may not be loaded uniformly and density gradients could form right from the start. In addition, when the green part is moved to be sintered, it could sag causing variations in the tube dimensions. Finally, if the tube is not supported correctly during sintering,

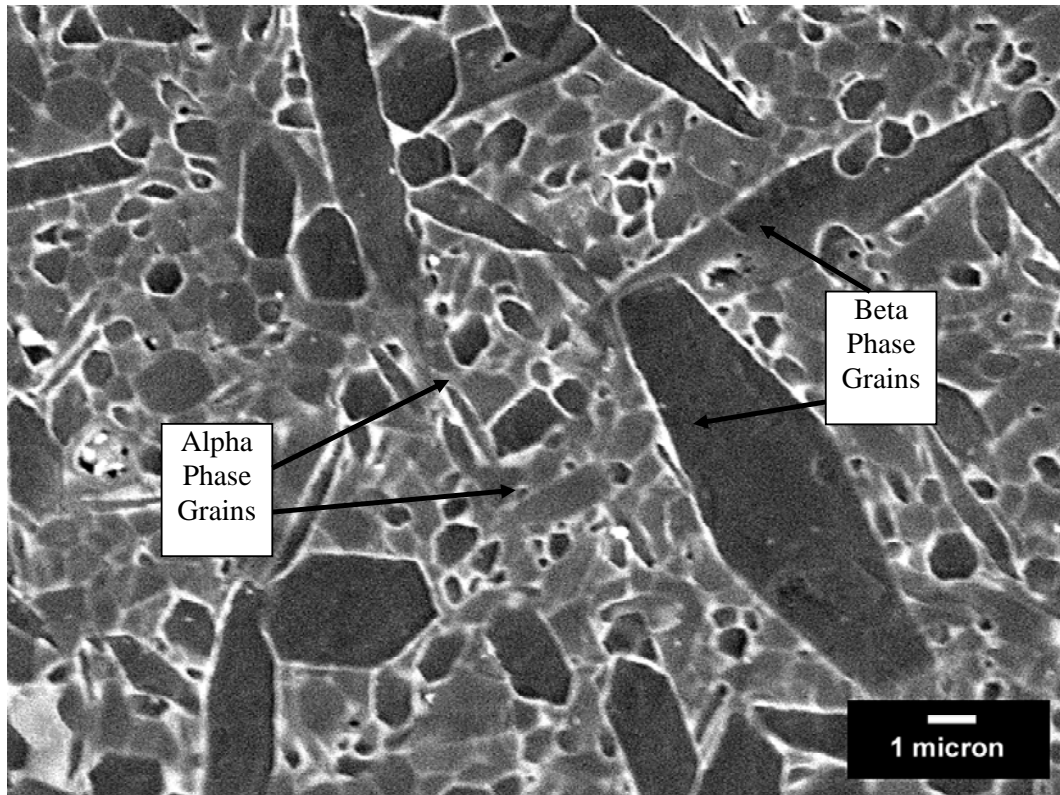


Figure 1. Microstructure of Kennametal TK4 SiAlON (STK4) with 60% alpha phase and 40% beta phase. Sample was etched in molten KOH (3).

it could sag further which would alter the final tube dimensions and could cause further gradients in the density of the final product. Because of all of this, it will be advantageous to examine how the density of the tube varies across its length. One way to determine this is to use immersion density techniques to find the density of sections of the tube. While water could be used for this process, kerosene is more commonly used due to its lower surface tension. This property allows the kerosene to enter the majority of any open porosity that may exist in the test specimen. The dimensional fidelity can be evaluated by making various measurements of samples of the tubes with calipers. While a method such as this may be a bit more primitive, it is less time-intensive and more cost-effective than using optical instrumentation. The measurements made using calipers should give a good representation of the samples and could indicate whether more intensive analysis needs to be performed.

The dimensional properties of the tube also have an effect on the strength of the tube. If some portions of the tube walls are thinner than others, then the strength of the tube at those points can potentially be compromised.

The configuration of the tubular samples allows for the use of diametral compression as a strength-testing technique. Much work has been done within recent years to develop and revise the methods for determining the strengths of samples tested under diametral compression (8). In

general, the ring is compressed while in the upright position until failure. The load required to promote failure and the initial dimensions of the ring are used to determine the strength of the ring. Once all the strength data is collected, the overall strength of the tube, as well as the identification of any gradients, can be determined through the use of the Weibull analysis. Weibull statistical analysis is based on the weakest link theory and relates the failure probability to the Weibull modulus, which is a measure of the scatter of the data, and the characteristic strength which corresponds to the strength of a unit volume specimen stressed in uniform tension (8). The Weibull modulus is useful in assessing how consistent the overall tube strength is. The higher the Weibull modulus, the less spread there is in the data, which is what is expected for a tube that has the same strength throughout its length. The characteristic strength gives a good estimate of the overall strength of all samples in a set and helps to compare the strength of several different sample sets to one another.

Based on the testing methods that have been discussed previously, it should be possible to critically examine the properties of ITK4 ceramic tubes and determine if these tubes are able to be produced without strength or density gradients, and with good dimensional fidelity.

3. Statement of Work

The combination of high stiffness, high temperature capability, and superior wear resistance inherent to ceramic materials make them ideal candidates as liners for military gun-barrel applications. It is anticipated that the use of a ceramic-lined gun barrel will increase muzzle kinetic energy and provide a significant increase in barrel life. Some small-caliber systems will require ceramic tubes approximately 500 mm long. While tubes of this length can be manufactured, there is a question of the quality and consistency of the material along the entire tube length. This will be determined by assessing material properties along the tube length and the statistical analysis of this data. The following tasks will be performed:

1. Perform wet density measurements on O-ring specimens from tubes supplied by ARL.
2. Perform diametral compression testing of O-ring specimens at room temperature to determine the strength.
3. Conduct 100% optical analysis of the strength specimens and scanning electron microscope (SEM) analysis of select specimens to determine the strength-limiting flaws.
4. Perform a statistical analysis of the density and strength data to determine the consistency of the material along the entire length of the tube.

4. Experimental Procedure

4.1 Materials Studied

A total of 67 specimens was received for testing. All of them were Kennametal ITK4 SiAlON. The specimens were O-rings machined from five different ITK4 tubes. Two of the tubes were originally 200 mm in length, and the other three tubes were 100 mm in length. The 200-mm-length tubes were labeled as ITK4-4 and ITK4-14. The 100-mm-length tubes were labeled ITK4-6, ITK4-7, and ITK4-8.

The specimens were supplied by ARL. Tubes ITK4-6, ITK4-7, and ITK4-8 were cut into 10 rings each. ITK4-4 produced 19 rings, of which only 18 were analyzed (specimen number 14 was not available for analysis). ITK4-14 produced 20 rings, of which only 19 were analyzed (specimen number 3 was not available for analysis). The nominal dimensions of the inner and outer diameters were 24.0 mm and 33.0 mm, respectively. The nominal width of the rings was 8 mm. Each ring had its edges chamfered.

4.2 Density Determination

In order to determine if there were any density gradients present in the tubes, each O-ring was subjected to immersion density testing. The densities were measured by Archimedes' method, by measuring the mass of the specimens in air and then again in kerosene which had previously had its density calibrated using ASTM D 891-95 (9). Since the density of the kerosene is temperature dependent, the kerosene was allowed to equilibrate at ambient temperature prior to density testing. In addition, the kerosene temperature was recorded along with the mass data each time a measurement was made. From all of this data, as well as the known temperature dependence for the density of the kerosene, the densities of the specimens were calculated using equations 1 and 2.

$$\rho_{\text{sample}} = \frac{m_{\text{air}}}{m_{\text{air}} - m_{\text{kerosene}}} \rho_{\text{kerosene}}, \quad (1)$$

and

$$\rho_{\text{kerosene}} = -0.0005T + 0.786, \quad (2)$$

where T = temperature ($^{\circ}\text{C}$) and ρ_{kerosene} = kerosene density (g/cm^3).

The densities of the specimens were measured three times each and then averaged. After the measurements were made, the specimens were set inside a fume hood to allow the fan to aid in the evaporation of the kerosene from the specimen surface. The three immersion tests of each specimen were made on different days to allow extra time for the kerosene to evaporate from the specimens.

4.3 Roundness Testing

The O-ring specimens were all tested for roundness by measuring inner and outer diameters of the specimens at various points. All specimens were measured along two arbitrary diameters which were perpendicular to each other. In addition to these measurements, specimens from ITK4-6 and ITK4-7 were also measured along a third diameter which was labeled as the vertical axis for diametral compression testing. It was then determined that more measurements were necessary in order to get a better sense of the overall roundness of the specimens. The specimens from ITK4-6 and ITK4-7 had at this point already been subjected to destructive strength testing. However, the remainder of the specimens were available for this additional analysis. Each of these specimens was measured at 4 diameters, each 45° from the last with the first measurement labeled as the vertical axis for compression testing (in addition to the two initial arbitrary measurements). All measurements were made using digital calipers.

The roundness was calculated by using equation 3:

$$\text{roundness} = \frac{d_{\text{least}}}{d_{\text{greatest}}}, \quad (3)$$

where d_{least} = smallest diameter and d_{greatest} = largest diameter.

$$\% \text{ out-of-roundness} = (1 - \text{roundness}) \times 100\%. \quad (4)$$

All measurements made for a given specimen were used together to calculate the roundness of that specimen. Since specimens from ITK4-4, ITK4-8, and ITK4-14 had many more measurements made for use in roundness calculations, the calculated roundness should be much closer to the actual roundness of the specimen than for specimens with fewer measurements made. This is due to the fact that fewer measurements may not show all of the potential diameter deviations present in the specimen, whereas a bigger sample size of measurements will better show these deviations.

4.4 Strength Testing

Diametral compression consists of compressing the specimen between two platens along the ring diameter. While the specimen is being compressed, some regions will be under a tensile stress while other regions will be under a compressive stress. Figure 2 shows where these regions lie on the specimen.

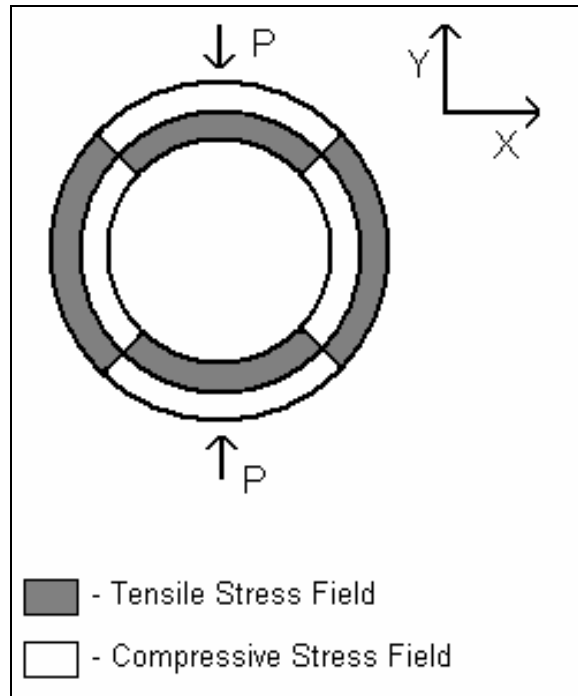


Figure 2. Schematic representation of the tangential stress field existing in a diametrically compressed O-ring specimen.

If the specimens are prepared and tested properly, the failure due to the compressive load applied along the diameter should occur on the inside diameter along the y-axis.

During testing for out-of-roundness, all the specimens were marked along the vertical axis used for compression as shown in figure 3. Specimens from ITK4-8, ITK4-4, and ITK4-14 were marked as shown in figure 4. The extra marks denote the placement of measurements made for roundness testing. All marks were made to allow the specimen pieces to be reoriented properly for post-fracture analysis of flaws contributing to failure.

Diametral compression was performed using an Instron Model 4202. Specimens from ITK4-6 and ITK4-7 were tested with pieces of Grafoil placed at the contact points of the platens and the specimen. The Grafoil was used to help avoid parasitic stresses at the contact points. However, the use of the Grafoil caused anomalies in the data due to deformation and failure of the Grafoil.

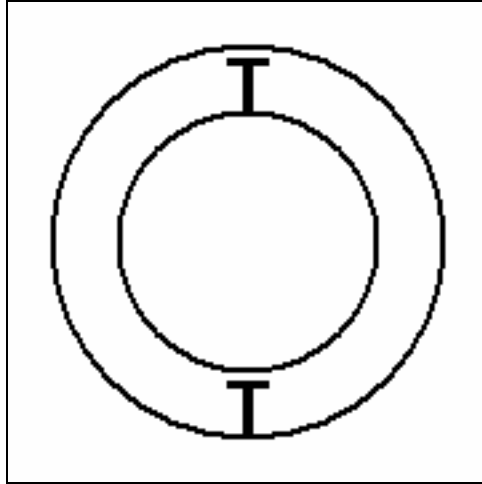


Figure 3. O-ring markings for specimens from ITK4-6 and ITK4-7.

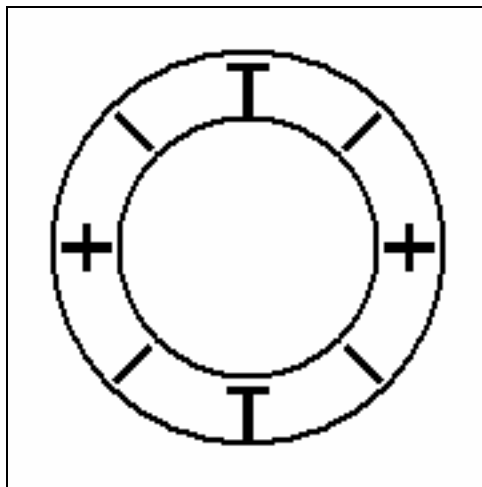


Figure 4. O-ring markings for specimens from ITK4-4, ITK4-8, and ITK4-14.

The remaining specimens were tested with manila folder paper placed at the contact points of the platens and the specimen. This removed the effect of the Grafoil from the compression data. Typical plots for specimens tested with and without Grafoil can be seen in figures 5 and 6, respectively.

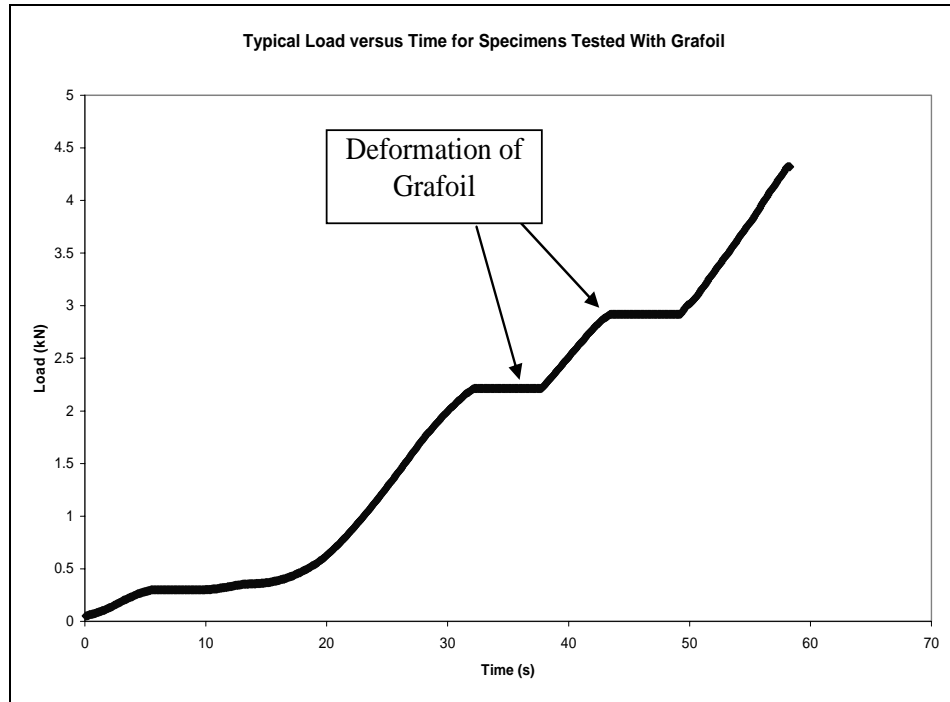


Figure 5. Typical load-vs.-time graph for specimens tested in diametral compression with Grafoil at contacts.

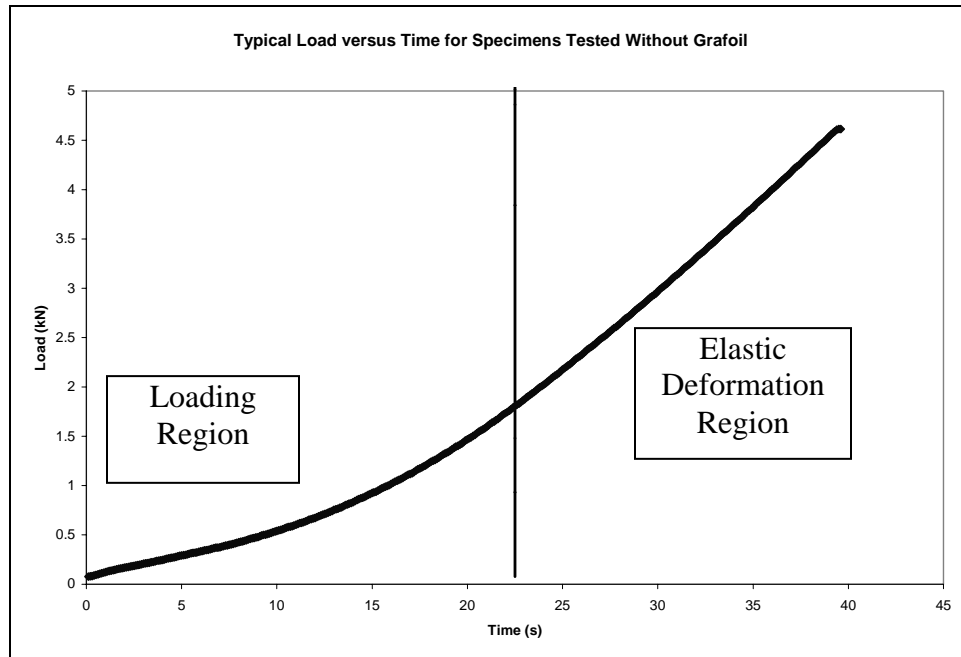


Figure 6. Typical load-vs.-time graph for specimens tested in diametral compression with manila folder paper at contacts instead of Grafoil.

All specimens were tested using a crosshead speed of 0.5 mm/min. The load-vs.-time data was recorded and stored in electronic form. The maximum load at failure was recorded for each specimen and was used, along with the specimen's dimensional measurements and failure angle, which are all shown in figure 7, to calculate the maximum stress on the specimen using equation 5 (8).

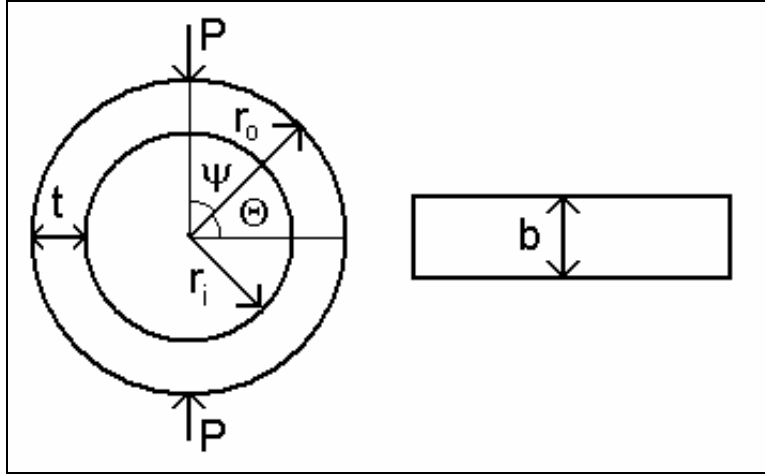


Figure 7. O-ring measurement schematic.

$$\sigma_{\theta} = \frac{P}{2} \left[0.637 \frac{r_a y}{I} - \cos \Theta \left(\frac{1}{A} + \frac{r_a y}{I} \right) \right], \quad (5)$$

where

P = load,

$\Theta = 90 - \Psi$,

$r_a = (r_i + r_o)/2$,

$y = r_a - r$,

$A = b(r_o - r_i) = bt$, and

$I = \frac{1}{12} b (r_o - r_i)^3 = \frac{1}{12} bt^3$.

5. Results and Discussion

5.1 Density Determination

Figure 8 displays the density of the calibrated kerosene used for the immersion density as a function of temperature as determined using ASTM D 891-95 (9).

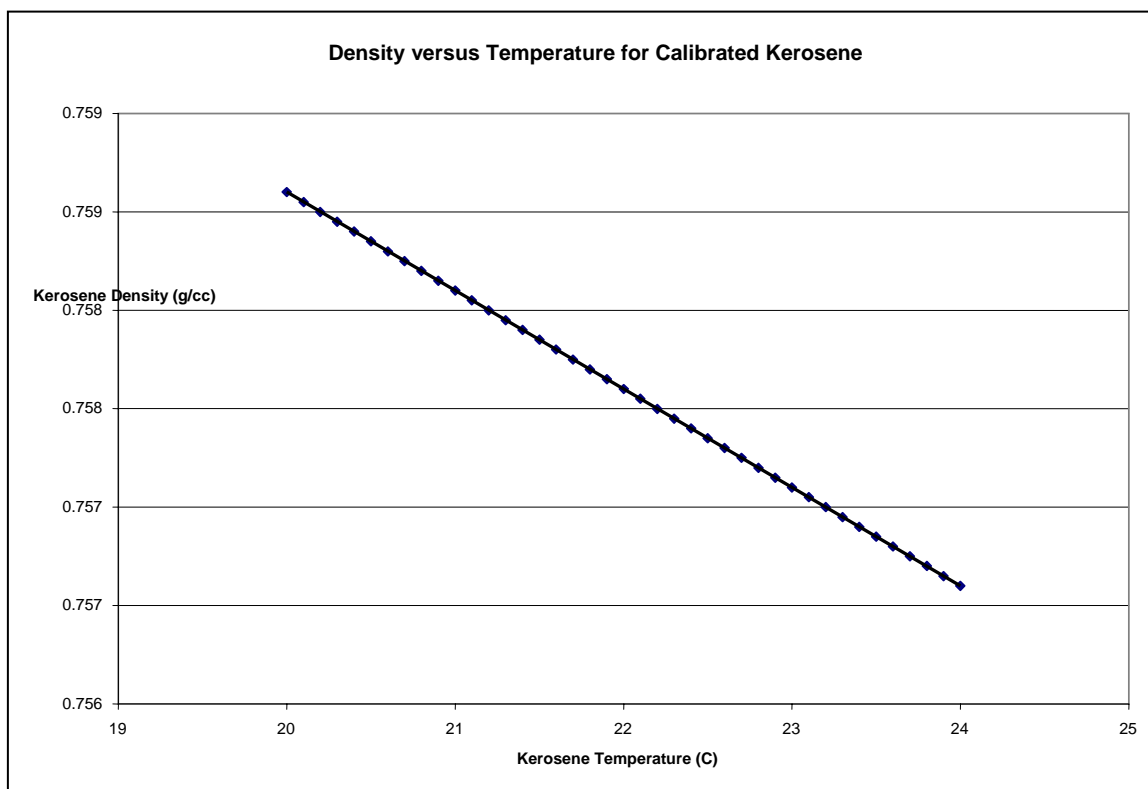


Figure 8. Density vs. temperature of calibrated kerosene used for immersion density measurements.

The densities of the specimens, which were calculated using Archimedes principle as described previously, are shown in figures 9 through 13. Although the initial mass measurements were made to five significant figures, there was fluctuation in the final digit and so the densities are reported to only four significant figures.

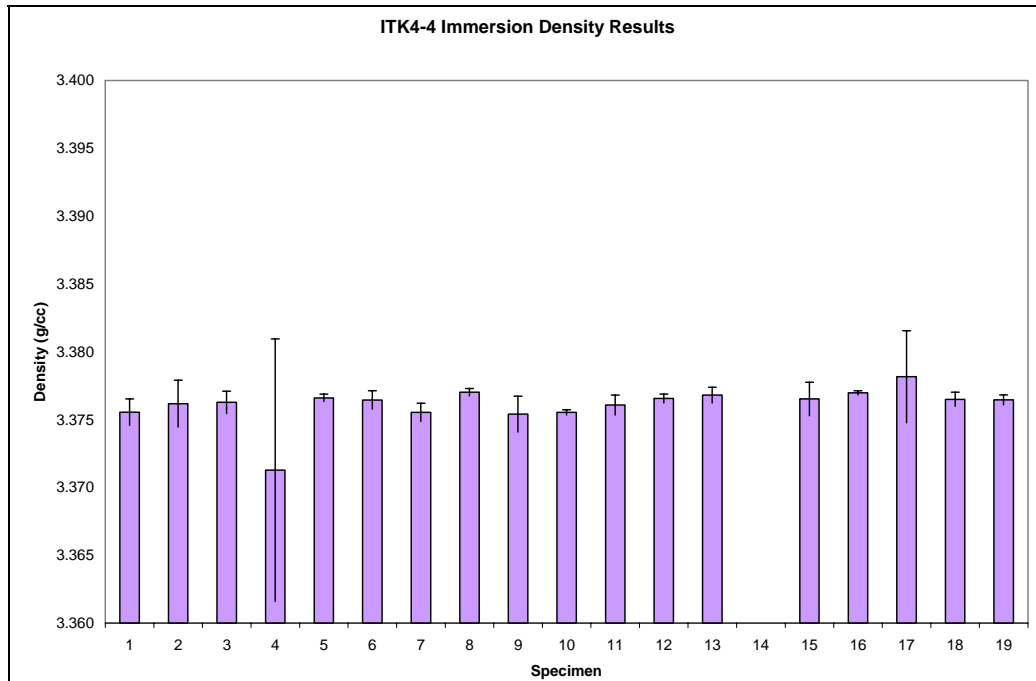


Figure 9. Plot showing immersion density results for specimens from ITK4-4. Bars represent one standard deviation of three measurements for the sample. ITK4-4 was initially a 200-mm-long tube. Specimen no. 14 was unavailable for analysis.

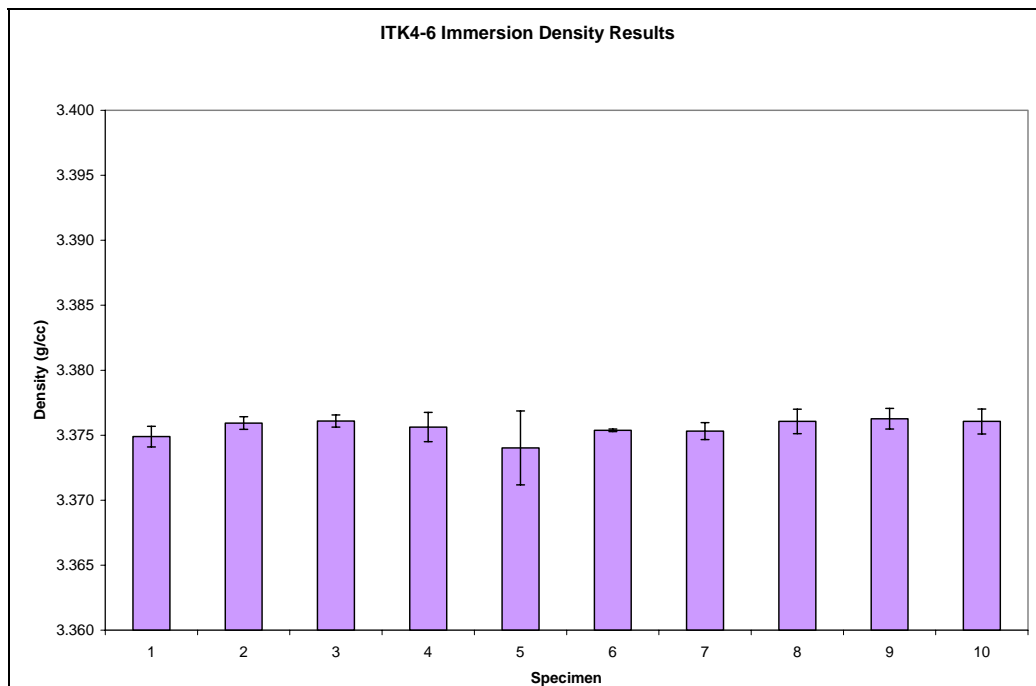


Figure 10. Plot showing immersion density results for specimens from ITK4-6. Bars represent one standard deviation of three measurements for the sample. ITK4-6 was initially a 100-mm-long tube.

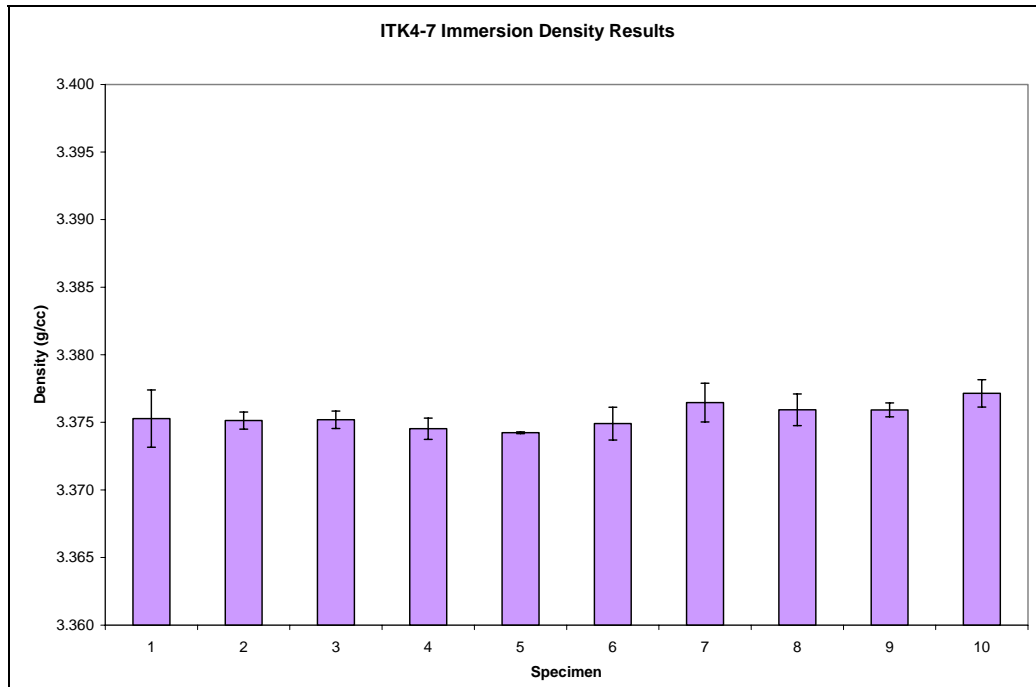


Figure 11. Plot showing immersion density results for specimens from ITK4-7. Bars represent one standard deviation of three measurements for the sample. ITK4-7 was initially a 100-mm-long tube.

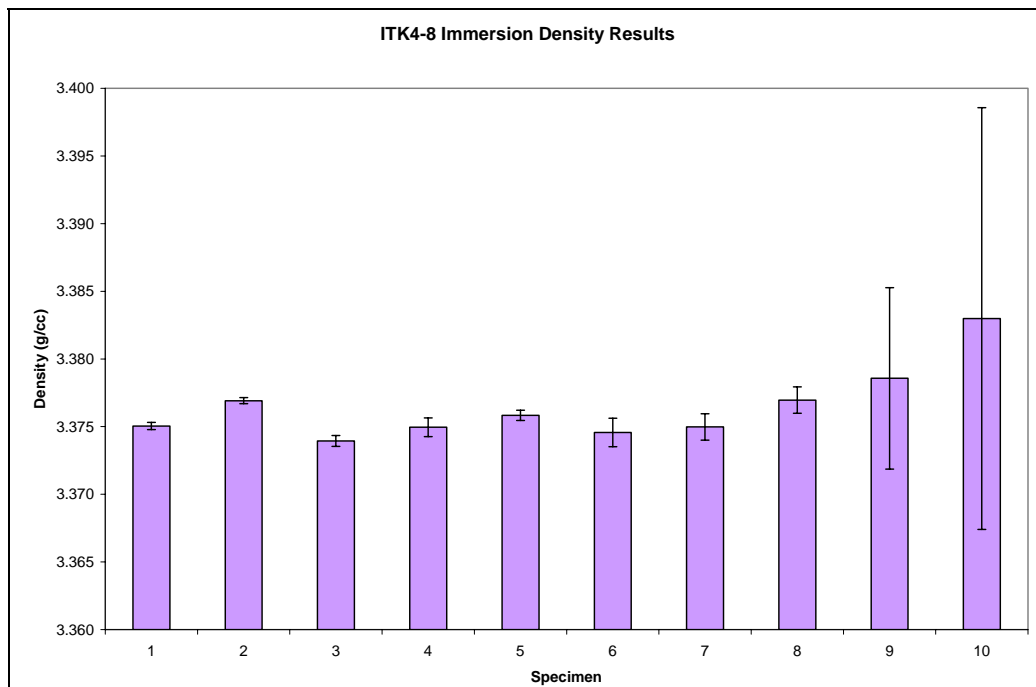


Figure 12. Plot showing immersion density results for specimens from ITK4-8. Bars represent one standard deviation of three measurements for the sample. ITK4-8 was initially a 100-mm-long tube.

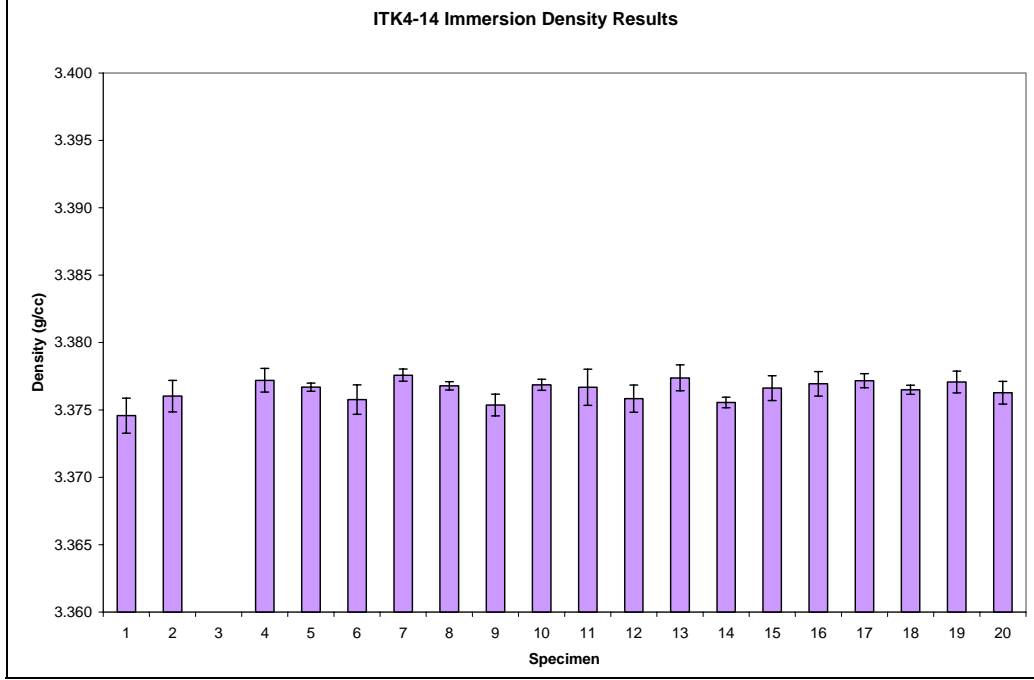


Figure 13. Plot showing immersion density results for specimens from ITK4-14. Bars represent one standard deviation of three measurements for the sample. ITK4-14 was initially a 200-mm-long tube. Specimen no. 3 was unavailable for analysis.

The large error bars present for specimens 9 and 10 of ITK4-8 (figure 12) are due to a single measurement for each specimen that was much larger than the other two measurements for that specimen. Eliminating the rogue measurements drops the averages for specimens 9 and 10 to 3.374 and 3.375 g/cm³, respectively. The resultant standard deviations are also very close in comparison to those found for the rest of the samples. This suggests that the apparent density gradient may not actually exist; however, the sample size for each statistical population is too small to determine this definitively.

ITK4-6 (figure 10) and ITK4-7 (figure 11) appear to have fairly uniform densities across their lengths. At first glance, it would appear that possible density gradients exist in tubes ITK4-4 (figure 9), ITK4-8 (figure 12), and ITK4-14 (figure 13). In order to check whether or not gradients exist for all of the tubes, the averages for the specimens were statistically tested against each other. A two-tailed z-test of averages was performed using equations 6 and 7. A confidence interval of 95% was used. The corresponding z-value at 95% confidence is 1.96, based on z tables (10).

$$\sigma_{X-Y} = \sqrt{\frac{\sigma_1^2}{m} + \frac{\sigma_2^2}{n}}, \quad (6)$$

where

σ_{X-Y} = standard deviation of X-Y,

σ_1 = standard deviation of X,

σ_2 = standard deviation of Y,

m = sample size of X, and

n = sample size of Y.

$$z = \frac{X - Y}{\sigma_{X-Y}}, \quad (7)$$

where

X = average 1,

Y = average 2, and

σ_{X-Y} = standard deviation of X-Y.

If the absolute value of the calculated value of z is <1.96, then the two averages are the same. If the absolute value of the calculated value of z is ≥ 1.96 , then the two averages are not the same.

Results of this analysis are found in tables 2 through 6.

Table 2. Statistical analysis of immersion density measurements for specimens from ITK4-4. Highlighted values denote dissimilar values based on the criteria.

	Sample 1	Sample 2	Sample 3	Sample 4	Sample 5	Sample 6	Sample 7	Sample 8	Sample 9
Sample 1	—	0.54	0.99	-0.76	1.81	1.30	-0.02	2.52	-0.15
Sample 2	-0.54	—	0.09	-0.86	0.43	0.25	-0.59	0.84	-0.61
Sample 3	-0.99	-0.09	—	-0.89	0.67	0.27	-1.21	1.50	-0.97
Sample 4	0.76	0.86	0.89	—	0.95	0.92	0.76	1.03	0.73
Sample 5	-1.81	-0.43	-0.67	-0.95	—	-0.39	-2.54	1.84	-1.54
Sample 6	-1.30	-0.25	-0.27	-0.92	0.39	—	-1.63	1.37	-1.21
Sample 7	0.02	0.59	1.21	-0.76	2.54	1.63	—	3.52	-0.15
Sample 8	-2.52	-0.84	-1.50	-1.03	-1.84	-1.37	-3.52	—	-2.07
Sample 9	0.15	0.61	0.97	-0.73	1.54	1.21	0.15	2.07	—
Sample 10	0.02	0.63	1.52	-0.76	5.58	2.21	-0.01	7.72	-0.17
Sample 11	-0.74	0.10	0.32	-0.86	1.19	0.64	-0.92	2.10	-0.76
Sample 12	-1.69	-0.37	-0.55	-0.94	0.21	-0.26	-2.34	1.87	-1.46
Sample 13	-1.92	-0.60	-0.92	-0.99	-0.54	-0.71	-2.47	0.58	-1.68
Sample 15	-1.06	-0.28	-0.28	-0.93	0.12	-0.09	-1.21	0.69	-1.07
Sample 16	-2.50	-0.80	-1.46	-1.02	-2.03	-1.32	-3.59	0.26	-2.04
Sample 17	-1.28	-0.90	-0.94	-1.16	-0.79	-0.86	-1.31	-0.58	-1.31
Sample 18	-1.49	-0.31	-0.40	-0.93	0.32	-0.12	-1.96	1.55	-1.34
Sample 19	-1.49	-0.27	-0.33	-0.92	0.60	-0.01	-2.04	2.14	-1.31

Table 2. Statistical analysis of immersion density measurements for specimens from ITK4-4. Highlighted values denote dissimilar values based on the criteria (continued).

	Sample 10	Sample 11	Sample 12	Sample 13	Sample 15	Sample 16	Sample 17	Sample 18	Sample 19
Sample 1	-0.02	0.74	1.69	1.92	1.06	2.50	1.28	1.49	1.49
Sample 2	-0.63	-0.10	0.37	0.60	0.28	0.80	0.90	0.31	0.27
Sample 3	-1.52	-0.32	0.55	0.92	0.28	1.46	0.94	0.40	0.33
Sample 4	0.76	0.86	0.94	0.99	0.93	1.02	1.16	0.93	0.92
Sample 5	-5.58	-1.19	-0.21	0.54	-0.12	2.03	0.79	-0.32	-0.60
Sample 6	-2.21	-0.64	0.26	0.71	0.09	1.32	0.86	0.12	0.01
Sample 7	0.01	0.92	2.34	2.47	1.21	3.59	1.31	1.96	2.04
Sample 8	-7.72	-2.10	-1.87	-0.58	-0.69	-0.26	0.58	-1.55	-2.14
Sample 9	0.17	0.76	1.46	1.68	1.07	2.04	1.31	1.34	1.31
Sample 10	—	1.21	4.61	3.62	1.36	10.35	1.34	3.03	3.75
Sample 11	-1.21	—	1.04	1.36	0.54	2.09	1.04	0.83	0.79
Sample 12	-4.61	-1.04	—	0.65	-0.05	1.98	0.82	-0.16	-0.38
Sample 13	-3.62	-1.36	-0.65	—	-0.37	0.49	0.68	-0.69	-0.91
Sample 15	-1.36	-0.54	0.05	0.37	—	0.63	0.79	-0.02	-0.10
Sample 16	-10.35	-2.09	-1.98	-0.49	-0.63	—	0.61	-1.53	-2.26
Sample 17	-1.34	-1.04	-0.82	-0.68	-0.79	-0.61	—	-0.84	-0.87
Sample 18	-3.03	-0.83	0.16	0.69	0.02	1.53	0.84	—	-0.14
Sample 19	-3.75	-0.79	0.38	0.91	0.10	2.26	0.87	0.14	—

Table 3. Statistical analysis of immersion density measurements for specimens from ITK4-6. Highlighted values denote dissimilar values based on the criteria.

	Sample 1	Sample 2	Sample 3	Sample 4	Sample 5	Sample 6	Sample 7	Sample 8	Sample 9	Sample 10
Sample 1	—	1.96	2.26	0.92	-0.51	1.05	0.72	1.65	2.12	1.62
Sample 2	-1.96	—	0.38	-0.44	-1.15	-2.01	-1.34	0.20	0.60	0.18
Sample 3	-2.26	-0.38	—	-0.66	-1.24	-2.63	-1.68	-0.05	0.33	-0.06
Sample 4	-0.92	0.44	0.66	—	-0.91	-0.39	-0.41	0.51	0.80	0.50
Sample 5	0.51	1.15	1.24	0.91	—	0.82	0.77	1.18	1.32	1.17
Sample 6	-1.05	2.01	2.63	0.39	-0.82	—	-0.15	1.26	1.92	1.22
Sample 7	-0.72	1.34	1.68	0.41	-0.77	0.15	—	1.13	1.60	1.10
Sample 8	-1.65	-0.20	0.05	-0.51	-1.18	-1.26	-1.13	—	0.29	-0.01
Sample 9	-2.12	-0.60	-0.33	-0.80	-1.32	-1.92	-1.60	-0.29	—	-0.29
Sample 10	-1.62	-0.18	0.06	-0.50	-1.17	-1.22	-1.10	0.01	0.29	—

Table 4. Statistical analysis of immersion density measurements for specimens from ITK4-7. Highlighted values denote dissimilar values based on the criteria.

	Sample 1	Sample 2	Sample 3	Sample 4	Sample 5	Sample 6	Sample 7	Sample 8	Sample 9	Sample 10
Sample 1	—	-0.11	-0.07	-0.58	-0.86	-0.26	0.80	0.47	0.51	1.37
Sample 2	0.11	—	0.10	-1.05	-2.46	-0.29	1.46	1.03	1.66	2.90
Sample 3	0.07	-0.10	—	-1.14	-2.57	-0.36	1.40	0.96	1.53	2.81
Sample 4	0.58	1.05	1.14	—	-0.64	0.46	2.05	1.73	2.57	3.53
Sample 5	0.86	2.46	2.57	0.64	—	0.97	2.69	2.51	5.59	4.96
Sample 6	0.26	0.29	0.36	-0.46	-0.97	—	1.43	1.05	1.33	2.45
Sample 7	-0.80	-1.46	-1.40	-2.05	-2.69	-1.43	—	-0.49	-0.61	0.67
Sample 8	-0.47	-1.03	-0.96	-1.73	-2.51	-1.05	0.49	—	-0.01	1.35
Sample 9	-0.51	-1.66	-1.53	-2.57	-5.59	-1.33	0.61	0.01	—	1.85
Sample 10	-1.37	-2.90	-2.81	-3.53	-4.96	-2.45	-0.67	-1.35	-1.85	—

Table 5. Statistical analysis of immersion density measurements for specimens from ITK4-8. Highlighted values denote dissimilar values based on the criteria.

	Sample 1	Sample 2	Sample 3	Sample 4	Sample 5	Sample 6	Sample 7	Sample 8	Sample 9	Sample 10
Sample 1	—	9.53	-4.00	-0.21	2.99	-0.76	-0.11	3.27	0.91	0.88
Sample 2	-9.53	—	-11.21	-4.68	-4.25	-3.78	-3.35	0.06	0.43	0.67
Sample 3	4.00	11.21	—	2.20	5.93	0.97	1.71	4.94	1.19	1.00
Sample 4	0.21	4.68	-2.20	—	1.94	-0.53	0.04	2.89	0.93	0.89
Sample 5	-2.99	4.25	-5.93	-1.94	—	-1.96	-1.41	1.85	0.70	0.79
Sample 6	0.76	3.78	-0.97	0.53	1.96	—	0.50	2.87	1.02	0.93
Sample 7	0.11	3.35	-1.71	-0.04	1.41	-0.50	—	2.47	0.92	0.89
Sample 8	-3.27	-0.06	-4.94	-2.89	-1.85	-2.87	-2.47	—	0.41	0.67
Sample 9	-0.91	-0.43	-1.19	-0.93	-0.70	-1.02	-0.92	-0.41	—	0.45
Sample 10	-0.88	-0.67	-1.00	-0.89	-0.79	-0.93	-0.89	-0.67	-0.45	—

From table 2, specimens 7, 10, and 16 from ITK4-4 appear to be quite different from the majority of the other specimens. Also, the dissimilarities found for specimens at the end of the tube tend to occur when paired with specimens from the middle of the tube. This is especially prevalent towards the end of the tube with the higher numbered specimens. This could suggest a density gradient for this tube.

From table 3, ITK4-6 shows very little dissimilarity between samples. This suggests a fairly uniform density across the length of the tube. This is consistent with figure 10.

Table 4 shows that specimens at the higher numbered end of ITK4-7 are dissimilar to the specimens located in the middle of the tube. This suggests a density gradient across the tube. Based on figure 11, it is possible that the density is slightly higher towards the higher numbered end of the tube.

From table 5, ITK4-8 appears to have many specimens that are dissimilar to each other. However, this is mainly due to the majority of the samples having such small standard deviations. Specimens 9 and 10, as seen in figure 12, have excessively large standard deviations which cause them to fall into the range of every other specimen when compared with a 95% confidence level.

Based on table 6 and figure 13, it seems highly possible that specimen 1 from ITK4-14 has a lower density than the rest of the tube. In addition, there may be decreased density present in the middle of the tube as shown by the data for specimens 7, 8, and 9. These density gradients could lead to strength gradients in the tubes. Whether or not this is true will be examined later on.

Table 6. Statistical analysis of immersion density measurements for specimens from ITK4-14. Highlighted values denote dissimilar values based on the criteria.

	Sample 1	Sample 2	Sample 4	Sample 5	Sample 6	Sample 7	Sample 8	Sample 9	Sample 10	
Sample 1	—	1.44	2.90	2.76	1.22	3.79	2.88	0.89	2.91	
Sample 2	−1.44	—	1.38	0.95	−0.28	2.13	1.09	−0.81	1.16	
Sample 4	−2.90	−1.38	—	−0.94	−1.77	0.66	−0.76	−2.65	−0.60	
Sample 5	−2.76	−0.95	0.94	—	−1.42	2.83	0.39	−2.66	0.58	
Sample 6	−1.22	0.28	1.77	1.42	—	2.66	1.57	−0.52	1.63	
Sample 7	−3.79	−2.13	−0.66	−2.83	−2.66	—	−2.48	−4.12	−2.03	
Sample 8	−2.88	−1.09	0.76	−0.39	−1.57	2.48	—	−2.84	0.24	
Sample 9	−0.89	0.81	2.65	2.66	0.52	4.12	2.84	—	2.85	
Sample 10	−2.91	−1.16	0.60	−0.58	−1.63	2.03	−0.24	−2.85	—	
Sample 11	−1.95	−0.64	0.56	0.01	−0.92	1.09	0.14	−1.45	0.22	
Sample 12	−1.33	0.21	1.75	1.40	−0.08	2.71	1.55	−0.64	1.62	
Sample 13	−3.00	−1.54	−0.24	−1.18	−1.92	0.33	−1.00	−2.77	−0.85	
Sample 14	−1.25	0.66	2.95	4.00	0.32	5.87	4.28	−0.37	3.99	
Sample 15	−2.23	−0.69	0.79	0.13	−1.04	1.63	0.31	−1.77	0.42	
Sample 16	−2.58	−1.06	0.36	−0.44	−1.43	1.09	−0.26	−2.23	−0.13	
Sample 17	−3.21	−1.54	0.05	−1.36	−2.01	1.02	−1.07	−3.22	−0.79	
Sample 18	−2.49	−0.67	1.29	0.76	−1.11	3.34	1.12	−2.23	1.20	
Sample 19	−2.83	−1.28	0.17	−0.77	−1.67	0.93	−0.57	−2.59	−0.41	
Sample 20	−1.91	−0.30	1.31	0.80	−0.64	2.36	0.99	−1.35	1.08	
	Sample 11	Sample 12	Sample 13	Sample 14	Sample 15	Sample 16	Sample 17	Sample 18	Sample 19	Sample 20
Sample 1	1.95	1.33	3.00	1.25	2.23	2.58	3.21	2.49	2.83	1.91
Sample 2	0.64	−0.21	1.54	−0.66	0.69	1.06	1.54	0.67	1.28	0.30
Sample 4	−0.56	−1.75	0.24	−2.95	−0.79	−0.36	−0.05	−1.29	−0.17	−1.31
Sample 5	−0.01	−1.40	1.18	−4.00	−0.13	0.44	1.36	−0.76	0.77	−0.80
Sample 6	0.92	0.08	1.92	−0.32	1.04	1.43	2.01	1.11	1.67	0.64
Sample 7	−1.09	−2.71	−0.33	−5.87	−1.63	−1.09	−1.02	−3.34	−0.93	−2.36
Sample 8	−0.14	−1.55	1.00	−4.28	−0.31	0.26	1.07	−1.12	0.57	−0.99
Sample 9	1.45	0.64	2.77	0.37	1.77	2.23	3.22	2.23	2.59	1.35
Sample 10	−0.22	−1.62	0.85	−3.99	−0.42	0.13	0.79	−1.20	0.41	−1.08
Sample 11	—	−0.87	0.73	−1.40	−0.07	0.27	0.58	−0.23	0.44	−0.44
Sample 12	0.87	—	1.90	−0.46	0.99	1.39	2.01	1.07	1.65	0.58
Sample 13	−0.73	−1.90	—	−3.04	−0.99	−0.57	−0.33	−1.50	−0.41	−1.49
Sample 14	1.40	0.46	3.04	—	1.85	2.41	4.26	3.18	2.93	1.35
Sample 15	0.07	−0.99	0.99	−1.85	—	0.43	0.90	−0.22	0.65	−0.47
Sample 16	−0.27	−1.39	0.57	−2.41	−0.43	—	0.38	−0.78	0.20	−0.92
Sample 17	−0.58	−2.01	0.33	−4.26	−0.90	−0.38	—	−1.87	−0.16	−1.55
Sample 18	0.23	−1.07	1.50	−3.18	0.22	0.78	1.87	—	1.15	−0.42
Sample 19	−0.44	−1.65	0.41	−2.93	−0.65	−0.20	0.16	−1.15	—	−1.19
Sample 20	0.44	−0.58	1.49	−1.35	0.47	0.92	1.55	0.42	1.19	—

5.2 Roundness Testing

The results from the out-of-roundness testing of the specimens are displayed in tables 7–11. It should be noted once again that specimens from ITK4-6 and ITK4-7 only had three measurements used in the calculations while the rest of the specimens had six measurements used.

Table 7. ITK4-4 roundness test results.

Sample	O. D. Roundness	O. D. % Out of Roundness	I. D. Roundness	I. D. % Out of Roundness
1	0.993	0.70	0.997	0.30
2	0.996	0.40	0.994	0.60
3	0.996	0.40	0.991	0.90
4	0.996	0.40	0.993	0.70
5	0.996	0.40	0.996	0.40
6	0.996	0.40	0.994	0.60
7	0.997	0.30	0.994	0.60
8	0.996	0.40	0.995	0.50
9	0.995	0.50	0.992	0.80
10	0.996	0.40	0.994	0.60
11	0.997	0.30	0.992	0.80
12	0.998	0.20	0.996	0.40
13	0.997	0.30	0.992	0.80
15	0.998	0.20	0.994	0.60
16	0.999	0.10	0.995	0.50
17	0.996	0.40	0.992	0.80
18	0.996	0.40	0.996	0.40
19	0.997	0.30	0.997	0.30
Average	0.996	0.361	0.994	0.589
Std. Dev.	0.001	0.129	0.002	0.184

Table 8. ITK4-6 roundness test results.

Sample	O. D. Roundness	O. D. % Out of Roundness	I. D. Roundness	I. D. % Out of Roundness
1	0.999	0.10	0.995	0.50
2	0.999	0.10	0.995	0.50
3	0.999	0.10	0.995	0.50
4	0.999	0.10	0.995	0.50
5	0.999	0.10	0.994	0.60
6	1.000	0.00	0.994	0.60
7	0.999	0.10	0.994	0.60
8	0.999	0.10	0.993	0.70
9	1.000	0.00	0.995	0.50
10	1.000	0.00	0.995	0.50
Average	0.999	0.070	0.994	0.550
Std. Dev.	0.000	0.048	0.001	0.071

Table 9. ITK4-7 roundness test results.

Sample	O. D. Roundness	O. D. % Out of Roundness	I. D. Roundness	I. D. % Out of Roundness
1	1.000	0.00	0.993	0.70
2	1.000	0.00	0.995	0.50
3	1.000	0.00	0.995	0.50
4	1.000	0.00	0.995	0.50
5	1.000	0.00	0.993	0.70
6	1.000	0.00	0.994	0.60
7	0.999	0.10	0.994	0.60
8	0.999	0.10	0.994	0.60
9	1.000	0.00	0.994	0.60
10	1.000	0.00	0.995	0.50
Average	1.000	0.020	0.994	0.580
Std. Dev.	0.000	0.042	0.001	0.079

Table 10. ITK4-8 roundness test results.

Sample	O. D. Roundness	O. D. % Out of Roundness	I. D. Roundness	I. D. % Out of Roundness
1	0.999	0.10	0.993	0.70
2	0.998	0.20	0.993	0.70
3	0.999	0.10	0.994	0.60
4	0.999	0.10	0.995	0.50
5	0.998	0.20	0.995	0.50
6	0.999	0.10	0.995	0.50
7	0.999	0.10	0.995	0.50
8	0.999	0.10	0.994	0.60
9	0.999	0.10	0.994	0.60
10	0.999	0.10	0.994	0.60
Average	0.999	0.120	0.994	0.580
Std. Dev.	0.000	0.042	0.001	0.079

Table 11. ITK4-14 roundness test results.

Sample	O. D. Roundness	O. D. % Out of Roundness	I. D. Roundness	I. D. % Out of Roundness
1	0.998	0.20	0.996	0.40
2	0.999	0.10	0.995	0.50
4	0.999	0.10	0.995	0.50
5	0.999	0.10	0.996	0.40
6	0.998	0.20	0.994	0.60
7	0.999	0.10	0.996	0.40
8	0.999	0.10	0.996	0.40
9	0.999	0.10	0.996	0.40
10	0.999	0.10	0.996	0.40
11	0.999	0.10	0.996	0.40
12	0.998	0.20	0.996	0.40
13	0.998	0.20	0.994	0.60
14	0.997	0.30	0.994	0.60
15	0.996	0.40	0.996	0.40
16	0.997	0.30	0.995	0.50
17	0.996	0.40	0.993	0.70
18	0.996	0.40	0.996	0.40
19	0.996	0.40	0.997	0.30
20	0.997	0.30	0.996	0.40
Average	0.998	0.216	0.995	0.458
Std. Dev.	0.001	0.121	0.001	0.102

All of the specimens from all tubes show out-of-roundness of less than 1% for both inner and outer diameters. ITK4-4, ITK4-8, and ITK4-14 have higher calculated out-of-roundness than ITK4-6 and ITK4-7, mainly due to the fact that more measurements were taken for the former specimens which allowed for greater variability. The inner diameters of all tubes displayed a greater tendency to be out-of-round than the outer diameters did. For the purposes of gun tubes, this may not be a good thing, even though the out-of-roundness is less than 1%. The projectiles that come through these tubes have a standard diameter and the tubes need to be standard as well in order to allow for the projectile to have maximum accuracy upon exiting the tube.

5.3 Strength Testing

All specimens with the exception of specimen 5 from ITK4-4 failed down through the vertical axis of the specimen. Specimen 5 from ITK4-4 failed at an angle of 30° from the vertical axis. The results from the diametral compression testing are shown in figures 14–23. The data was also plotted using Weib Par and maximum likelihood estimators of the Weibull modulus and characteristic strength. All of the data used for these plots and calculations can be found in appendix C.

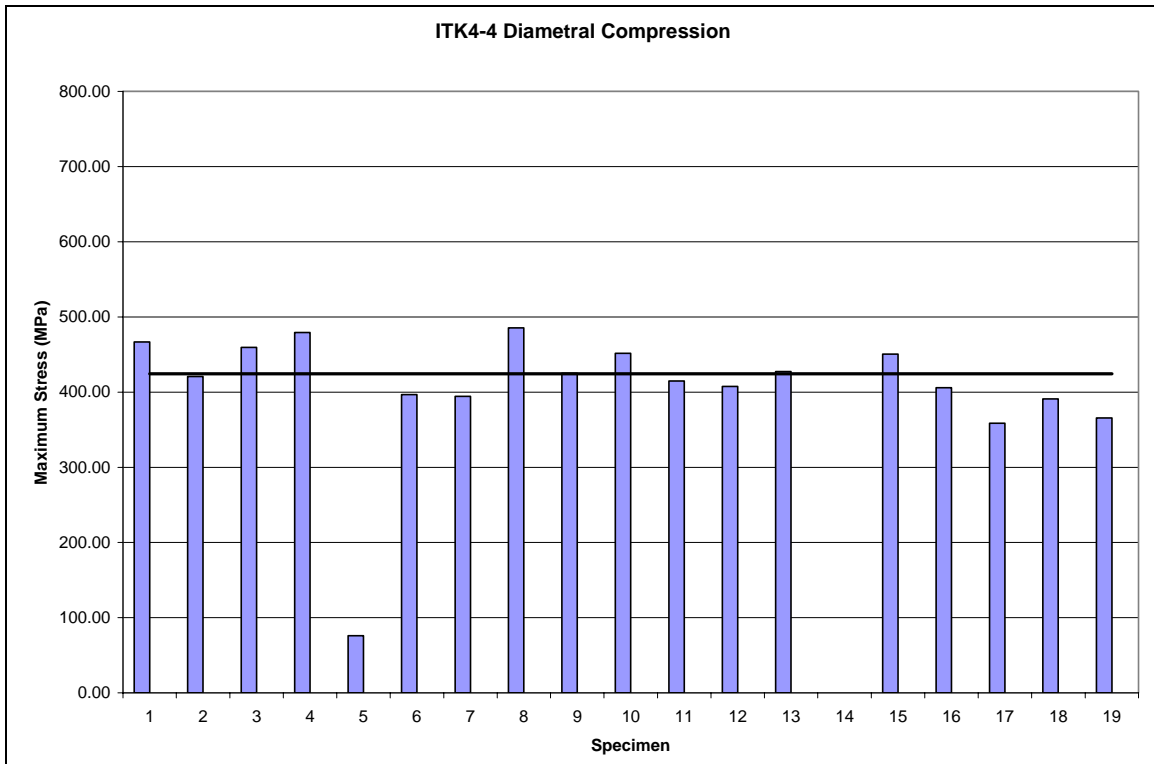


Figure 14. ITK4-4 diametral compression results. Average is shown as dark horizontal line.

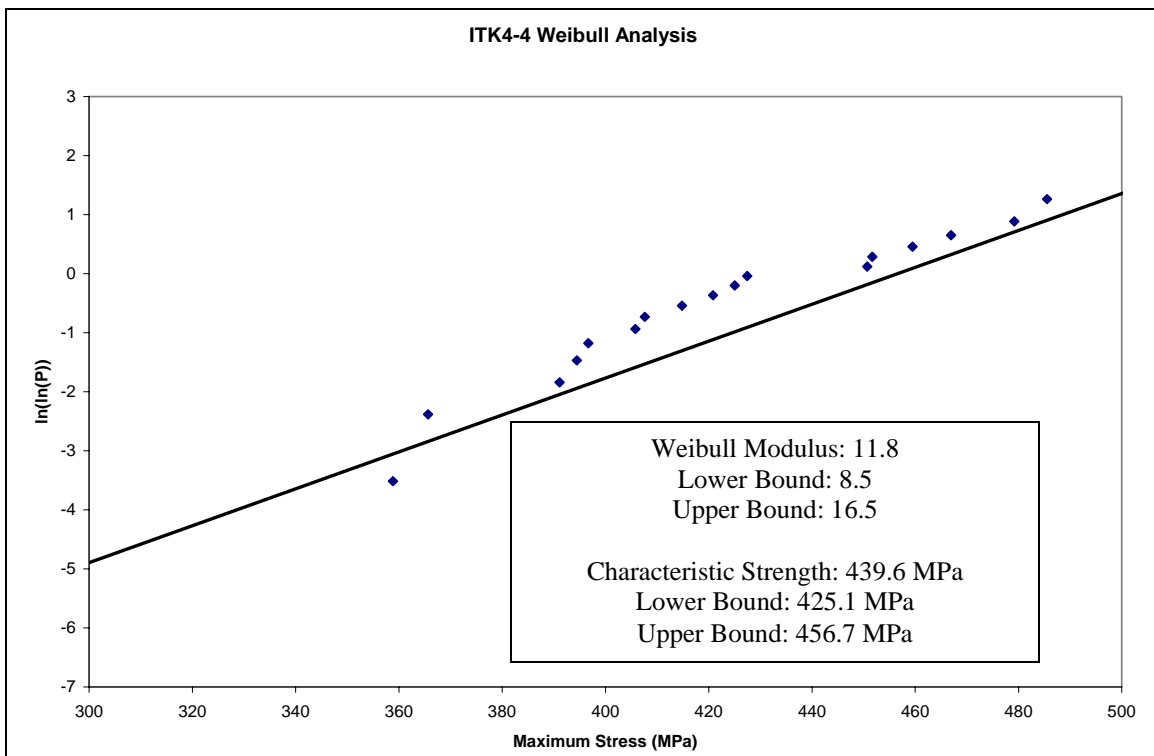


Figure 15. ITK4-4 Weibull analysis of maximum stress using Weib Par and maximum likelihood.

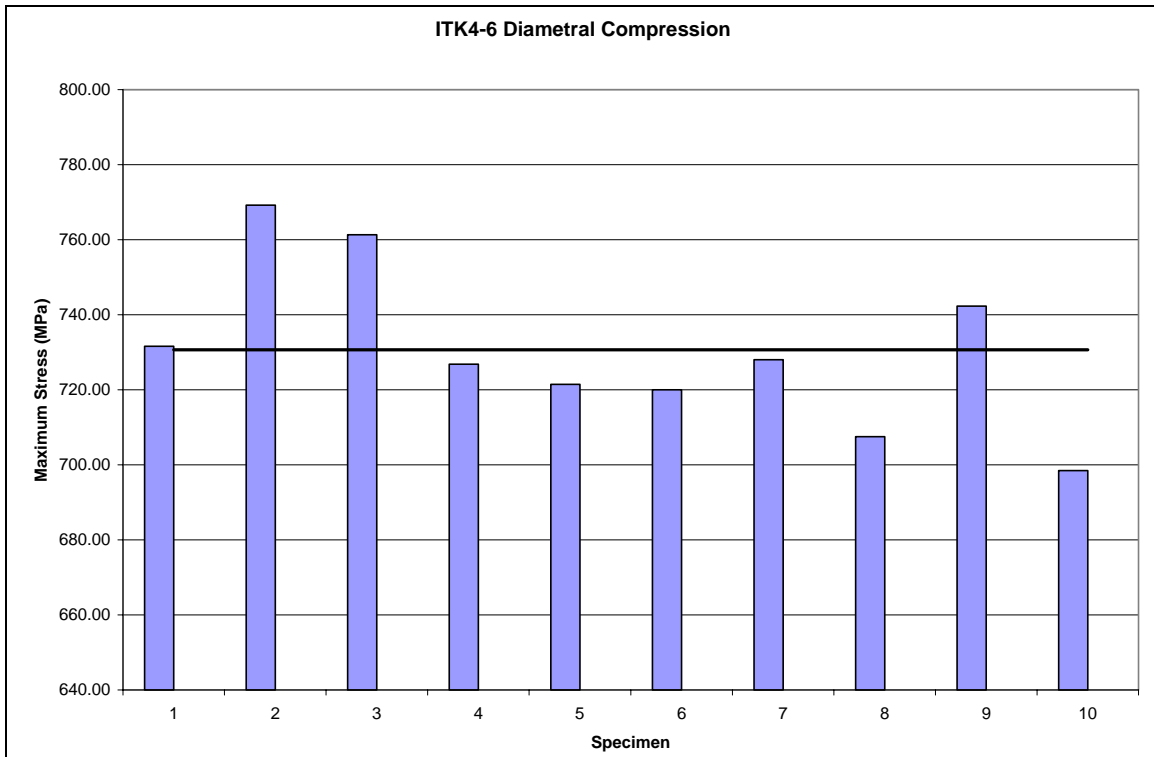


Figure 16. ITK4-6 diametral compression results. Average is shown as dark horizontal line.

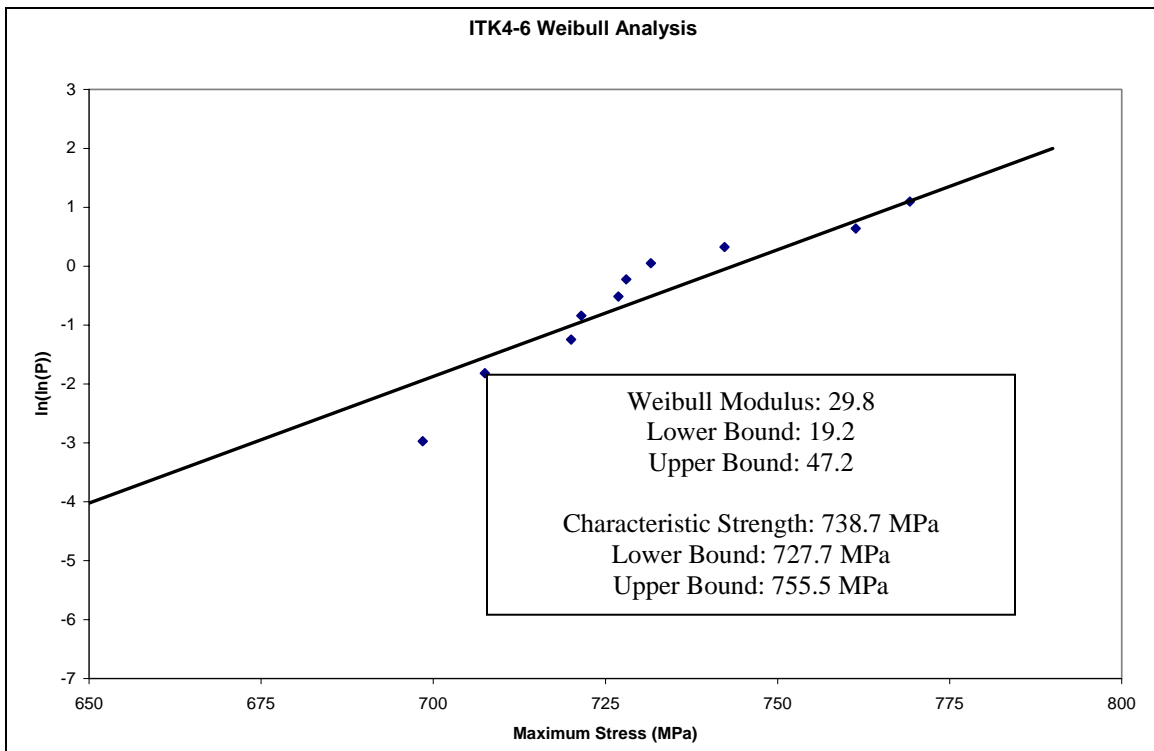


Figure 17. ITK4-6 Weibull analysis of maximum stress using Weib Par and maximum likelihood.

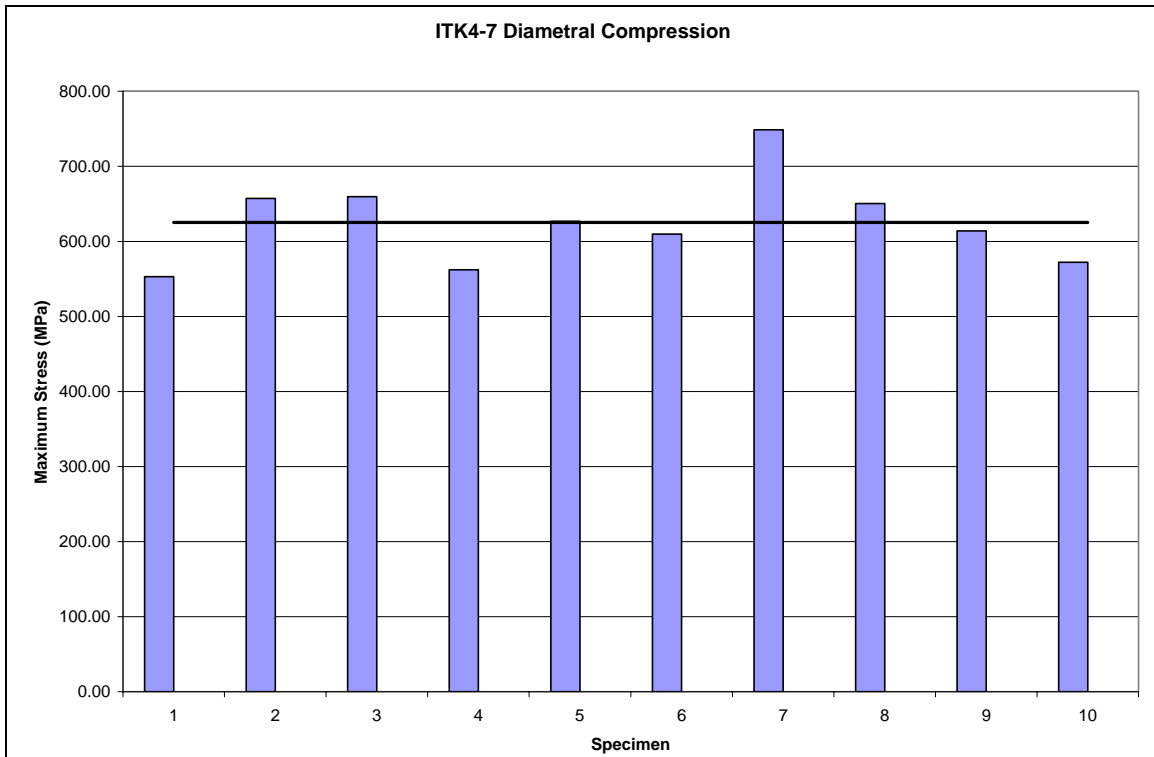


Figure 18. ITK4-7 diametral compression results. Average is shown as dark horizontal line.

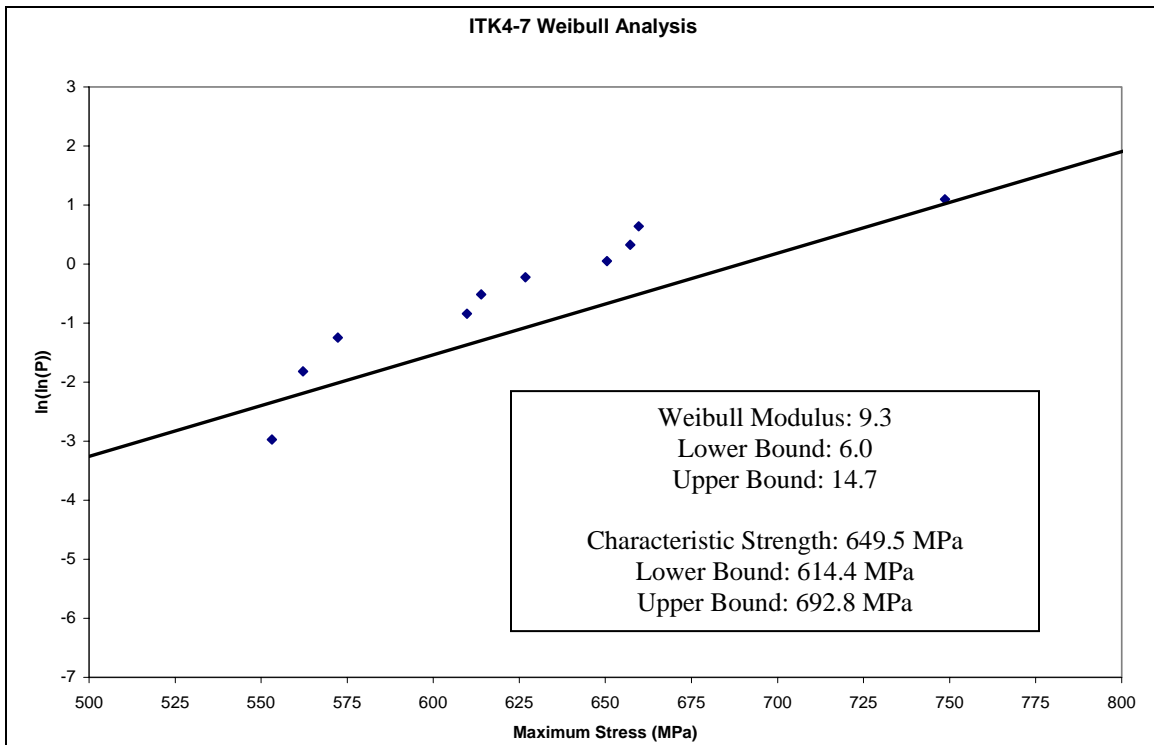


Figure 19. ITK4-7 Weibull analysis of maximum stress using Weib Par and maximum likelihood.

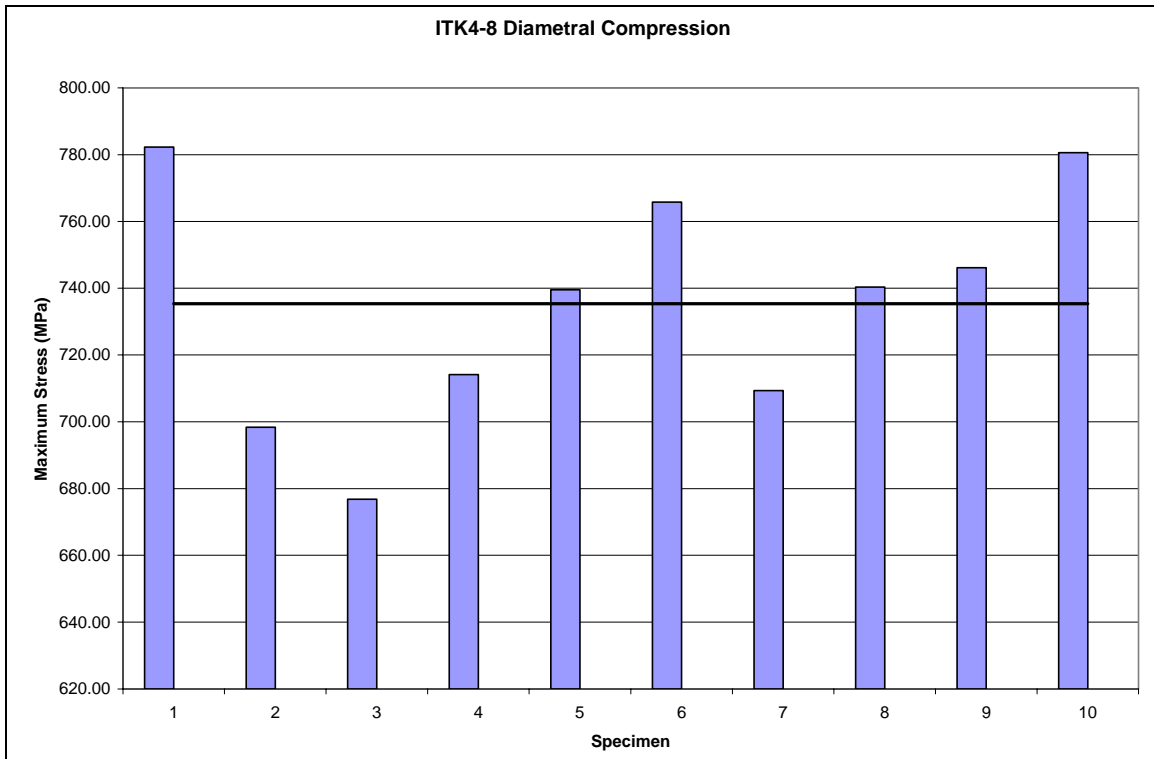


Figure 20. ITK4-8 diametral compression results. Average is shown as dark horizontal line.

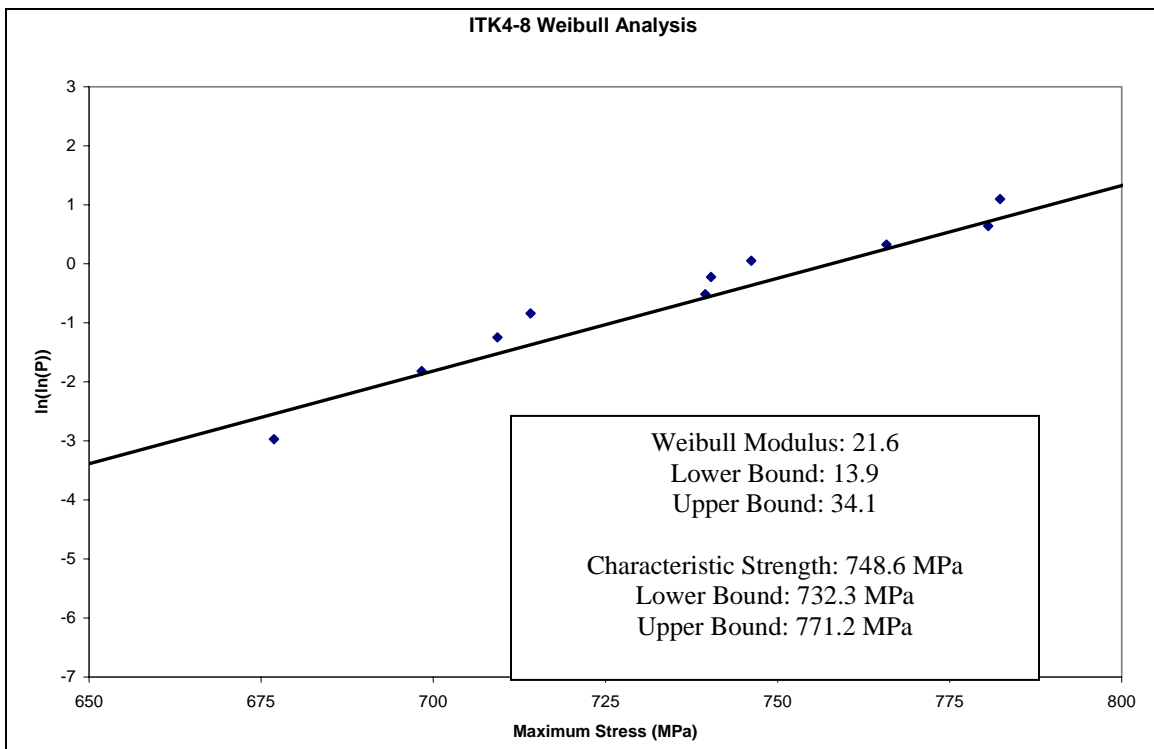


Figure 21. ITK4-8 Weibull analysis of maximum stress using Weib Par and maximum likelihood.

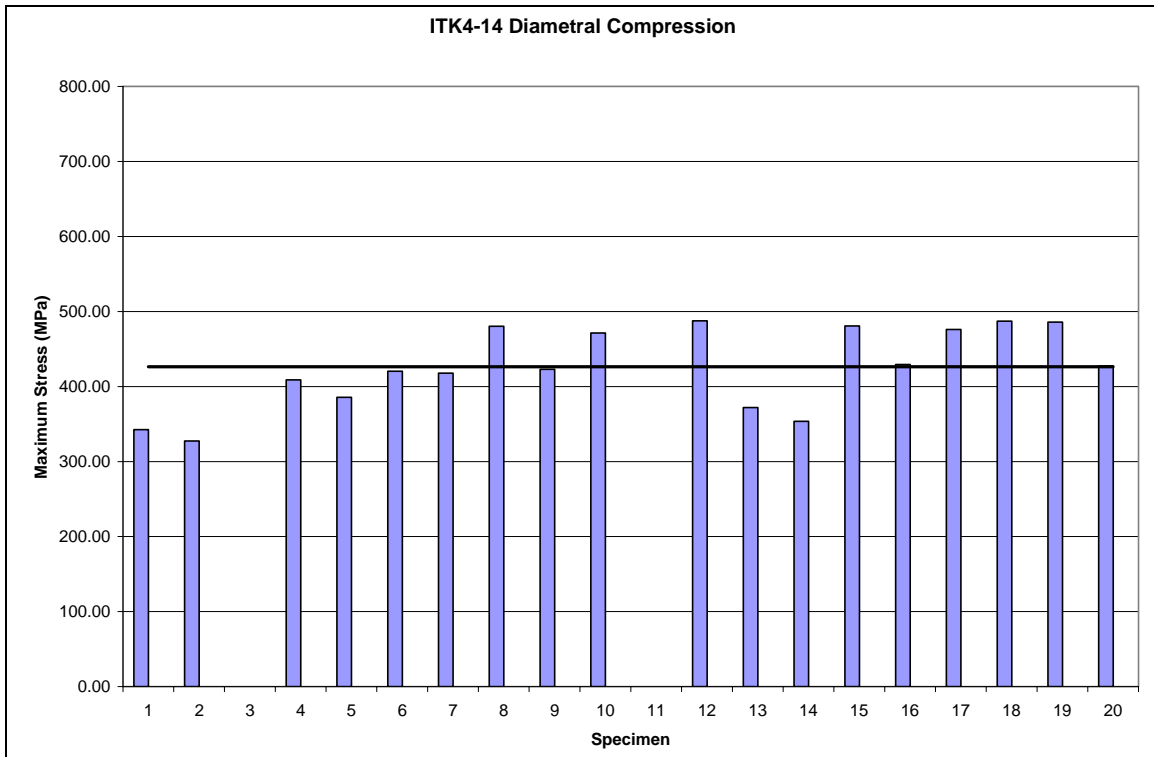


Figure 22. ITK4-14 diametral compression results. Average is shown as dark horizontal line.

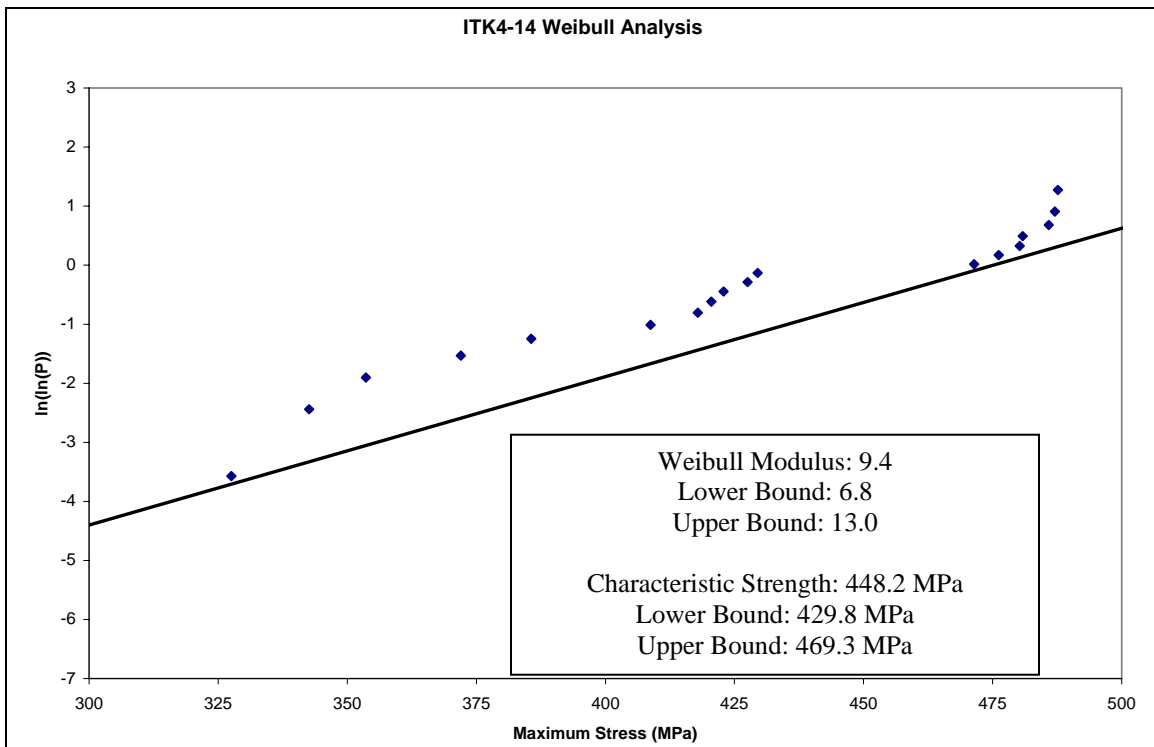


Figure 23. ITK4-14 Weibull analysis of maximum stress using Weib Par and maximum likelihood.

The data suggests a possible strength gradient for ITK4-4, with the higher strength specimens existing at the low numbered end of the tube and lower strength specimens existing at the high numbered end of the tube. A comparison of the strength data and the density data can be found in section 5.4.

Because specimen 5 from ITK4-4 had a different failure mode from the other specimens, it was not included in the Weibull analysis for the tube.

The data highly suggests a strength gradient running from one end of the tube to the other. A comparison of the strength data and the density data can be found in section 5.4.

The data suggests that ITK4-8 has higher strength at one end than the other. A comparison of the strength data and the density data can be found in section 5.4.

The data presented for ITK4-14 shows a potential strength gradient with lower strength towards the lower numbered side than towards the higher numbered side. A comparison of the strength data and the density data can be found in section 5.4.

A plot comparing the Weibull plots for the data from the specimens from all tubes is shown in figure 24.

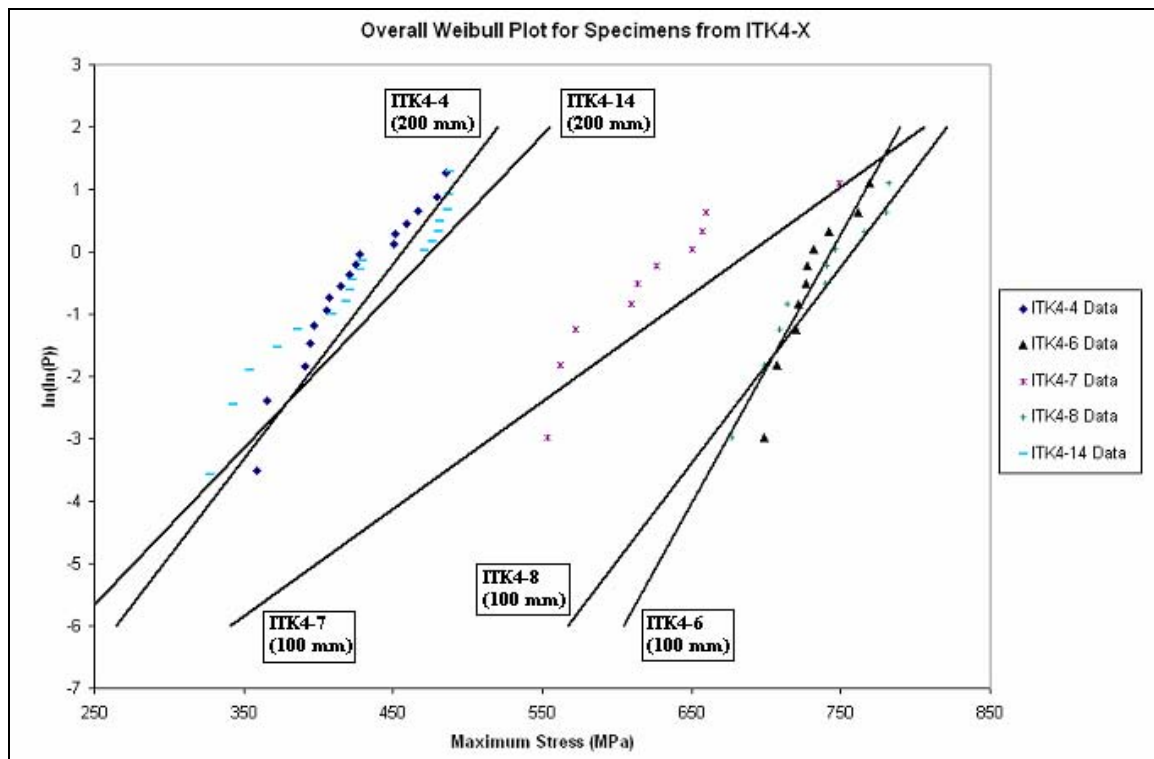


Figure 24. Weibull plots of strength data from specimens from ITK4-X sorted by tube of origin.

Based on this analysis, it appears that the longer tubes exhibited a lower characteristic strength than the shorter tubes. With the exception of ITK4-7, the shorter tubes show much less variability in strength values over the length of the tube, although this could very well be due to the fact that there are almost twice as many samples in each long tube as there are in each short tube. Table 12 contains an overall strength data comparison for ITK4-X tubes.

Table 12. Comparison of overall strength data for ITK4-X tubes.

Tube	Average Strength (MPa)	Std. Dev. (MPa)	Characteristic Strength (MPa)	Lower Bound (MPa)	Upper Bound (MPa)	Weibull Modulus	Lower Bound	Upper Bound
ITK4-4 (200-mm-long)	404.33	89.63	439.6	425.1	456.7	11.8	8.5	16.5
ITK4-14 (200-mm-long)	426.54	53.40	448.2	429.8	469.3	9.4	6.8	13.0
ITK4-6 (100-mm-long)	730.68	22.01	738.7	727.7	755.5	29.8	19.2	47.2
ITK4-7 (100-mm-long)	625.40	58.15	649.5	614.4	692.8	9.3	6.0	14.7
ITK4-8 (100-mm-long)	735.34	35.37	748.6	732.3	771.2	21.6	13.9	34.1

ITK4-7 appears to be different from the other two short tubes. The Weibull analysis for this tube appears to be influenced by a potential outlying data point which may be abnormally higher than the rest. This data point was removed in further analysis and the recalculated Weibull modulus and characteristic strength were 16.0 and 627.2 MPa. While the recalculated Weibull modulus is closer to the Weibull moduli of the other short tubes, the recalculated characteristic strength is dropping farther from the characteristic strengths of the other short tubes.

5.4 Strength/Density Comparisons

Plots comparing the strength of samples within a tube with their individual density are shown in figures 25–29.

The data for the density of ITK4-4 suggests, with the exclusion of a few specimens with abnormal standard deviations, that there is no real density gradient across the tube. The strength data however shows decreased strength towards the higher numbered end of the tube. Overall, there is about a 20% difference in strength between the two ends.

The density data for ITK4-6 does not suggest any kind of a gradient. The strength data, however, shows a decrease in strength across the tube length with ~5% variability in strength.

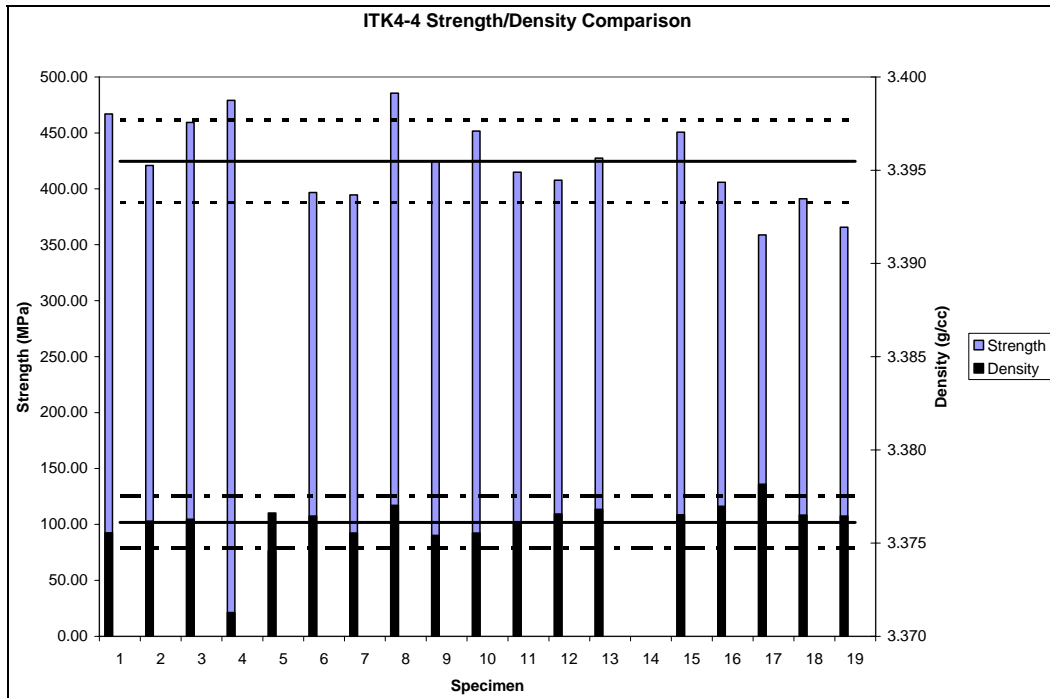


Figure 25. Comparison of strength and density values for specimens from ITK4-4. ITK4-4 was initially a 200-mm-long tube. Specimen 14 was not available for analysis. The solid lines represent the averages of the data while the dotted lines represent one standard deviation.

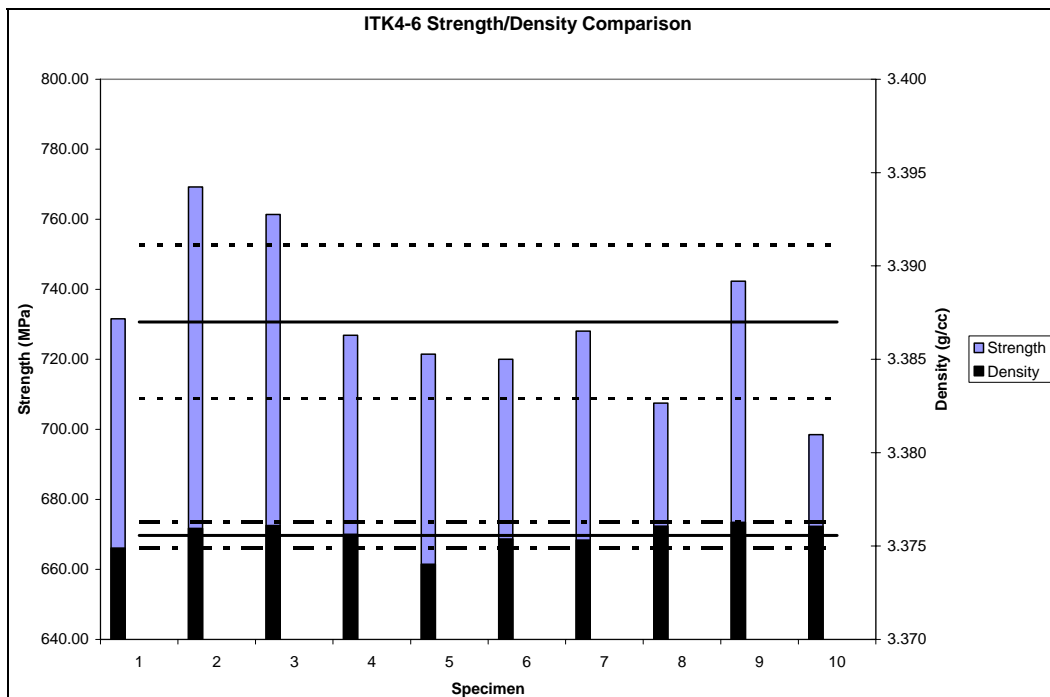


Figure 26. Comparison of strength and density values for specimens from ITK4-6. ITK4-6 was initially a 100-mm-long tube. The solid lines represent the averages of the data while the dotted lines represent one standard deviation.

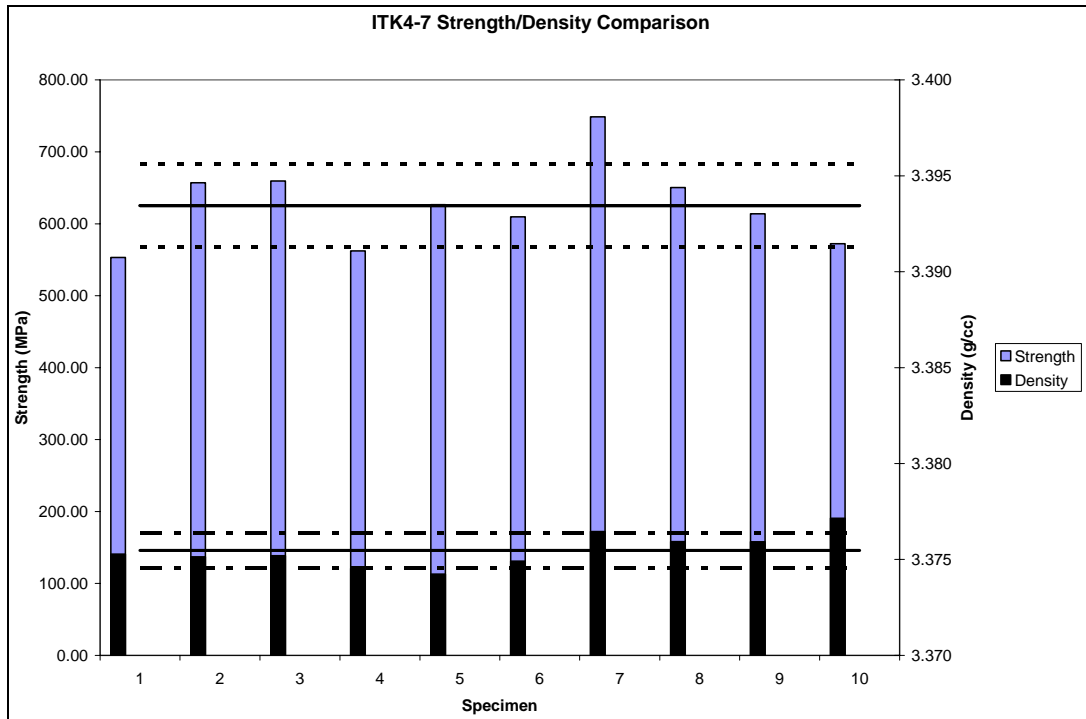


Figure 27. Comparison of strength and density values for specimens from ITK4-7. ITK4-7 was initially a 100-mm-long tube. The solid lines represent the averages of the data while the dotted lines represent one standard deviation.

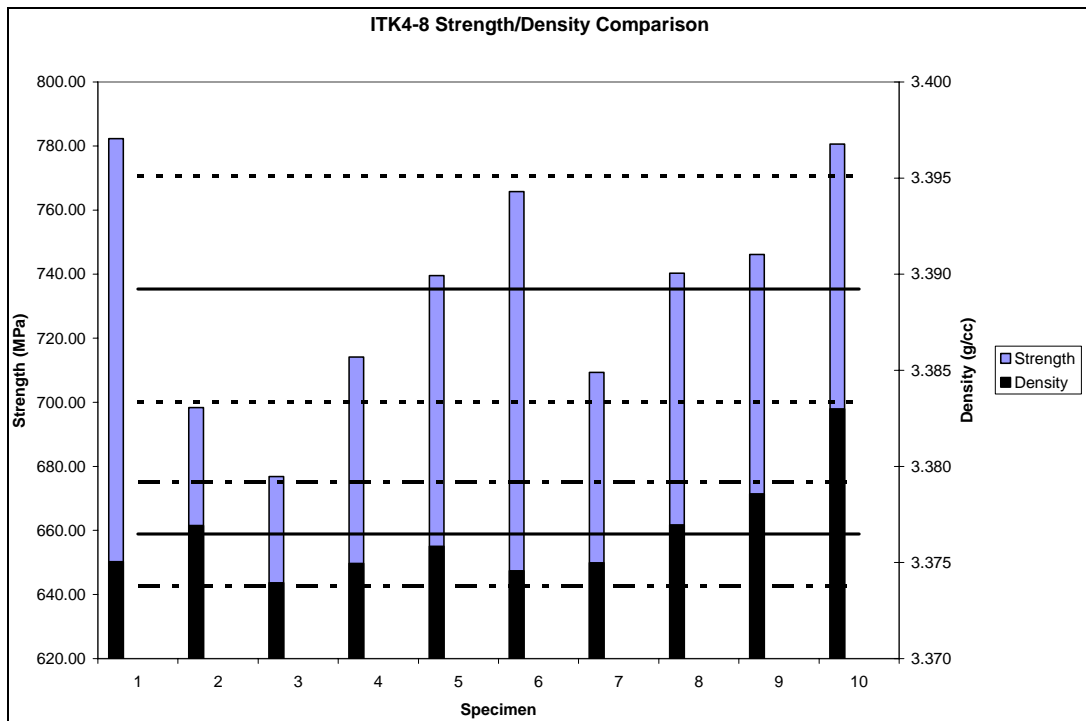


Figure 28. Comparison of strength and density values for specimens from ITK4-8. ITK4-8 was initially a 100-mm-long tube. The solid lines represent the averages of the data while the dotted lines represent one standard deviation.

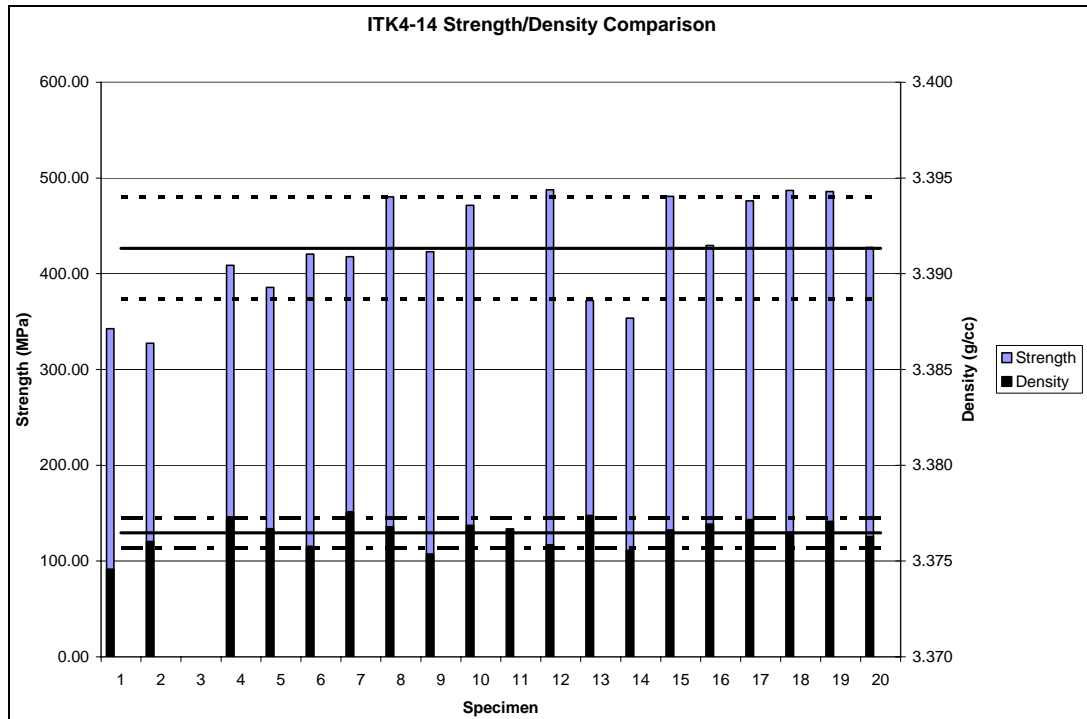


Figure 29. Comparison of strength and density values for specimens from ITK4-14. ITK4-14 was initially a 100-mm-long tube. Specimen 3 was not available for testing. Specimen 11 was broken during preloading and no data was available for strength analysis. The solid lines represent the averages of the data while the dotted lines represent one standard deviation.

Density data suggests a slight density gradient for ITK4-7 with the higher numbered specimens having a higher density. However, the decrease in density is at most about 0.5% which tells us that, overall, the density is fairly uniform. Strength data suggests decreased strength at the ends of the tube with about an 8% decline from the strength of the middle.

The density data for ITK4-8 shows a gradient with higher density at the higher numbered end. In truth, this gradient leaves only about 0.5% denser than the other. This means that the tube has a fairly uniform density across its length. The strength data also suggests higher strength (about 5%) towards the higher numbered end. Even though the density is uniform and the strength data shows somewhat of a gradient, in this case, the strength data and density data correspond well with each other. The specimens that exhibited higher densities than their neighbors also exhibited higher strengths than their neighbors. Overall, a higher density correlated directly with a higher strength on a specimen by specimen basis.

The density of ITK4-14 varies only by about 0.6% over its length. The strength, however, shows a tendency towards lower strength at the lower numbered end of the tube. Overall, there is about a 30% change in strength across the tube length.

The majority of the tubes show very little deviation in the density of any given tube (no tube showed more than a 1% change along its length). However, all of the tubes show a trend of one form or another in strength along their lengths. The extent to which these trends occur across the tube length help determine the overall fidelity of the tube. In general, an extreme gradient in either density or strength is a sign that the tube is not being manufactured uniformly and something in the production process needs to be changed. Even if the tube meets strength and density requirements with the extreme fluctuation in properties, something in the production process should be changed to try to produce the tubes more uniformly as the variations in properties could eventually get out of control and lead to non-conformal tubes. If the gradients are fairly small, and the properties are all well within their limits, then the tubes are being manufactured uniformly and no changes in production methods are absolutely necessary.

In addition, there appears to be no real correlation between the roundness of the tube and the strength/density of the tube. This may be due to the small amount of roundness measurements made for the tubes and the lack of precision that can be obtained from these measurements.

5.5 Fractography

All of the specimens showed flaws occurring from the inner surface of the O-ring, in the tensile stress field. There don't appear to be any specimens that failed due to an edge flaw. Figure 30 shows a typical failure origin for the O-rings. Many of the pictures display a silvery-white area around the failure origin similar to that seen in figure 30. In order to try and determine what this discoloration was, the failure origin of one of the specimens was examined using energy dispersive spectroscopy (EDS). The specimen was examined at four spots in and around the failure origin. All of the spectra from these spots were very similar in elemental composition. One of these spectra is shown in figure 31. The only elements found were silicon, aluminum, nitrogen, oxygen, and yttrium. This suggests that there is no steel, or any other impurity, present in the composition.

Specimen 5 from ITK4-4 was the only O-ring tested that did not fail down through the vertical axis upon testing. It failed at an angle of 30° from the vertical axis. Figures 31 and 32 show the two sides of the failure origin for this specimen. The failure here is due to some sort of processing flaw, most likely an agglomerate or inclusion of some sort.

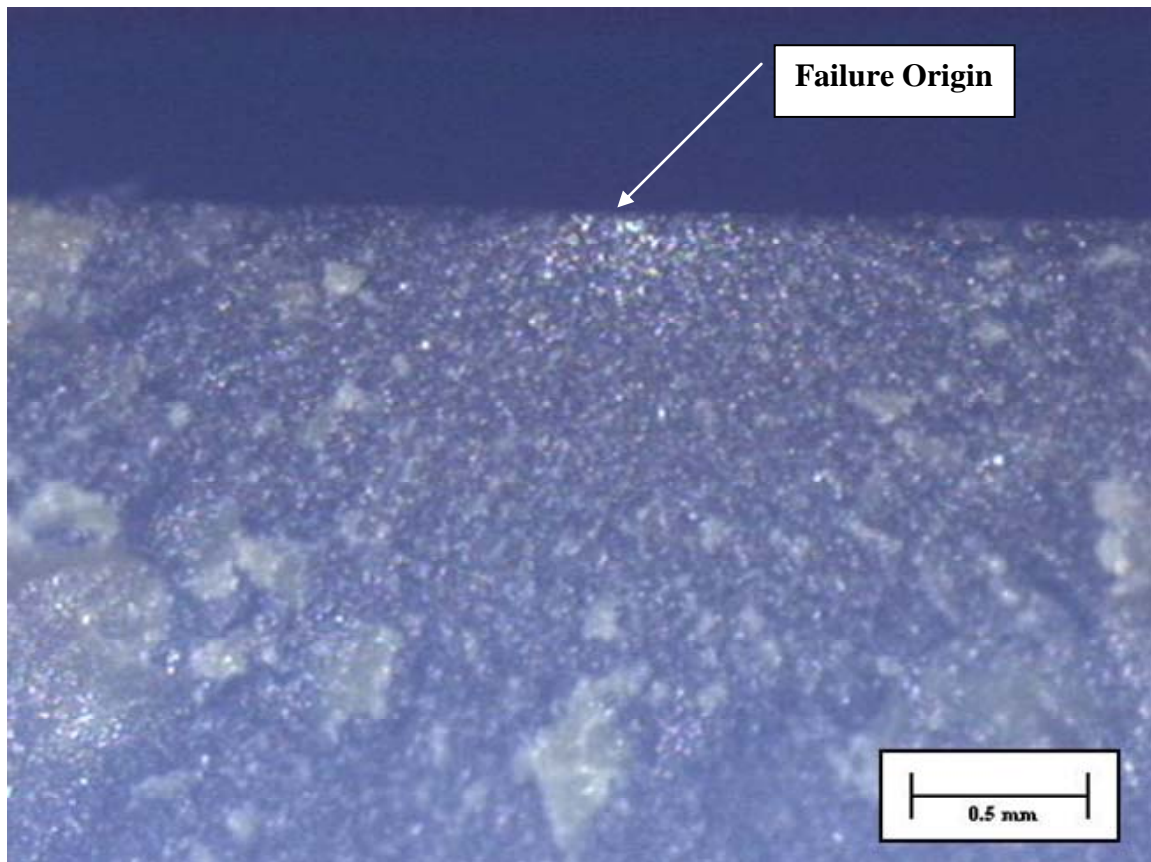


Figure 30. Typical micrograph of failure origin for O-rings tested under diametral compression.

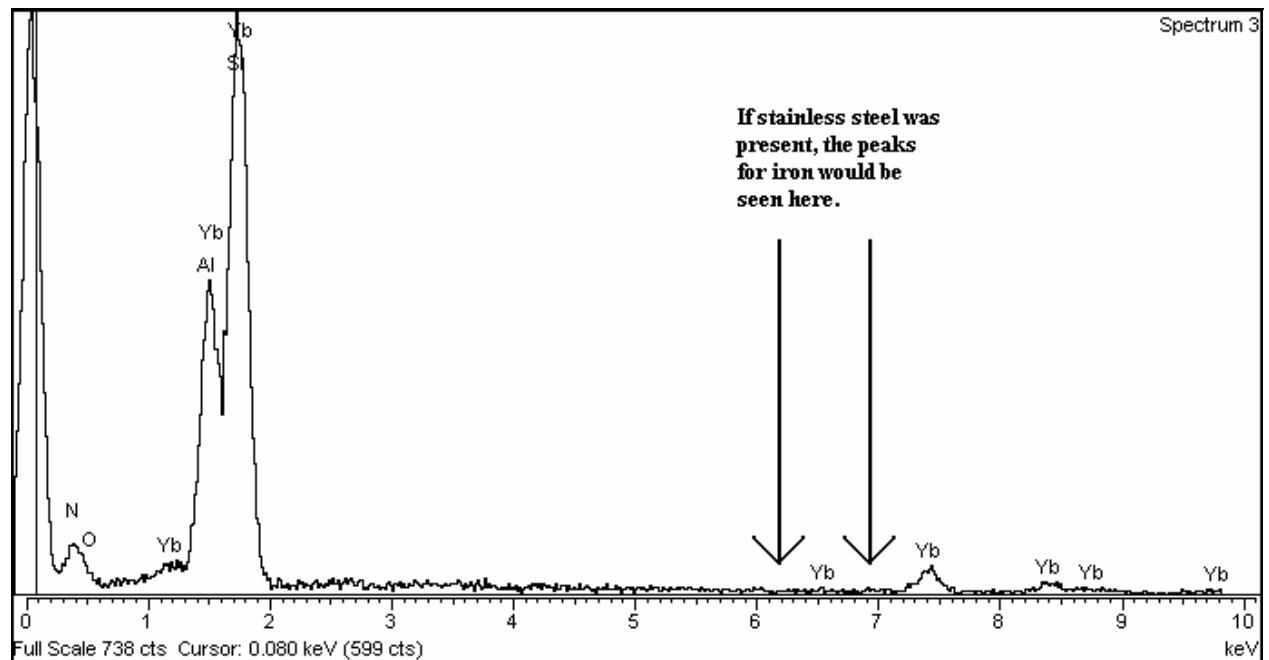


Figure 31. Typical EDS spectrum in and around failure origins of ITK4-X specimens.

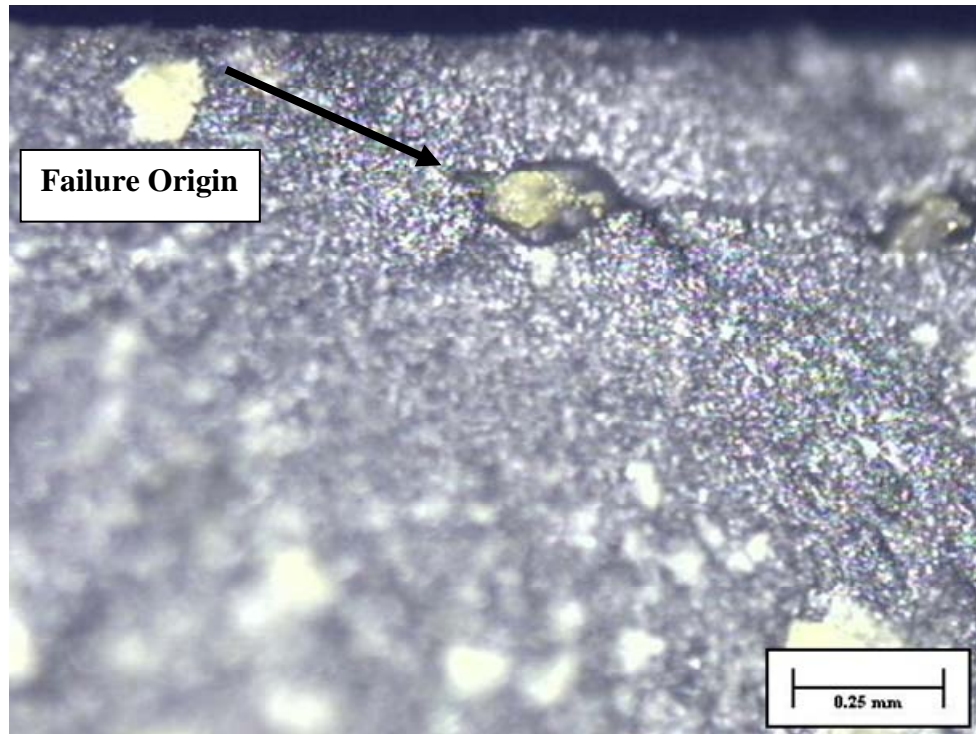


Figure 32. Fracture origin of specimen 5 from ITK4-4, side 1. Failure appears to have been caused by an agglomerate or inclusion of some sort.



Figure 33. Fracture origin of specimen 5 from ITK4-4, side 2. Failure appears to have been caused by an agglomerate or inclusion of some sort.

6. Conclusions

The densities of all specimens tested are fairly similar with few exceptions. All of the tubes studied showed less than a 1% difference (approximately 0.034 g/cm^3) in density between any two specimens.

In regards to dimensional properties, all tubes were within 1% out-of-roundness with the majority of samples less than 0.5% out-of-round.

The shorter tubes (ITK4-6, ITK4-7, and ITK4-8) displayed higher overall strength values than the longer tubes (ITK4-4 and ITK4-14).

ITK4-4 displayed a strength gradient that left one end 20% (77 MPa) stronger than the other end. The strength steadily declined from one end to the other.

ITK4-6 showed a steady decline in strength from one end of the tube to the other, with one end 5% (38 MPa) stronger than the other. ITK4-7 displayed approximately an 8% (50 MPa) difference in strength between the middle of the tube and the ends with the ends of the tube displaying a lower strength. ITK4-8 and ITK4-14 both showed a steady decline in strength from one end of the tube to the other. ITK4-8 showed an overall change of about 5% (37 MPa) in strength. ITK4-14 showed a 30% (100 MPa) difference in strength from end to end.

Overall, there seems to be (for the most part) a correlation between strength and density. The specimens that showed higher densities also tended to show higher strengths. This may seem contrary to the previous statements which discussed the absence of density gradients and the presence of strength gradients. However, these were mainly due to the small scale on which the densities could be compared to each other. The strength values, however, are big enough that even small differences between samples are magnified and easier to see. Therefore, whatever gradients exist for the strengths, tend to exist for the densities as well, just on a much smaller scale which is why there is no more than a 1% difference between any of the densities of any of the specimens.

7. Future Work

While some trends can be seen from the data and work shown here, further research is necessary to validate the results and expand this research further. It would be advantageous to procure more tube samples and perform immersion density again but with more runs to allow for better statistical analysis of this data. With only three runs per specimen, one outlying data point had

the potential to greatly skew the final data for that specimen and produced abnormal standard deviations.

In addition, the roundness of new samples should probably be verified with a machine that can determine those properties optically by making thousands of diameter measurements at various points all around the sample.

INTENTIONALLY LEFT BLANK.

8. References

1. Kohnken, K. H. Ceramic Gun Barrels. *Advanced Materials & Processes* **2002**, 160 (9), 47–48.
2. Van Akin, D. Ceramic/Propellant Interactions in Gun Barrel Applications. B.S. Thesis in Materials Science and Engineering, The Pennsylvania State University, University Park, PA, 2004.
3. Swab, J. J.; Wereszczak, A. A.; Tice, J.; Caspe, R.; Kraft, R. H.; Adams, J. W. *Mechanical and Thermal Properties of Advanced Ceramics for Gun Barrel Applications*; ARL-TR-3417; U.S. Army Research Laboratory: Aberdeen Proving Ground, MD, 2005.
4. Grujicic, M.; DeLong, J. R.; Derosset, W. S. Reliability Analysis of Hybrid Ceramic/Steel Gun Barrels. *Fatigue Fract. Engng. Mater. Struct.* **2003**, 26, 405–420.
5. Swab, J. J. U.S. Army Research Laboratory, Aberdeen Proving Ground, MD. Private communication, ITK4 discussion, 2005.
6. Bhatnagar, A.; Hoffman, M. J.; Dauskardt, R. H. Fracture and Subcritical Crack Growth Behavior of Y-Si-Al-O-N Glasses and Si₃N₄ Ceramics. *J. Am. Ceram. Soc.* **2000**, 83 (3), 585–596.
7. Yang, J.; Zhang, G.; She, J.; Ohji, T.; Kanzaki, S. Improvement of Mechanical Properties and Corrosion Resistance of Porous β -SiAlON Ceramics by Low Y₂O₃ Additions. *J. Am. Ceram. Soc.* **2004**, 87 (9), 1714–1719.
8. Jadaan, O. M.; Shelleman, D. L.; Conway, J. C.; Mecholsky, J. J.; Tressler, R. E. Prediction of the Strength of Ceramic Tubular Components: Part I – Analysis. *ASTM Journal of Testing and Evaluation* **1991**, 19 (3), 181–191.
9. *ASTM D 891-95*. Standard Test Methods for Specific Gravity, Apparent, of Liquid Industrial Chemicals. *Annu. Book ASTM Stand.* **2003**, Vol. 15.05.
10. Devore, J. L. *Probability and Statistics: For Engineering and the Sciences*; 6th ed.; Thomson, Brooks/Cole: Belmont, CA, 2004.

INTENTIONALLY LEFT BLANK.

Appendix A. Immersion Density Measurements

Table A-1. ITK4-4 immersion density run no. 1.

Specimen	Mass in Air (g)	Immersion Mass (g)	Kerosene Temp. (°C)	Kerosene Density (g/cm ³)	Sample Density (g/cm ³)
1	11.432	2.567	21.7	0.7578	3.3746
2	11.490	2.580	21.8	0.7577	3.3744
3	11.501	2.581	21.9	0.7577	3.3761
4	11.508	2.581	22.0	0.7576	3.3779
5	11.500	2.580	22.0	0.7576	3.3769
6	11.527	2.587	22.0	0.7576	3.3757
7	11.533	2.589	22.0	0.7576	3.3748
8	11.520	2.584	22.1	0.7576	3.3773
9	11.515	2.584	22.2	0.7575	3.3756
10	11.511	2.583	22.2	0.7575	3.3758
11	11.527	2.587	22.2	0.7575	3.3752
12	11.473	2.574	22.2	0.7575	3.3764
13	11.441	2.567	22.2	0.7575	3.3761
14	Sample Does Not Exist				
15	11.469	2.572	22.3	0.7575	3.3776
16	11.440	2.566	22.3	0.7575	3.3769
17	11.427	2.563	22.4	0.7574	3.3768
18	11.391	2.555	22.4	0.7574	3.3767
19	11.353	2.547	22.4	0.7574	3.3760
Average	—	—	—	—	3.3762
Std. Dev.	—	—	—	—	0.0010

Table A-2. ITK4-4 immersion density run no. 2.

Specimen	Mass in Air (g)	Immersion Mass (g)	Kerosene Temp. (°C)	Kerosene Density (g/cm ³)	Sample Density (g/cm ³)
1	11.432	2.564	22.6	0.7573	3.3765
2	11.489	2.577	22.6	0.7573	3.3763
3	11.501	2.579	22.6	0.7573	3.3772
4	11.506	2.593	22.7	0.7573	3.3602
5	11.499	2.579	22.7	0.7573	3.3764
6	11.527	2.585	22.7	0.7573	3.3767
7	11.533	2.587	22.8	0.7572	3.3756
8	11.519	2.583	22.8	0.7572	3.3768
9	11.514	2.582	22.8	0.7572	3.3766
10	11.510	2.582	22.8	0.7572	3.3754
11	11.527	2.585	22.8	0.7572	3.3765
12	11.473	2.573	22.8	0.7572	3.3764
13	11.440	2.565	22.8	0.7572	3.3771
14	Sample Does Not Exist				
15	11.469	2.573	22.8	0.7572	3.3752
16	11.439	2.565	22.8	0.7572	3.3768
17	11.426	2.563	22.8	0.7572	3.3756
18	11.390	2.554	22.8	0.7572	3.3769
19	11.354	2.546	22.8	0.7572	3.3768
Average	—	—	—	—	3.3755
Std. Dev.	—	—	—	—	0.0039

Table A-3. ITK4-4 immersion density run no. 3.

Specimen	Mass in Air (g)	Immersion Mass (g)	Kerosene Temp. (°C)	Kerosene Density (g/cm ³)	Sample Density (g/cm ³)
1	11.433	2.565	22.6	0.7573	3.3755
2	11.490	2.576	22.6	0.7573	3.3779
3	11.500	2.580	22.6	0.7573	3.3756
4	11.505	2.581	22.6	0.7573	3.3757
5	11.499	2.579	22.6	0.7573	3.3766
6	11.527	2.585	22.6	0.7573	3.3769
7	11.534	2.587	22.7	0.7573	3.3762
8	11.519	2.583	22.7	0.7573	3.3770
9	11.514	2.584	22.8	0.7572	3.3740
10	11.510	2.582	22.8	0.7572	3.3754
11	11.527	2.585	22.8	0.7572	3.3765
12	11.475	2.573	22.8	0.7572	3.3769
13	11.440	2.565	22.8	0.7572	3.3771
14	Sample Does Not Exist				
15	11.470	2.572	22.8	0.7572	3.3768
16	11.440	2.565	22.8	0.7572	3.3771
17	11.426	2.558	22.9	0.7572	3.3820
18	11.392	2.555	22.9	0.7572	3.3759
19	11.354	2.546	22.9	0.7572	3.3765
Average	—	—	—	—	3.3767
Std. Dev.	—	—	—	—	0.0016

Table A-4. ITK4-4 immersion density summary.

Specimen	Run 1	Run 2	Run 3	Average (g/cm ³)	Std. Dev.
1	3.3746	3.3765	3.3755	3.3756	0.0010
2	3.3744	3.3763	3.3779	3.3762	0.0017
3	3.3761	3.3772	3.3756	3.3763	0.0008
4	3.3779	3.3602	3.3757	3.3713	0.0097
5	3.3769	3.3764	3.3766	3.3766	0.0003
6	3.3757	3.3767	3.3769	3.3764	0.0007
7	3.3748	3.3756	3.3762	3.3755	0.0007
8	3.3773	3.3768	3.3770	3.3770	0.0003
9	3.3756	3.3766	3.3740	3.3754	0.0013
10	3.3758	3.3754	3.3754	3.3755	0.0002
11	3.3752	3.3765	3.3765	3.3761	0.0007
12	3.3764	3.3764	3.3769	3.3766	0.0003
13	3.3761	3.3771	3.3771	3.3768	0.0006
14	Sample Does Not Exist				
15	3.3776	3.3752	3.3768	3.3765	0.0012
16	3.3769	3.3768	3.3771	3.3770	0.0002
17	3.3768	3.3756	3.3820	3.3782	0.0034
18	3.3767	3.3769	3.3759	3.3765	0.0005
19	3.3760	3.3768	3.3765	3.3764	0.0004
Overall	—	—	—	3.3761	0.0013

Table A-5. ITK4-6 immersion density run no. 1.

Specimen	Initial Mass (g)	Immersion Mass (g)	Kerosene Temp. (°C)	Kerosene Density (g/cm ³)	Sample Density (g/cm ³)
1	10.821	2.429	22.4	0.7574	3.3742
2	10.810	2.425	22.4	0.7574	3.3763
3	10.824	2.428	22.4	0.7574	3.3765
4	10.826	2.430	22.4	0.7574	3.3743
5	10.837	2.435	22.4	0.7574	3.3708
6	10.825	2.429	22.4	0.7574	3.3754
7	10.823	2.429	22.4	0.7574	3.3748
8	10.813	2.426	22.4	0.7574	3.3758
9	10.809	2.425	22.6	0.7573	3.3755
10	10.843	2.433	22.6	0.7573	3.3750
Average	—	—	—	—	3.3749
Std. Dev.	—	—	—	—	0.0016

Table A-6. ITK4-6 immersion density run no. 2.

Specimen	Initial Mass (g)	Immersion Mass (g)	Kerosene Temp. (°C)	Kerosene Density (g/cm ³)	Sample Density (g/cm ³)
1	10.820	2.428	22.6	0.7573	3.3748
2	10.811	2.425	22.6	0.7573	3.3762
3	10.827	2.429	22.6	0.7573	3.3756
4	10.825	2.428	22.6	0.7573	3.3763
5	10.838	2.431	22.6	0.7573	3.3762
6	10.826	2.429	22.6	0.7573	3.3753
7	10.824	2.428	22.6	0.7573	3.3760
8	10.811	2.424	22.8	0.7572	3.3771
9	10.808	2.424	22.8	0.7572	3.3762
10	10.844	2.432	22.8	0.7572	3.3763
Average	—	—	—	—	3.3760
Std. Dev.	—	—	—	—	0.0006

Table A-7. ITK4-6 immersion density run no. 3.

Specimen	Initial Mass (g)	Immersion Mass (g)	Kerosene Temp. (°C)	Kerosene Density (g/cm ³)	Sample Density (g/cm ³)
1	10.820	2.427	22.8	0.7572	3.3757
2	10.810	2.425	22.8	0.7572	3.3754
3	10.826	2.428	22.8	0.7572	3.3762
4	10.826	2.428	22.8	0.7572	3.3762
5	10.837	2.431	23.0	0.7571	3.3750
6	10.825	2.428	23.0	0.7571	3.3755
7	10.824	2.428	23.0	0.7571	3.3751
8	10.811	2.425	23.0	0.7571	3.3753
9	10.808	2.423	23.0	0.7571	3.3771
10	10.843	2.431	23.0	0.7571	3.3769
Average	—	—	—	—	3.3758
Std. Dev.	—	—	—	—	0.0007

Table A-8. ITK4-6 immersion density summary.

Specimen	Run 1	Run 2	Run 3	Average (g/cm ³)	Std. Dev.
1	3.3742	3.3748	3.3757	3.3749	0.0008
2	3.3763	3.3762	3.3754	3.3759	0.0005
3	3.3765	3.3756	3.3762	3.3761	0.0005
4	3.3743	3.3763	3.3762	3.3756	0.0011
5	3.3708	3.3762	3.3750	3.3740	0.0028
6	3.3754	3.3753	3.3755	3.3754	0.0001
7	3.3748	3.3760	3.3751	3.3753	0.0006
8	3.3758	3.3771	3.3753	3.3761	0.0009
9	3.3755	3.3762	3.3771	3.3763	0.0008
10	3.3750	3.3763	3.3769	3.3761	0.0010
Overall	—	—	—	3.3756	0.0007

Table A-9. ITK4-7 immersion density run no. 1.

Specimen	Initial Mass (g)	Immersion Mass (g)	Kerosene Temp. (°C)	Kerosene Density (g/cm ³)	Sample Density (g/cm ³)
1	10.888	2.442	22.6	0.7573	3.3765
2	10.878	2.441	22.4	0.7574	3.3753
3	10.865	2.438	22.8	0.7572	3.3745
4	10.864	2.438	22.7	0.7573	3.3744
5	10.868	2.439	22.7	0.7573	3.3742
6	10.856	2.437	22.6	0.7573	3.3735
7	10.849	2.433	22.6	0.7573	3.3769
8	10.845	2.432	22.6	0.7573	3.3770
9	10.844	2.433	22.6	0.7573	3.3753
10	10.844	2.431	22.6	0.7573	3.3781
Average	—	—	—	—	3.3756
Std. Dev.	—	—	—	—	0.0015

Table A-10. ITK4-7 immersion density run no. 2.

Specimen	Initial Mass (g)	Immersion Mass (g)	Kerosene Temp. (°C)	Kerosene Density (g/cm ³)	Sample Density (g/cm ³)
1	10.888	2.443	22.0	0.7576	3.3765
2	10.877	2.442	22.0	0.7576	3.3745
3	10.864	2.438	22.1	0.7576	3.3757
4	10.863	2.439	22.2	0.7575	3.3738
5	10.869	2.440	22.2	0.7575	3.3743
6	10.856	2.436	22.3	0.7575	3.3756
7	10.850	2.435	22.4	0.7574	3.3749
8	10.845	2.434	22.4	0.7574	3.3747
9	10.841	2.432	22.4	0.7574	3.3762
10	10.845	2.433	22.4	0.7574	3.3761
Average	—	—	—	—	3.3752
Std. Dev.	—	—	—	—	0.0009

Table A-11. ITK4-7 immersion density run no. 3.

Specimen	Initial Mass (g)	Immersion Mass (g)	Kerosene Temp. (°C)	Kerosene Density (g/cm ³)	Sample Density (g/cm ³)
1	10.888	2.445	22.4	0.7574	3.3728
2	10.875	2.440	22.4	0.7574	3.3757
3	10.865	2.438	22.4	0.7574	3.3754
4	10.865	2.438	22.4	0.7574	3.3754
5	10.870	2.440	22.4	0.7574	3.3742
6	10.857	2.436	22.4	0.7574	3.3757
7	10.850	2.433	22.4	0.7574	3.3776
8	10.845	2.433	22.4	0.7574	3.3761
9	10.841	2.432	22.4	0.7574	3.3762
10	10.845	2.432	22.5	0.7574	3.3772
Average	—	—	—	—	3.3756
Std. Dev.	—	—	—	—	0.0014

Table A-12. ITK4-7 immersion density summary.

Specimen	Run 1	Run 2	Run 3	Average (g/cm ³)	Std. Dev.
1	3.3765	3.3765	3.3728	3.3753	0.0021
2	3.3753	3.3745	3.3757	3.3751	0.0006
3	3.3745	3.3757	3.3754	3.3752	0.0006
4	3.3744	3.3738	3.3754	3.3745	0.0008
5	3.3742	3.3743	3.3742	3.3742	0.0001
6	3.3735	3.3756	3.3757	3.3749	0.0012
7	3.3769	3.3749	3.3776	3.3765	0.0014
8	3.3770	3.3747	3.3761	3.3759	0.0012
9	3.3753	3.3762	3.3762	3.3759	0.0005
10	3.3781	3.3761	3.3772	3.3771	0.0010
Overall	—	—	—	3.3755	0.0009

Table A-13. ITK4-8 immersion density run no. 1.

Specimen	Initial Mass (g)	Immersion Mass (g)	Kerosene Temp. (°C)	Kerosene Density (g/cm ³)	Sample Density (g/cm ³)
1	10.909	2.448	22.4	0.7574	3.3752
2	10.893	2.443	22.4	0.7574	3.3771
3	10.897	2.446	22.4	0.7574	3.3742
4	10.895	2.445	22.4	0.7574	3.3750
5	10.899	2.445	22.4	0.7574	3.3762
6	10.902	2.446	22.4	0.7574	3.3758
7	10.903	2.446	22.4	0.7574	3.3761
8	10.896	2.443	22.4	0.7574	3.3781
9	10.892	2.436	22.5	0.7574	3.3863
10	10.886	2.424	22.6	0.7573	3.4010
Average	—	—	—	—	3.3795
Std. Dev.	—	—	—	—	0.0083

Table A-14. ITK4-8 immersion density run no. 2.

Specimen	Initial Mass (g)	Immersion Mass (g)	Kerosene Temp. (°C)	Kerosene Density (g/cm ³)	Sample Density (g/cm ³)
1	10.909	2.448	22.4	0.7574	3.3752
2	10.893	2.443	22.5	0.7574	3.3769
3	10.896	2.446	22.6	0.7573	3.3735
4	10.894	2.445	22.6	0.7573	3.3742
5	10.899	2.445	22.6	0.7573	3.3758
6	10.902	2.447	22.6	0.7573	3.3740
7	10.904	2.447	22.6	0.7573	3.3746
8	10.896	2.444	22.6	0.7573	3.3762
9	10.891	2.444	22.6	0.7573	3.3747
10	10.886	2.443	22.6	0.7573	3.3745
Average	—	—	—	—	3.3750
Std. Dev.	—	—	—	—	0.0011

Table A-15. ITK4-8 immersion density run no. 3.

Specimen	Initial Mass (g)	Immersion Mass (g)	Kerosene Temp. (°C)	Kerosene Density (g/cm ³)	Sample Density (g/cm ³)
1	10.909	2.448	22.6	0.7573	3.3747
2	10.893	2.443	22.6	0.7573	3.3767
3	10.898	2.446	22.6	0.7573	3.3741
4	10.894	2.444	22.6	0.7573	3.3756
5	10.898	2.445	22.6	0.7573	3.3755
6	10.902	2.447	22.6	0.7573	3.3740
7	10.903	2.447	22.6	0.7573	3.3743
8	10.897	2.444	22.6	0.7573	3.3766
9	10.891	2.444	22.6	0.7573	3.3747
10	10.887	2.444	22.6	0.7573	3.3735
Average	—	—	—	—	3.3750
Std. Dev.	—	—	—	—	0.0011

Table A-16. ITK4-8 immersion density summary.

Specimen	Run 1	Run 2	Run 3	Average (g/cm ³)	Std. Dev.
1	3.3752	3.3752	3.3747	3.3750	0.0003
2	3.3771	3.3769	3.3767	3.3769	0.0002
3	3.3742	3.3735	3.3741	3.3739	0.0004
4	3.3750	3.3742	3.3756	3.3750	0.0007
5	3.3762	3.3758	3.3755	3.3758	0.0004
6	3.3758	3.3740	3.3740	3.3746	0.0011
7	3.3761	3.3746	3.3743	3.3750	0.0010
8	3.3781	3.3762	3.3766	3.3770	0.0010
9	3.3863	3.3747	3.3747	3.3786	0.0067
10	3.4010	3.3745	3.3735	3.3830	0.0156
Overall	—	—	—	3.3765	0.0027

Table A-17. ITK4-14 immersion density run no. 1.

Specimen	Initial Mass (g)	Immersion Mass (g)	Kerosene Temp. (°C)	Kerosene Density (g/cm ³)	Sample Density (g/cm ³)
1	11.292	2.533	22.6	0.7573	3.3760
2	11.353	2.546	22.6	0.7573	3.3769
3	Sample Does Not Exist				
4	11.406	2.557	22.6	0.7573	3.3781
5	11.418	2.561	22.6	0.7573	3.3764
6	11.446	2.567	22.7	0.7573	3.3765
7	11.467	2.571	22.7	0.7573	3.3774
8	11.473	2.573	22.7	0.7573	3.3766
9	11.493	2.578	22.8	0.7572	3.3757
10	11.493	2.577	22.8	0.7572	3.3770
11	11.497	2.579	22.8	0.7572	3.3755
12	11.500	2.579	22.8	0.7572	3.3764
13	11.513	2.582	22.8	0.7572	3.3763
14	11.501	2.580	22.8	0.7572	3.3754
15	11.464	2.571	22.8	0.7572	3.3763
16	11.474	2.573	22.8	0.7572	3.3766
17	11.452	2.568	22.8	0.7572	3.3767
18	11.455	2.569	22.8	0.7572	3.3763
19	11.379	2.552	22.8	0.7572	3.3762
20	11.319	2.538	22.8	0.7572	3.3770
Average	—	—	—	—	3.3765
Std. Dev.	—	—	—	—	0.0006

Table A-18. ITK4-14 immersion density run no. 2.

Specimen	Initial Mass (g)	Immersion Mass (g)	Kerosene Temp. (°C)	Kerosene Density (g/cm ³)	Sample Density (g/cm ³)
1	11.292	2.534	22.8	0.7572	3.3742
2	11.353	2.546	22.8	0.7572	3.3765
3	Sample Does Not Exist				
4	11.406	2.558	22.8	0.7572	3.3763
5	11.417	2.560	22.8	0.7572	3.3769
6	11.446	2.567	22.8	0.7572	3.3763
7	11.467	2.571	22.8	0.7572	3.3772
8	11.474	2.573	22.8	0.7572	3.3766
9	11.494	2.578	22.8	0.7572	3.3760
10	11.491	2.577	22.8	0.7572	3.3764
11	11.497	2.577	22.8	0.7572	3.3782
12	11.500	2.579	22.8	0.7572	3.3764
13	11.513	2.581	22.8	0.7572	3.3776
14	11.503	2.580	22.8	0.7572	3.3760
15	11.464	2.570	22.8	0.7572	3.3776
16	11.474	2.572	22.8	0.7572	3.3780
17	11.451	2.567	22.8	0.7572	3.3778
18	11.455	2.569	22.8	0.7572	3.3763
19	11.380	2.551	22.8	0.7572	3.3779
20	11.318	2.539	22.8	0.7572	3.3753
Average	—	—	—	—	3.3767
Std. Dev.	—	—	—	—	0.0010

Table A-19. ITK4-14 immersion density run no. 3.

Specimen	Initial Mass (g)	Immersion Mass (g)	Kerosene Temp. (°C)	Kerosene Density (g/cm ³)	Sample Density (g/cm ³)
1	11.291	2.534	23.0	0.7571	3.3735
2	11.353	2.547	23.0	0.7571	3.3747
3	Sample Does Not Exist				
4	11.406	2.557	23.0	0.7571	3.3772
5	11.418	2.560	23.0	0.7571	3.3768
6	11.446	2.568	23.0	0.7571	3.3745
7	11.467	2.570	23.0	0.7571	3.3781
8	11.472	2.572	22.9	0.7572	3.3771
9	11.494	2.579	22.9	0.7572	3.3744
10	11.490	2.576	22.9	0.7572	3.3772
11	11.496	2.578	22.9	0.7572	3.3763
12	11.500	2.580	23.0	0.7571	3.3747
13	11.512	2.580	23.0	0.7571	3.3782
14	11.502	2.580	23.0	0.7571	3.3753
15	11.464	2.571	23.0	0.7571	3.3759
16	11.474	2.573	23.0	0.7571	3.3762
17	11.450	2.567	23.0	0.7571	3.3770
18	11.454	2.568	23.0	0.7571	3.3769
19	11.379	2.551	23.0	0.7571	3.3771
20	11.319	2.538	23.0	0.7571	3.3765
Average	—	—	—	—	3.3762
Std. Dev.	—	—	—	—	0.0013

Table A-20. ITK4-14 immersion density summary.

Specimen	Run 1	Run 2	Run 3	Average (g/cm ³)	Std. Dev.
1	3.3760	3.3742	3.3735	3.3746	0.0013
2	3.3769	3.3765	3.3747	3.3760	0.0012
3	Sample Does Not Exist				
4	3.3781	3.3763	3.3772	3.3772	0.0009
5	3.3764	3.3769	3.3768	3.3767	0.0003
6	3.3765	3.3763	3.3745	3.3758	0.0011
7	3.3774	3.3772	3.3781	3.3776	0.0005
8	3.3766	3.3766	3.3771	3.3768	0.0003
9	3.3757	3.3760	3.3744	3.3754	0.0008
10	3.3770	3.3764	3.3772	3.3769	0.0004
11	3.3755	3.3782	3.3763	3.3767	0.0013
12	3.3764	3.3764	3.3747	3.3758	0.0010
13	3.3763	3.3776	3.3782	3.3774	0.0010
14	3.3754	3.3760	3.3753	3.3756	0.0004
15	3.3763	3.3776	3.3759	3.3766	0.0009
16	3.3766	3.3780	3.3762	3.3769	0.0009
17	3.3767	3.3778	3.3770	3.3772	0.0005
18	3.3763	3.3763	3.3769	3.3765	0.0003
19	3.3762	3.3779	3.3771	3.3771	0.0008
20	3.3770	3.3753	3.3765	3.3763	0.0008
Overall	—	—	—	3.3765	0.0008

INTENTIONALLY LEFT BLANK.

Appendix B. Roundness Measurements

B.1 ITK4-4 Roundness Measurements

Table B-1. Arbitrary measurements: made at a randomly chosen diameter and the diameter perpendicular to it.

Specimen	O. D. 1 (mm)	O. D. 2 (mm)	I. D. 1 (mm)	I. D. 2 (mm)
1	33.98	33.75	24.46	24.40
2	33.98	33.85	24.47	24.40
3	33.96	33.97	24.40	24.45
4	33.98	33.96	24.40	24.35
5	33.91	33.96	24.42	24.42
6	33.88	33.99	24.43	24.44
7	33.92	33.98	24.40	24.46
8	33.90	33.97	24.39	24.47
9	33.89	33.96	24.40	24.42
10	33.89	33.98	24.39	24.46
11	33.93	33.92	24.41	24.41
12	33.86	33.91	24.40	24.43
13	33.85	33.91	24.39	24.47
15	33.83	33.88	24.41	24.41
16	33.83	33.85	24.42	24.45
17	33.82	33.87	24.39	24.43
18	33.84	33.80	24.40	24.41
19	33.74	33.79	24.41	24.42

Table B-2. Specific measurements: made based on orientation for strength testing.

Specimen	0°		45°		90°		135°	
	O. D.	I. D.	O. D.	I. D.	O. D.	I. D.	O. D.	I. D.
1	33.75	24.48	33.88	24.47	33.87	24.47	33.73	24.42
2	33.85	24.54	33.83	24.44	33.94	24.49	33.95	24.54
3	33.92	24.61	33.93	24.53	33.85	24.46	33.88	24.48
4	33.83	24.52	33.89	24.49	33.93	24.53	33.86	24.49
5	33.83	24.51	33.93	24.50	33.92	24.51	33.84	24.45
6	33.94	24.57	33.91	24.51	33.85	24.45	33.89	24.50
7	33.89	24.54	33.87	24.47	33.94	24.53	33.95	24.55
8	33.84	24.51	33.89	24.49	33.92	24.50	33.84	24.46
9	33.94	24.59	33.91	24.50	33.79	24.44	33.90	24.49
10	33.83	24.52	33.89	24.47	33.94	24.53	33.93	24.50
11	33.92	24.60	33.86	24.47	33.84	24.45	33.92	24.51
12	33.84	24.51	33.89	24.51	33.89	24.51	33.84	24.47
13	33.88	24.58	33.89	24.50	33.84	24.45	33.82	24.42
15	33.84	24.55	33.89	24.46	33.85	24.47	33.88	24.52
16	33.80	24.54	33.80	24.45	33.82	24.49	33.82	24.50
17	33.84	24.58	33.78	24.46	33.75	24.45	33.79	24.47
18	33.75	24.50	33.72	24.44	33.79	24.48	33.78	24.48
19	33.74	24.48	33.73	24.44	33.74	24.46	33.70	24.42

B.2 ITK4-6 Roundness Measurements

Table B-3. Arbitrary measurements: made at a randomly chosen diameter and the diameter perpendicular to it.

Specimen	O. D. 1 (mm)	O. D. 2 (mm)	I. D. 1 (mm)	I. D. 2 (mm)
1	33.03	33.02	23.93	23.92
2	33.05	33.05	23.91	23.93
3	33.03	33.02	23.92	23.94
4	33.05	33.03	23.93	23.93
5	33.03	33.03	23.90	23.91
6	33.04	33.03	23.91	23.93
7	33.05	33.02	23.91	23.93
8	33.04	33.02	23.93	23.90
9	33.04	33.03	23.93	23.90
10	33.04	33.03	23.93	23.92

Table B-4. Specific measurements: made based on orientation for strength testing.

	0°	
Specimen	O. D.	I. D.
1	33.05	24.03
2	33.03	24.04
3	33.04	24.04
4	33.04	24.05
5	33.05	24.05
6	33.04	24.05
7	33.04	24.05
8	33.04	24.06
9	33.04	24.03
10	33.04	24.05

B.3 ITK4-7 Roundness Measurements

Table B-5. Arbitrary measurements: made at a randomly chosen diameter and the diameter perpendicular to it.

Specimen	O. D. 1 (mm)	O. D. 2 (mm)	I. D. 1 (mm)	I. D. 2 (mm)
1	33.03	33.02	23.87	23.85
2	33.04	33.04	23.87	23.88
3	33.04	33.05	23.89	23.89
4	33.04	33.03	23.88	23.91
5	33.05	33.04	23.88	23.90
6	33.04	33.03	23.88	23.91
7	33.03	33.04	23.92	23.90
8	33.03	33.05	23.92	23.91
9	33.05	33.04	23.90	23.92
10	33.04	33.04	23.92	23.93

Table B-6. Specific measurements: made based on orientation for strength testing.

Specimen	0°	
	O. D.	I. D.
1	33.03	24.03
2	33.04	24.00
3	33.04	24.00
4	33.04	24.00
5	33.04	24.04
6	33.04	24.03
7	33.05	24.05
8	33.04	24.05
9	33.04	24.05
10	33.04	24.05

B.4 ITK4-8 Roundness Measurements

Table B-7. Arbitrary measurements: made at a randomly chosen diameter and the diameter perpendicular to it.

Specimen	O. D. 1 (mm)	O. D. 2 (mm)	I. D. 1 (mm)	I. D. 2 (mm)
1	33.05	33.05	23.84	23.84
2	33.06	33.04	23.83	23.86
3	33.04	33.03	23.85	23.86
4	33.03	33.04	23.84	23.86
5	33.05	33.03	23.85	23.86
6	33.05	33.03	23.86	23.87
7	33.04	33.03	23.85	23.85
8	33.03	33.02	23.85	23.85
9	33.05	33.04	23.87	23.86
10	33.04	33.03	23.87	23.85

Table B-8. Specific measurements: made based on orientation for strength testing.

Specimen	0°		45°		90°		135°	
	O. D.	I. D.	O. D.	I. D.	O. D.	I. D.	O. D.	I. D.
1	33.03	24.01	33.02	23.88	33.03	23.89	33.02	23.88
2	33.02	24.00	33.01	23.88	33.01	23.88	33.01	23.88
3	33.04	24.00	33.02	23.90	33.00	23.89	33.01	23.90
4	33.03	23.97	33.03	23.87	33.02	23.89	33.01	23.87
5	33.04	23.98	33.01	23.87	33.02	23.86	33.00	23.88
6	33.04	23.98	33.02	23.90	33.03	23.88	33.02	23.90
7	33.04	23.98	33.03	23.88	33.01	23.89	33.02	23.90
8	33.04	24.00	33.02	23.91	33.03	23.89	33.02	23.90
9	33.03	24.01	33.02	23.91	33.04	23.91	33.02	23.91
10	33.04	24.00	33.02	23.88	33.03	23.90	33.03	23.90

B.5 ITK4-14 Roundness Measurements

Table B-9. Arbitrary measurements: made at a randomly chosen diameter and the diameter perpendicular to it.

Specimen	O. D. 1 (mm)	O. D. 2 (mm)	I. D. 1 (mm)	I. D. 2 (mm)
1	33.64	33.68	24.38	24.38
2	33.74	33.76	24.40	24.42
4	33.80	33.80	24.43	24.42
5	33.81	33.84	24.43	24.44
6	33.84	33.86	24.43	24.40
7	33.85	33.86	24.44	24.44
8	33.86	33.88	24.42	24.44
9	33.86	33.88	24.42	24.44
10	33.89	33.88	24.44	24.44
11	33.89	33.91	24.44	24.45
12	33.89	33.91	24.43	24.45
13	33.92	33.89	24.43	24.41
14	33.93	33.84	24.44	24.41
15	33.87	33.91	24.44	24.44
16	33.85	33.91	24.42	24.48
17	33.92	33.85	24.41	24.42
18	33.80	33.91	24.43	24.46
19	33.79	33.90	24.46	24.46
20	33.80	33.72	24.44	24.44

Table B-10. Specific measurements: made based on orientation for strength testing.

Specimen	0°		45°		90°		135°	
	O. D.	I. D.	O. D.	I. D.	O. D.	I. D.	O. D.	I. D.
1	33.70	24.49	33.70	24.46	33.70	24.46	33.66	24.43
2	33.75	24.53	33.74	24.48	33.74	24.49	33.75	24.51
4	33.80	24.54	33.80	24.51	33.80	24.51	33.76	24.49
5	33.80	24.54	33.82	24.52	33.80	24.51	33.79	24.51
6	33.85	24.54	33.84	24.52	33.82	24.51	33.80	24.51
7	33.84	24.53	33.83	24.48	33.85	24.52	33.84	24.51
8	33.85	24.51	33.85	24.51	33.85	24.52	33.85	24.52
9	33.85	24.49	33.85	24.51	33.85	24.51	33.85	24.52
10	33.90	24.55	33.88	24.52	33.87	24.52	33.88	24.53
11	33.89	24.52	33.88	24.53	33.87	24.52	33.87	24.51
12	33.85	24.50	33.89	24.52	33.89	24.53	33.89	24.52
13	33.90	24.55	33.85	24.48	33.87	24.52	33.90	24.53
14	33.83	24.50	33.88	24.48	33.90	24.56	33.87	24.52
15	33.82	24.49	33.76	24.48	33.90	24.54	33.90	24.53
16	33.88	24.54	33.80	24.48	33.83	24.51	33.90	24.54
17	33.90	24.57	33.89	24.51	33.82	24.48	33.79	24.48
18	33.87	24.54	33.88	24.54	33.79	24.49	33.79	24.49
19	33.80	24.50	33.88	24.53	33.80	24.51	33.76	24.48
20	33.80	24.55	33.70	24.51	33.73	24.48	33.80	24.46

Appendix C. Diametral Compression Results

Table C-1. ITK4-4 diametral compression results.

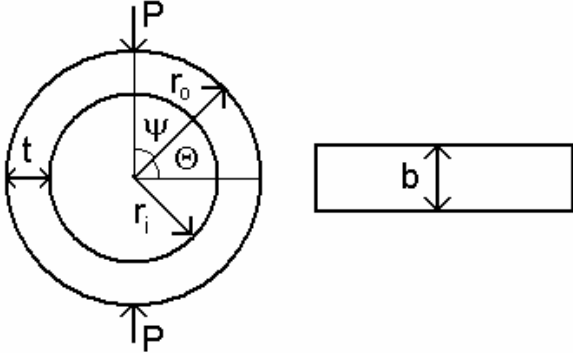
Sample	Max Load (N)	$r_a = (r_o + r_i)/2$ (mm)	b (mm)	t (mm)	$y = r_a - r$ (mm)	I (mm)	Ψ (°)	Stress (MPa)
1	2856	14.56	7.92	4.64	2.32	65.72	0	466.96
2	2589	14.60	7.92	4.66	2.33	66.57	0	420.83
3	2820	14.63	7.92	4.66	2.33	66.57	0	459.48
4	2950	14.59	7.92	4.66	2.33	66.57	0	479.18
5	2706	14.59	7.92	4.66	2.33	66.75	30	76.03
6	2467	14.63	7.92	4.69	2.34	67.87	0	396.69
7	2446	14.61	7.92	4.68	2.34	67.44	0	394.46
8	3000	14.59	7.92	4.67	2.33	66.96	0	485.52
9	2631	14.63	7.92	4.68	2.34	67.44	0	425.02
10	2779	14.59	7.92	4.66	2.33	66.53	0	451.69
11	2552	14.63	7.92	4.66	2.33	66.79	0	414.85
12	2517	14.59	7.91	4.67	2.33	66.92	0	407.61
13	2611	14.62	7.89	4.65	2.33	66.11	0	427.45
14	Does Not Exist							
15	2761	14.60	7.92	4.65	2.32	66.15	0	450.72
16	2472	14.59	7.92	4.63	2.32	65.51	0	405.82
17	2183	14.61	7.92	4.63	2.32	65.51	0	358.86
18	2381	14.56	7.92	4.63	2.31	65.29	0	391.12
19	2232	14.56	7.92	4.63	2.32	65.51	0	365.66
Average	—	—	—	—	—	—	—	424.49
Std. Dev.	—	—	—	—	—	—	—	36.53
Average Strength (MPa)	Std. Dev. (MPa)	Characteristic Strength (MPa)	Lower Bound (MPa)	Upper Bound (MPa)	Weibull Modulus	Lower Bound	Upper Bound	
424.49	36.53	440.01	426.33	455.91	12.29	8.95	17.02	
								

Table C-2. ITK4-6 diametral compression results.

Sample	Max Load (N)	$r_a = (r_o+r_i)/2$ (mm)	b (mm)	t (mm)	$y = r_a-r$ (mm)	I (mm)	Ψ (°)	Stress (MPa)
1	4319	14.27	7.92	4.51	2.26	60.51	0	731.58
2	4509	14.27	7.91	4.50	2.25	59.87	0	769.22
3	4489	14.27	7.94	4.50	2.25	60.29	0	761.36
4	4270	14.27	7.93	4.50	2.25	60.02	0	726.87
5	4247	14.28	7.93	4.50	2.25	60.22	0	721.47
6	4227	14.27	7.93	4.50	2.25	59.98	0	720.00
7	4274	14.27	7.93	4.50	2.25	59.98	0	728.01
8	4141	14.28	7.92	4.49	2.25	59.74	0	707.50
9	4379	14.27	7.93	4.51	2.25	60.38	0	742.33
10	4098	14.27	7.92	4.50	2.25	59.94	0	698.47
Average	—	—	—	—	—	—	—	730.68
Std. Dev.	—	—	—	—	—	—	—	22.01

Average Strength (MPa)	Std. Dev. (MPa)	Characteristic Strength (MPa)	Lower Bound (MPa)	Upper Bound (MPa)	Weibull Modulus	Lower Bound	Upper Bound
730.68	22.01	738.69	727.69	755.46	29.80	19.17	47.19

The diagram illustrates a thick-walled cylinder under diametral compression. The cylinder has an outer radius r_o , an inner radius r_i , and a thickness t . Vertical loads P are applied at the top and bottom. A horizontal line through the center shows the angle ψ between the vertical load direction and the radius. The angle θ is also indicated. To the right, a rectangular cross-section of width b is shown.

Table C-3. ITK4-7 diametral compression results.

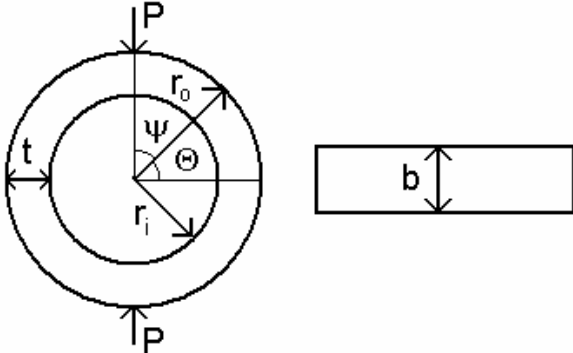
Sample	Max Load (N)	$r_a = (r_o + r_i)/2$ (mm)	b (mm)	t (mm)	$y = r_a - r$ (mm)	I (mm)	Ψ (°)	Stress (MPa)
1	3258	14.27	7.93	4.50	2.25	60.22	0	553.08
2	3905	14.26	7.93	4.52	2.26	60.99	0	657.24
3	3917	14.26	7.92	4.52	2.26	60.95	0	659.68
4	3338	14.26	7.92	4.52	2.26	60.95	0	562.17
5	3691	14.27	7.93	4.50	2.25	60.22	0	626.80
6	3597	14.27	7.93	4.51	2.25	60.38	0	609.76
7	4407	14.28	7.93	4.50	2.25	60.22	0	748.66
8	3816	14.27	7.92	4.50	2.25	59.94	0	650.41
9	3604	14.27	7.93	4.50	2.25	59.98	0	613.89
10	3360	14.27	7.93	4.50	2.25	59.98	0	572.32
Average	—	—	—	—	—	—	—	625.40
Std. Dev.	—	—	—	—	—	—	—	58.15
Average Strength (MPa)	Std. Dev. (MPa)	Characteristic Strength (MPa)	Lower Bound (MPa)	Upper Bound (MPa)	Weibull Modulus	Lower Bound	Upper Bound	
625.40	58.15	649.54	614.40	692.79	9.29	5.98	14.72	
								

Table C-4. ITK4-8 diametral compression results.

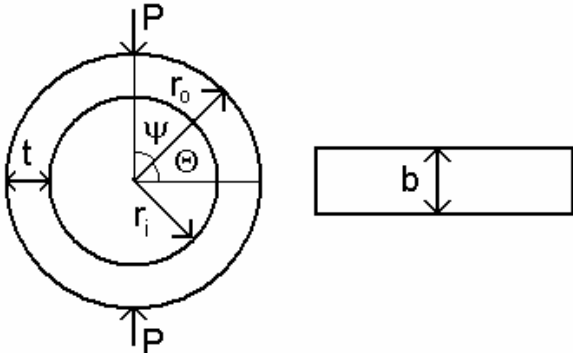
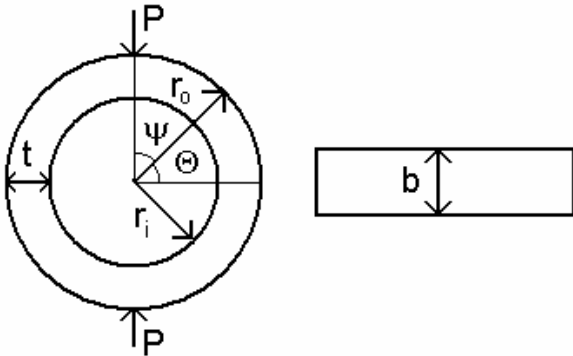
Sample	Max Load (N)	$r_a = (r_o + r_i)/2$ (mm)	b (mm)	t (mm)	$y = r_a - r$ (mm)	I (mm)	Ψ (°)	Stress (MPa)
1	4613	14.26	7.90	4.51	2.26	60.39	0	782.32
2	4114	14.26	7.89	4.51	2.26	60.32	0	698.33
3	4019	14.26	7.92	4.52	2.26	60.95	0	676.86
4	4262	14.25	7.92	4.53	2.27	61.35	0	714.11
5	4412	14.26	7.92	4.53	2.27	61.35	0	739.51
6	4569	14.26	7.92	4.53	2.27	61.35	0	765.82
7	4232	14.26	7.92	4.53	2.27	61.35	0	709.34
8	4396	14.26	7.92	4.52	2.26	60.95	0	740.35
9	4411	14.26	7.92	4.51	2.26	60.54	0	746.17
10	4635	14.26	7.92	4.52	2.26	60.95	0	780.60
Average	—	—	—	—	—	—	—	735.34
Std. Dev.	—	—	—	—	—	—	—	35.37
Average Strength (MPa)	Std. Dev. (MPa)	Characteristic Strength (MPa)	Lower Bound (MPa)	Upper Bound (MPa)	Weibull Modulus	Lower Bound	Upper Bound	
735.34	35.37	748.65	732.33	771.23	21.56	13.87	34.14	
								

Table C-5. ITK4-14 diametral compression results.

Sample	Max Load (N)	$r_a = (r_o + r_i)/2$ (mm)	b (mm)	t (mm)	$y = r_a - r$ (mm)	I (mm)	Ψ (°)	Stress (MPa)
1	2070	14.55	7.92	4.61	2.30	64.45	0	342.64
2	1980	14.57	7.92	4.61	2.31	64.66	0	327.54
3	Does Not Exist							
4	2490	14.59	7.92	4.63	2.32	65.51	0	408.77
5	2349	14.59	7.92	4.63	2.32	65.51	0	385.62
6	2587	14.60	7.92	4.66	2.33	66.57	0	420.51
7	2572	14.59	7.92	4.66	2.33	66.57	0	417.92
8	2975	14.59	7.92	4.67	2.34	67.22	0	480.22
9	2632	14.59	7.92	4.68	2.34	67.65	0	422.90
10	2922	14.61	7.92	4.68	2.34	67.44	0	471.39
11	NO DATA	14.60	7.92	4.69	2.34	67.87	NO DATA	
12	3026	14.59	7.92	4.68	2.34	67.39	0	487.64
13	2306	14.61	7.92	4.68	2.34	67.44	0	372.01
14	2187	14.58	7.92	4.67	2.33	67.00	0	353.60
15	2973	14.58	7.92	4.67	2.33	66.96	0	480.82
16	2658	14.61	7.92	4.67	2.34	67.22	0	429.50
17	2936	14.62	7.92	4.67	2.33	66.96	0	476.14
18	3008	14.60	7.92	4.67	2.33	67.00	0	487.01
19	2976	14.58	7.89	4.65	2.33	66.11	0	485.87
20	2595	14.59	7.91	4.63	2.31	65.21	0	427.54
Average	—	—	—	—	—	—	—	426.54
Std. Dev.	—	—	—	—	—	—	—	53.40
Average Strength (MPa)	Std. Dev. (MPa)	Characteristic Strength (MPa)	Lower Bound (MPa)	Upper Bound (MPa)	Weibull Modulus	Lower Bound	Upper Bound	
426.54	53.4	448.18	429.76	469.26	9.38	6.83	12.98	
								

Appendix D. Fractography

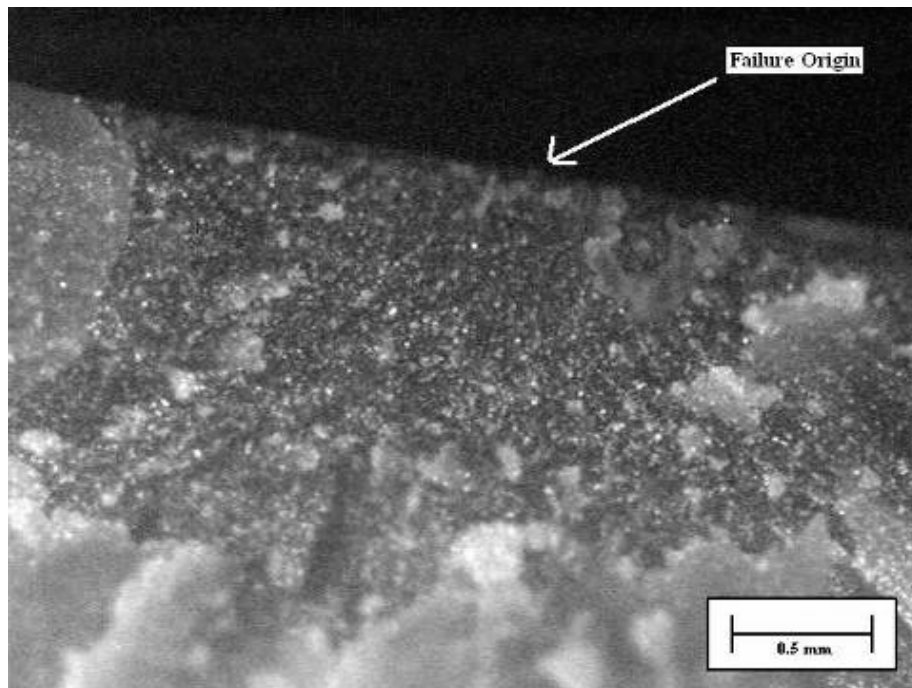


Figure D-1. ITK4-4 specimen 1.

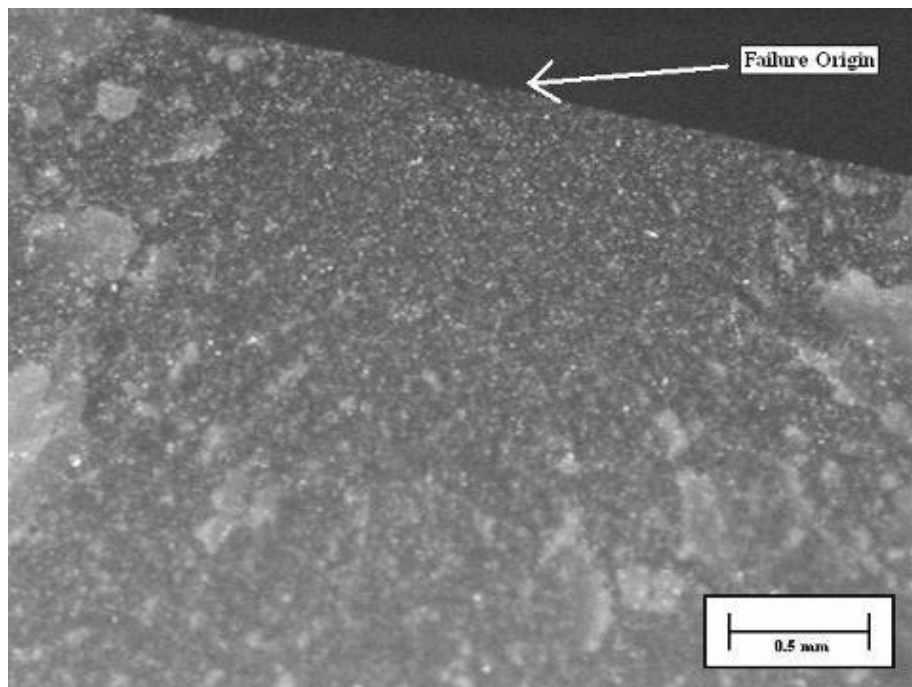


Figure D-2. ITK4-4 specimen 2.

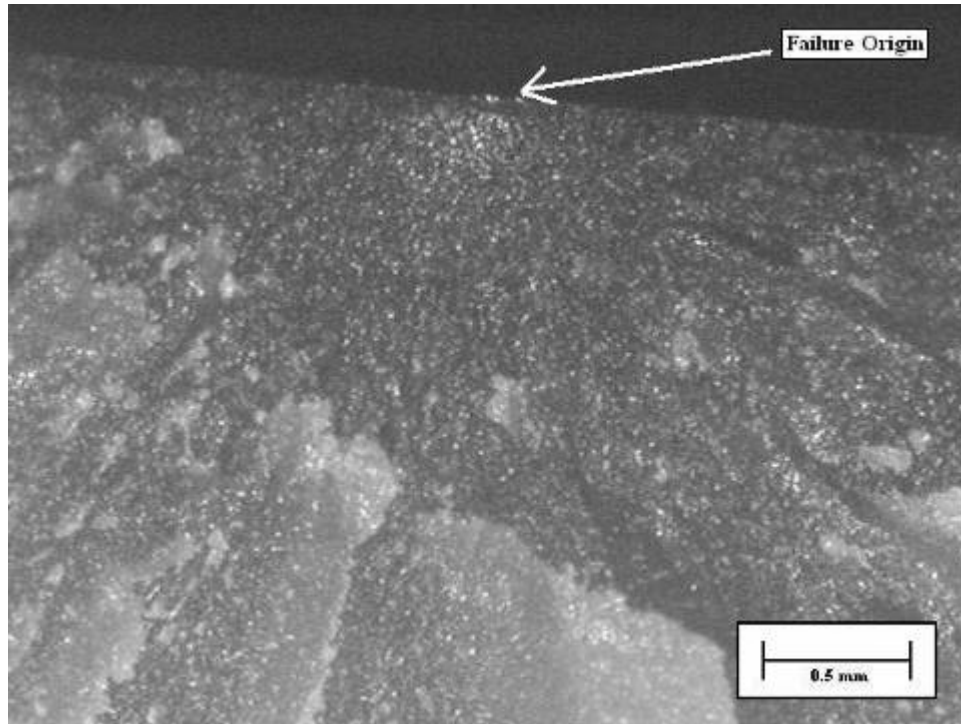


Figure D-3. ITK4-4 specimen 3.

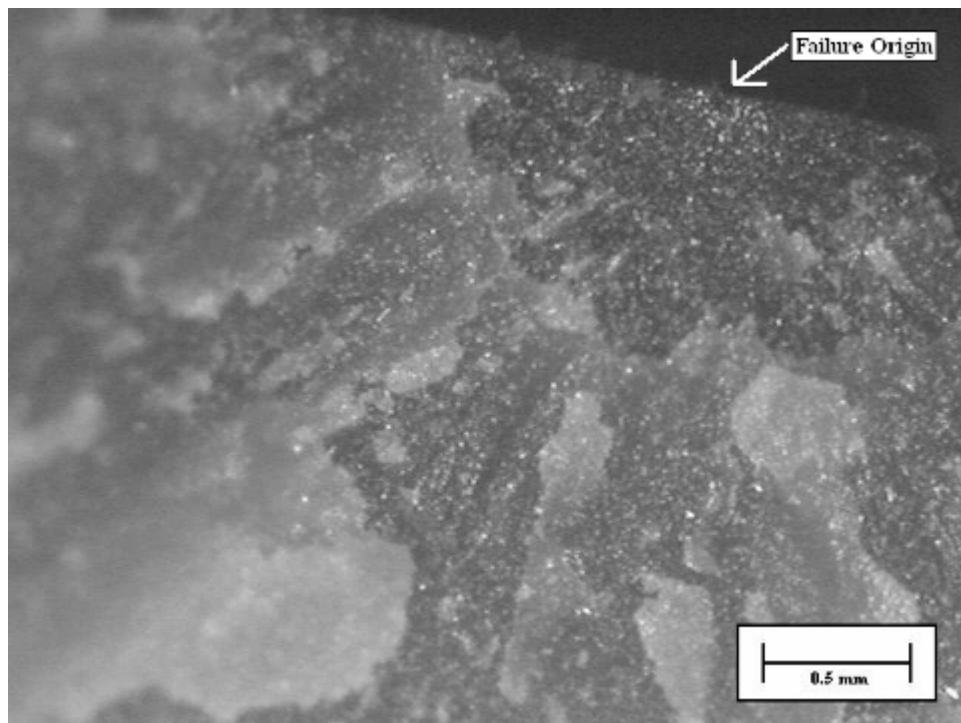


Figure D-4. ITK4-4 specimen 4.

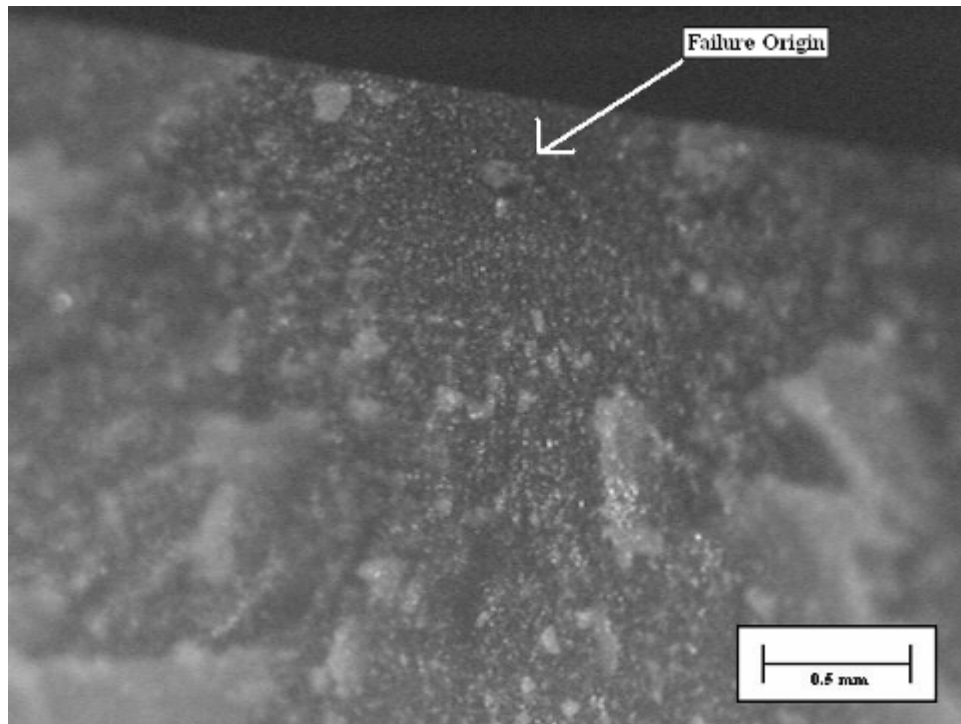


Figure D-5. ITK4-4 specimen 5.

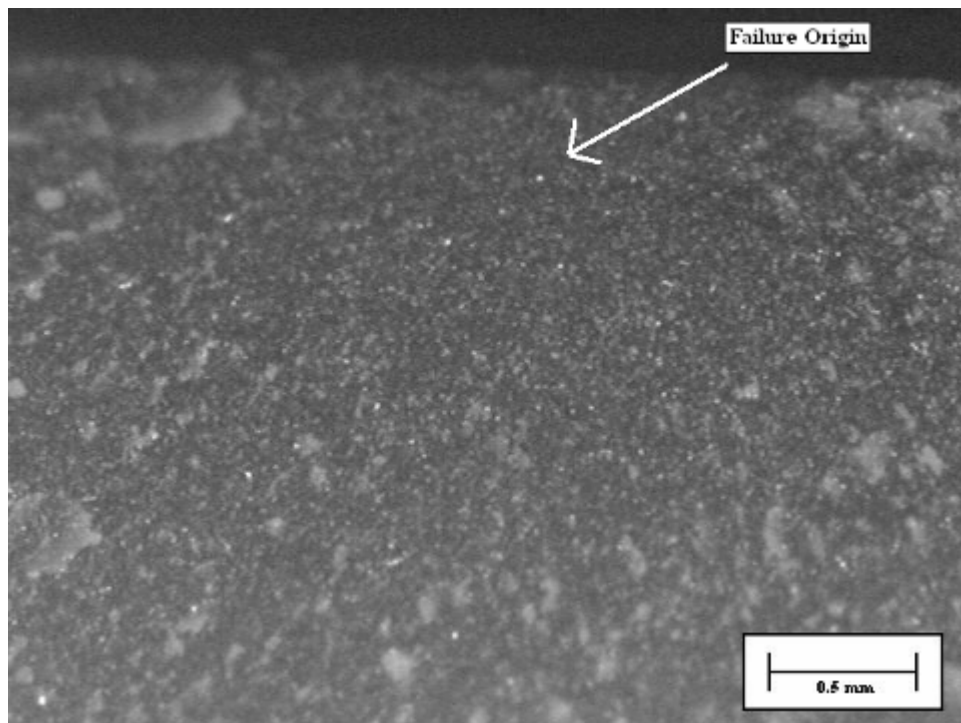


Figure D-6. ITK4-4 specimen 6.

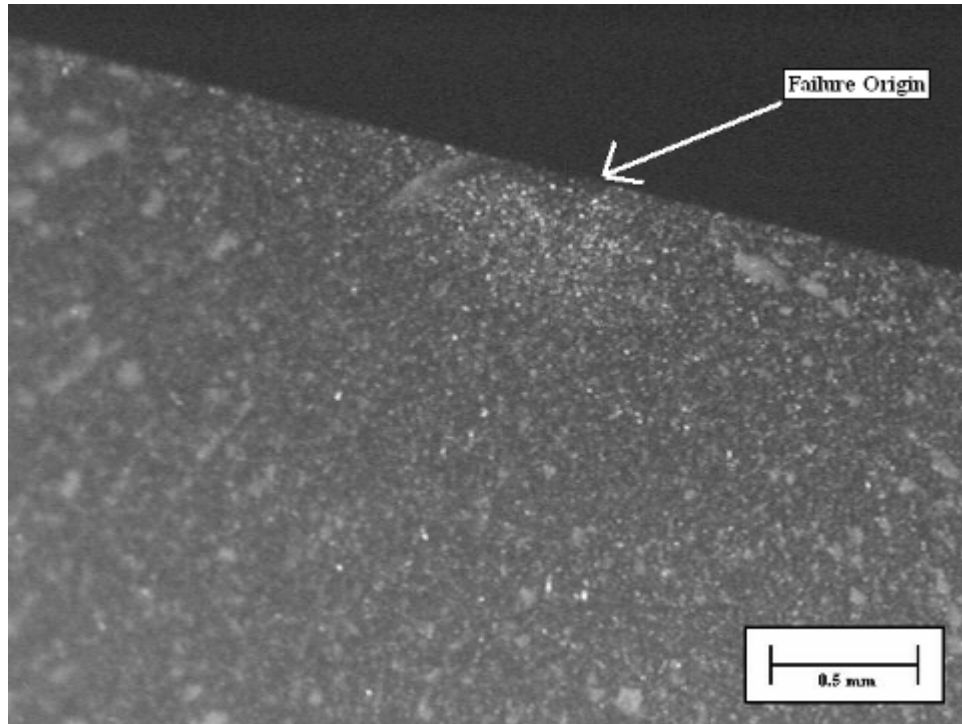


Figure D-7. ITK4-4 specimen 7.

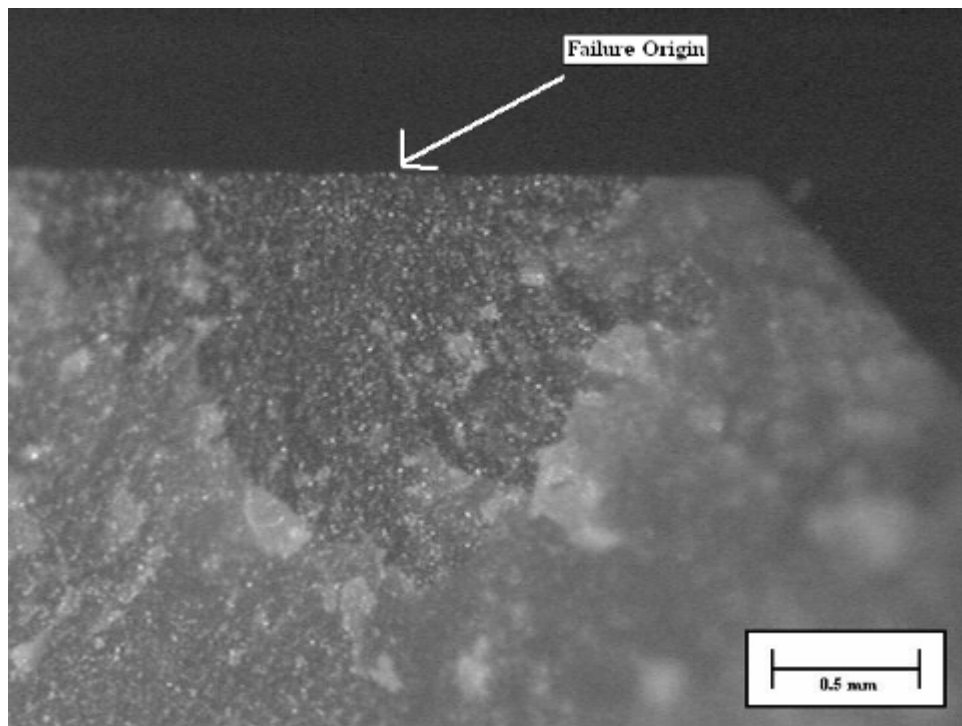


Figure D-8. ITK4-4 specimen 8.

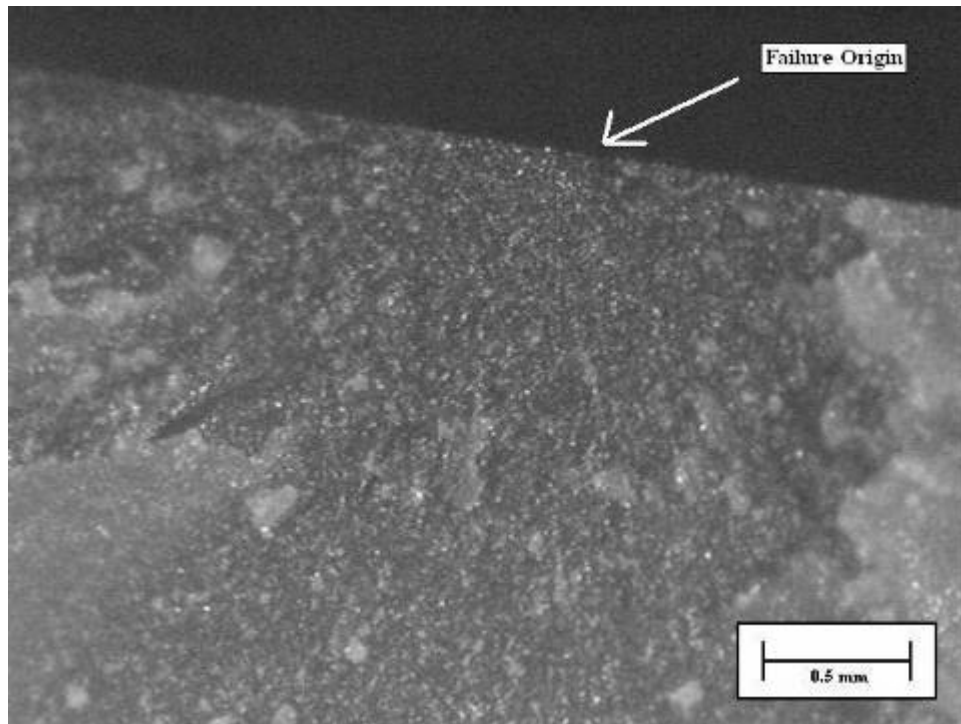


Figure D-9. ITK4-4 specimen 9.

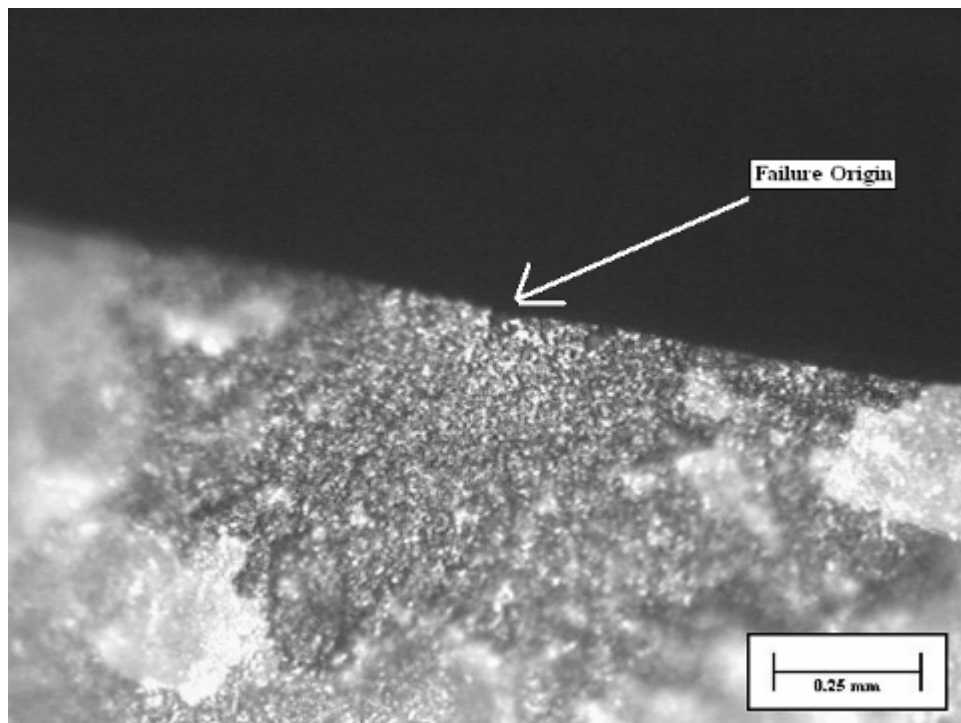


Figure D-10. ITK4-4 specimen 10.

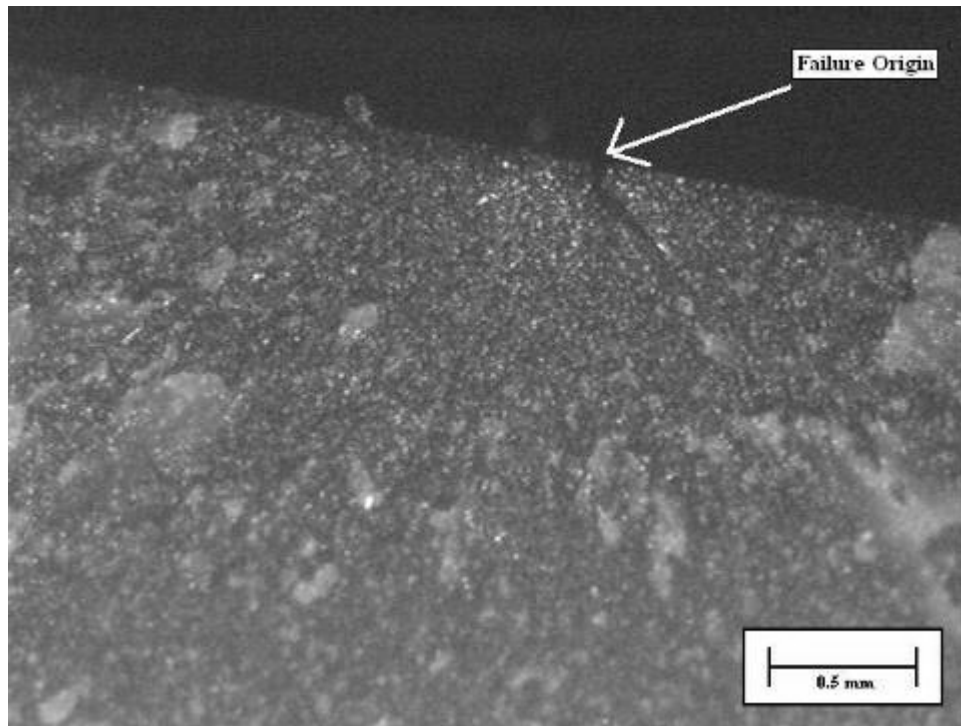


Figure D-11. ITK4-4 specimen 11.

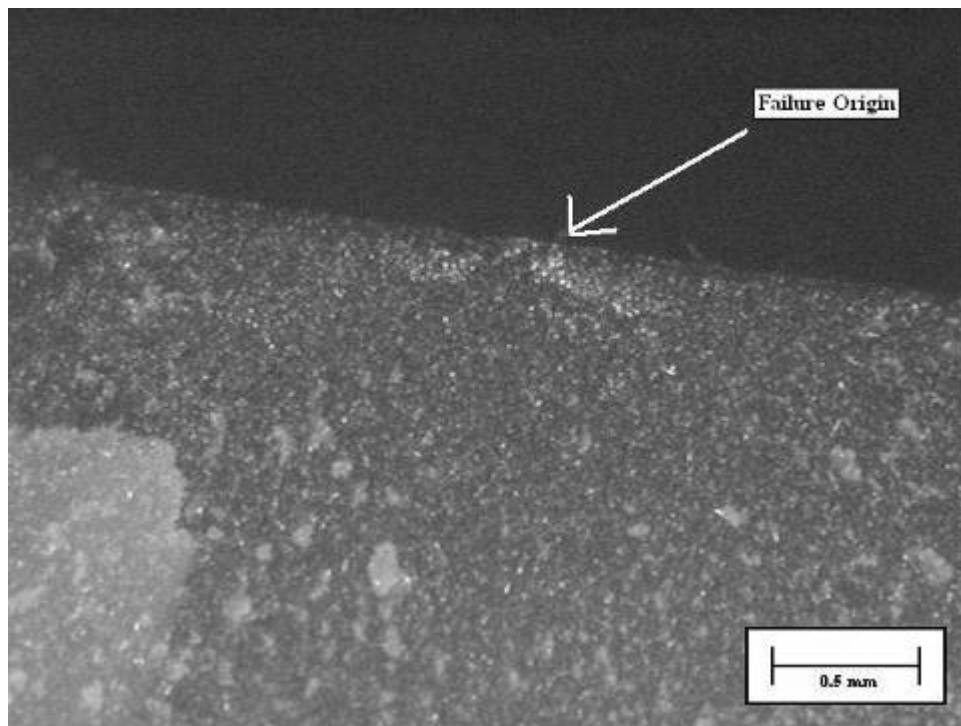


Figure D-12. ITK4-4 specimen 12.

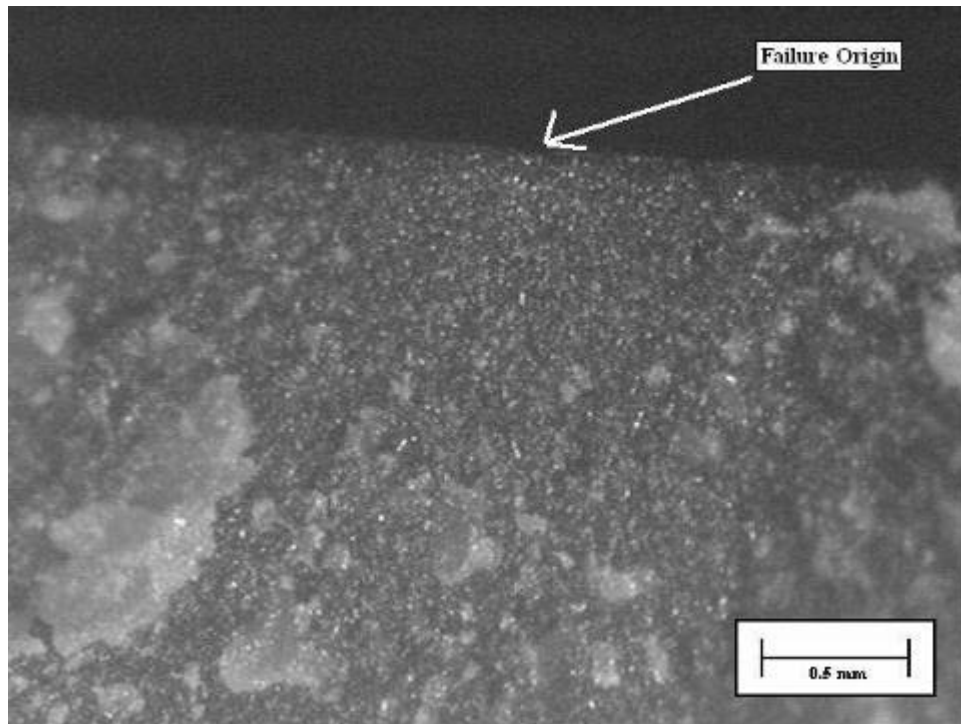


Figure D-13. ITK4-4 specimen 13.

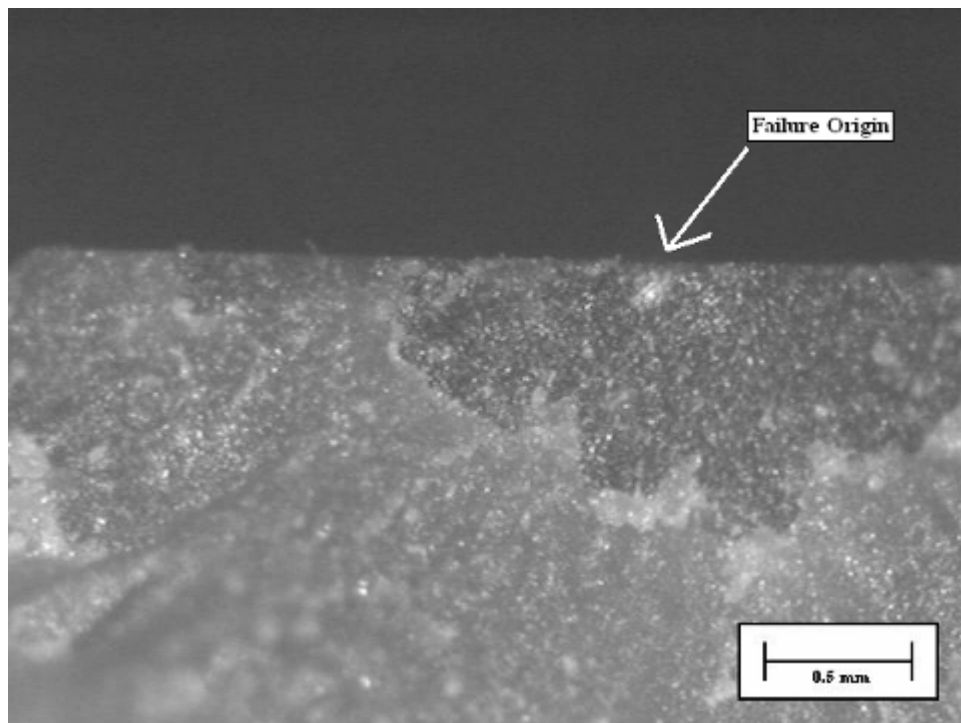


Figure D-14. ITK4-4 specimen 15.

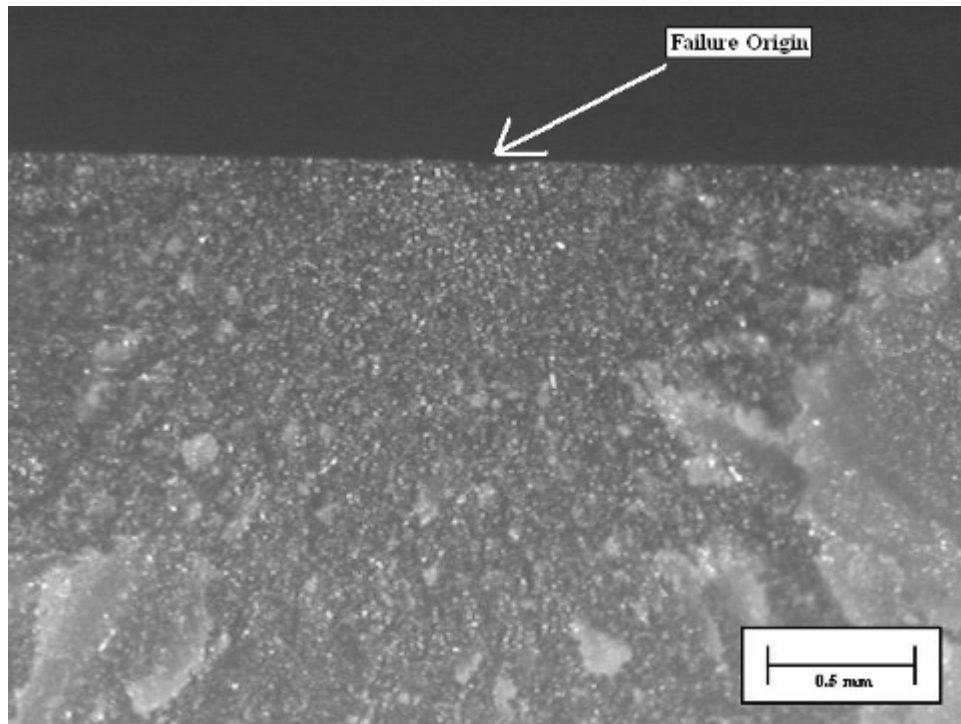


Figure D-15. ITK4-4 specimen 16.

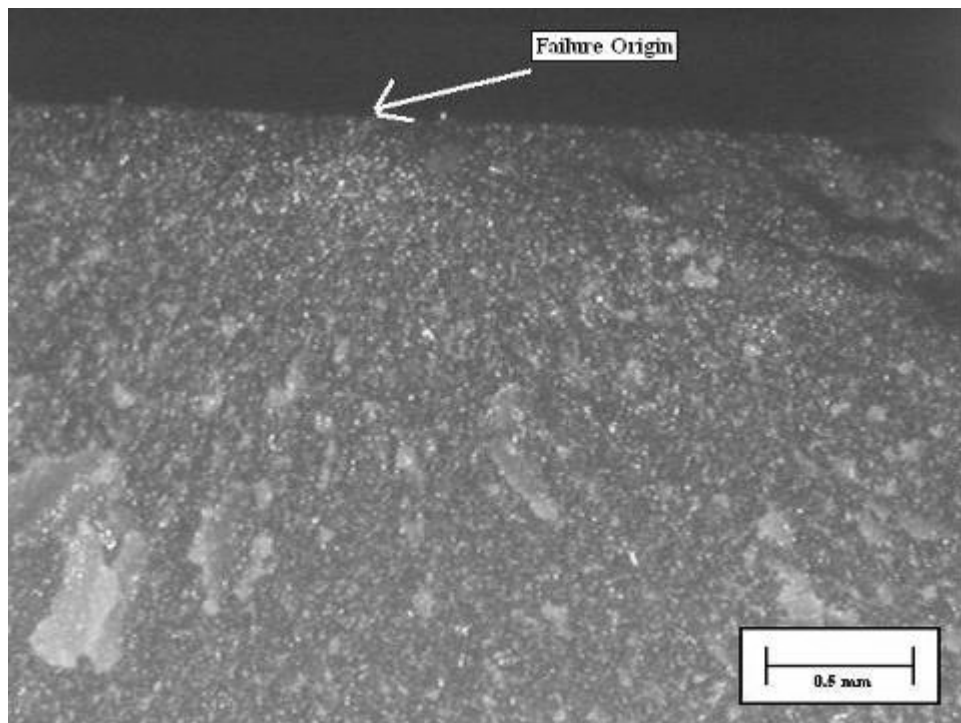


Figure D-16. ITK4-4 specimen 17.

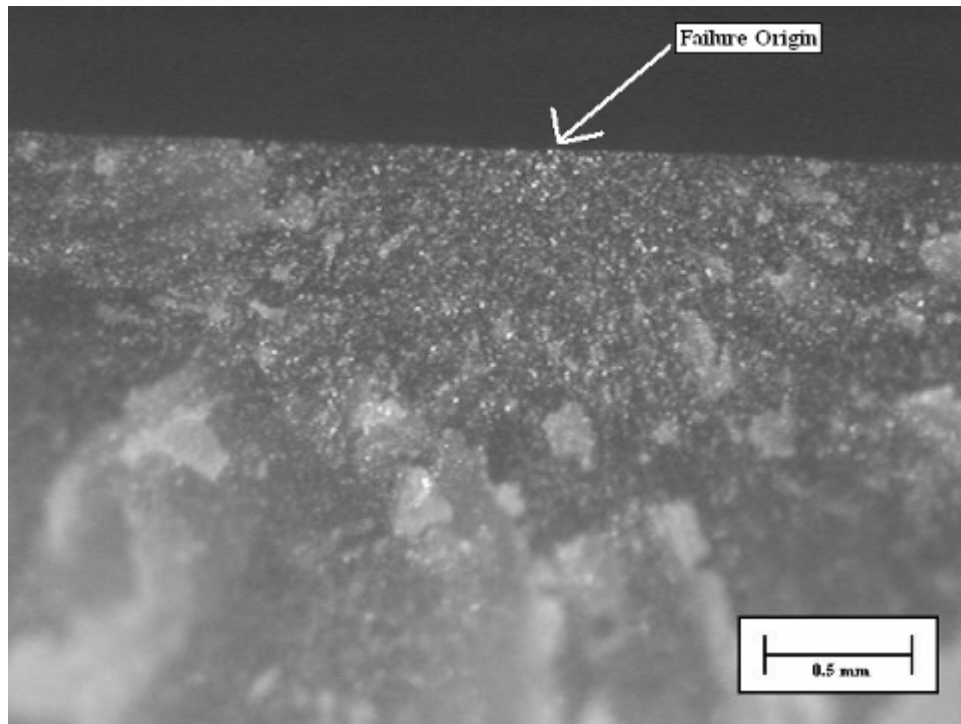


Figure D-17. ITK4-4 specimen 18.

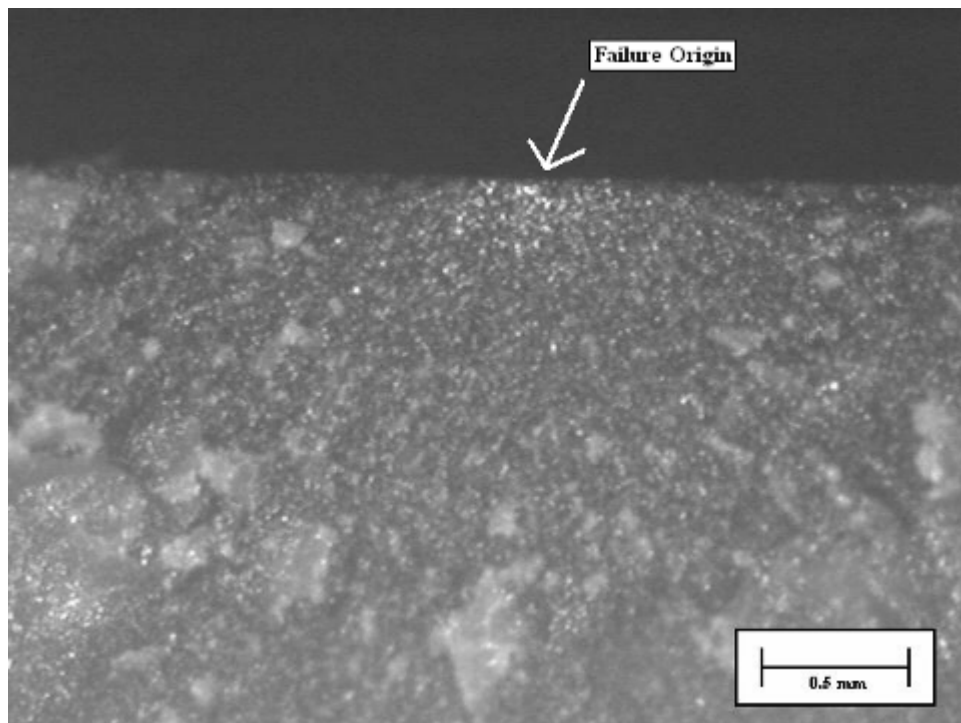


Figure D-18. ITK4-4 specimen 19.

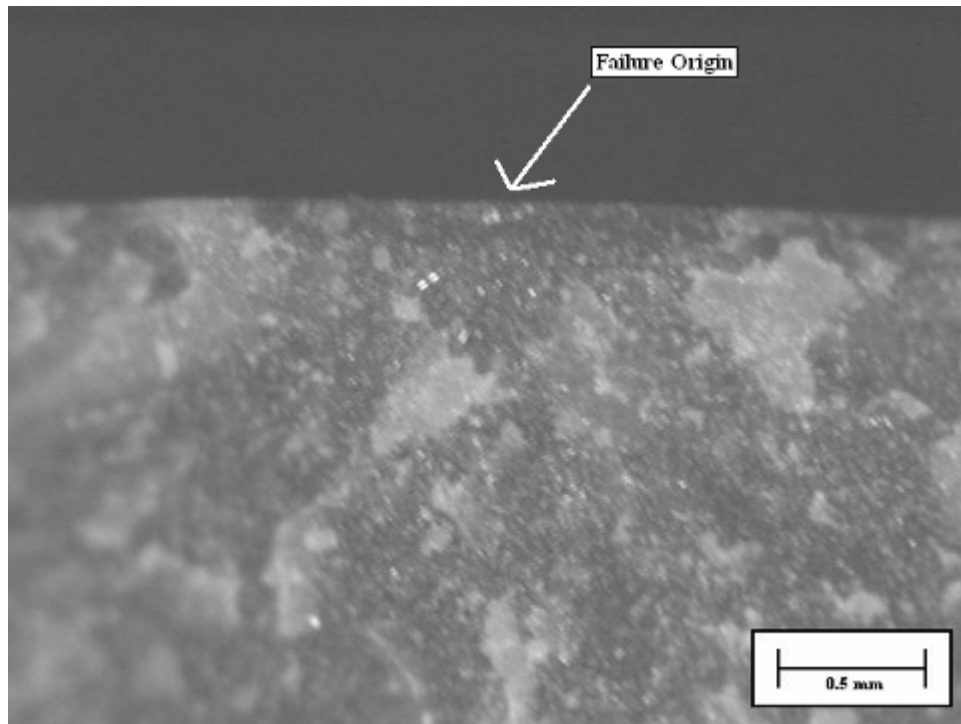


Figure D-19. ITK4-6 specimen 1.

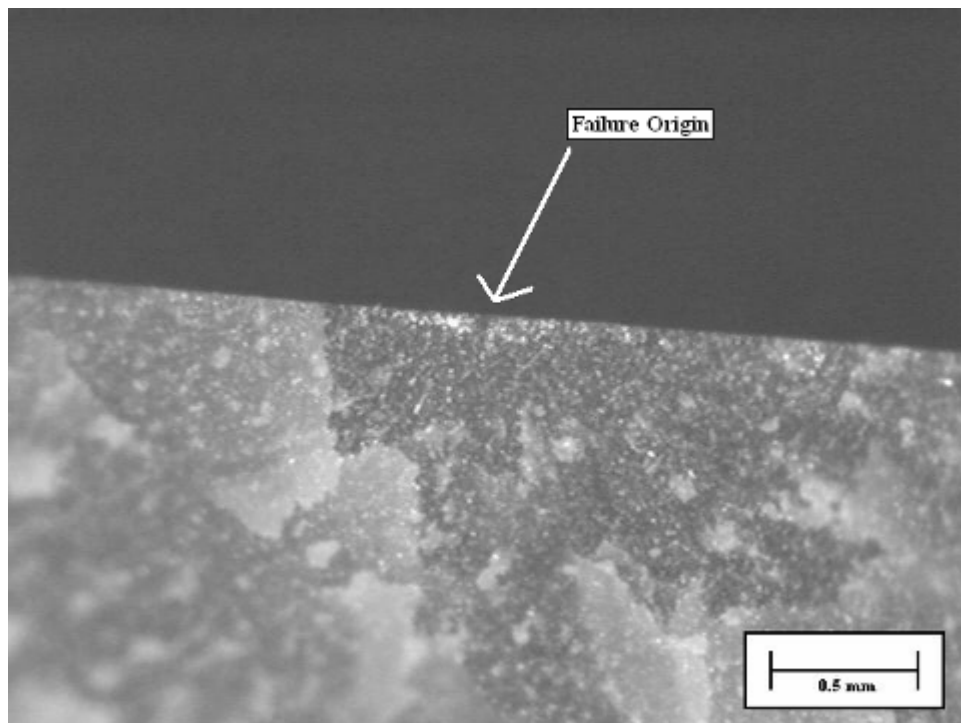


Figure D-20. ITK4-6 specimen 2.

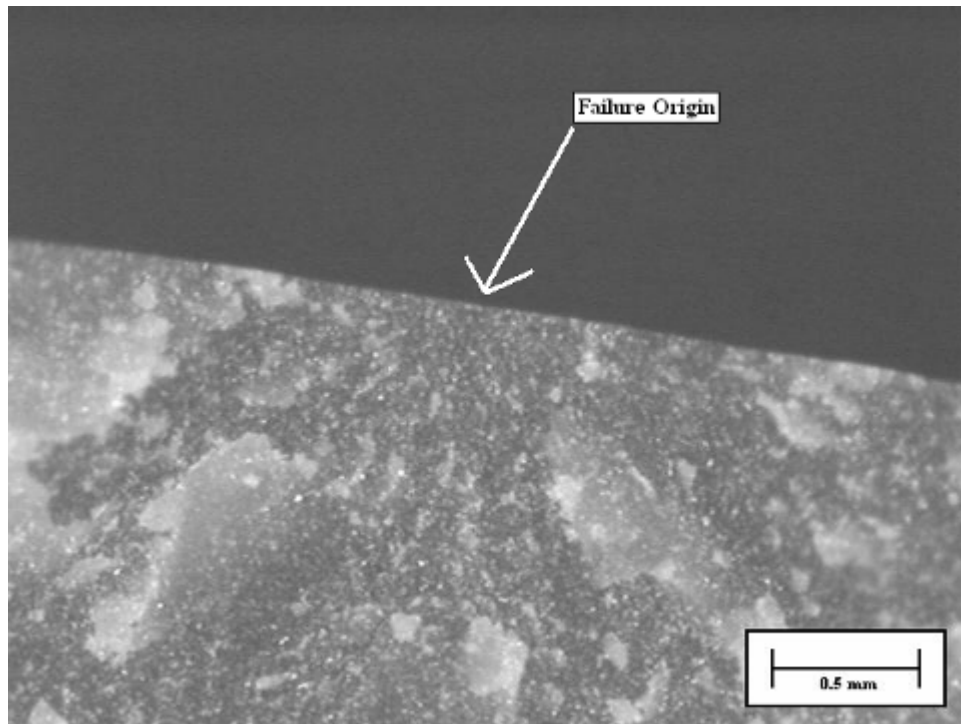


Figure D-21. ITK4-6 specimen 3.

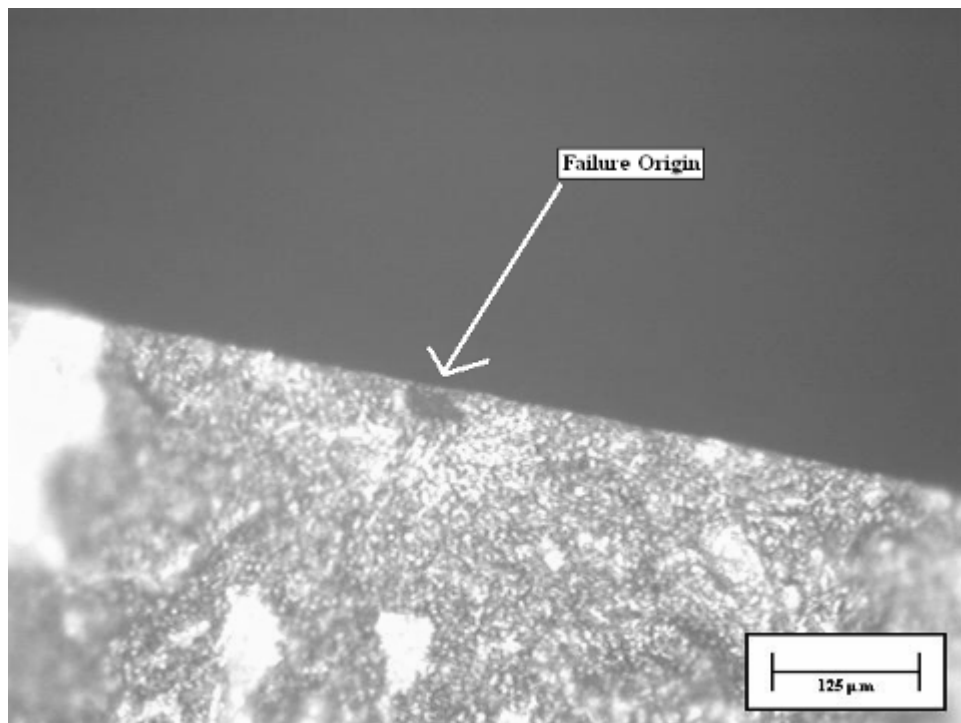


Figure D-22. ITK4-6 specimen 4.

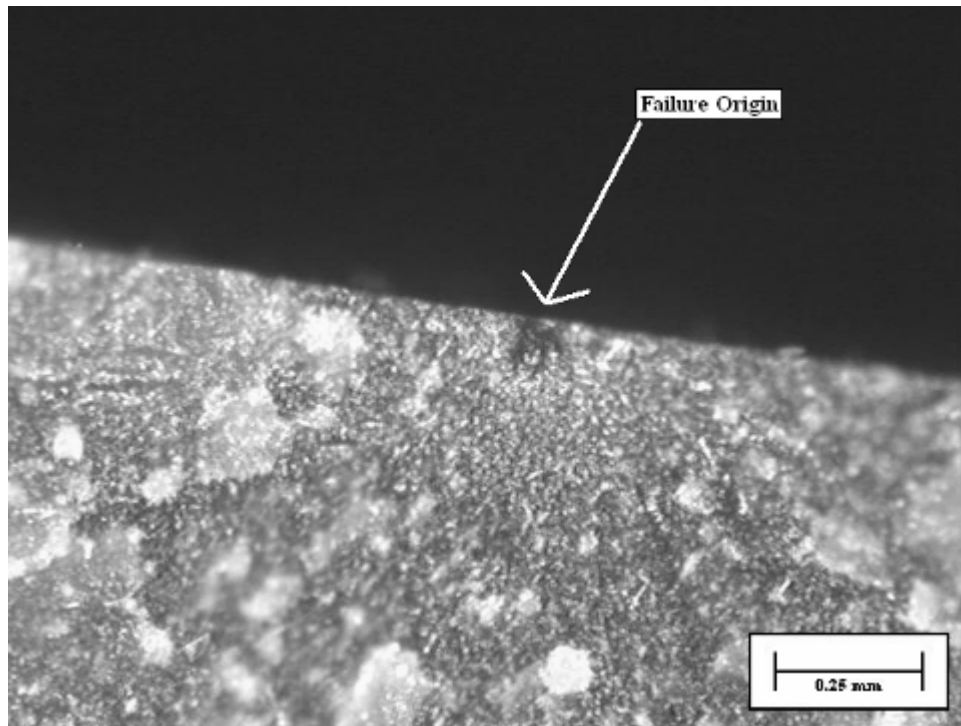


Figure D-23. ITK4-6 specimen 5.

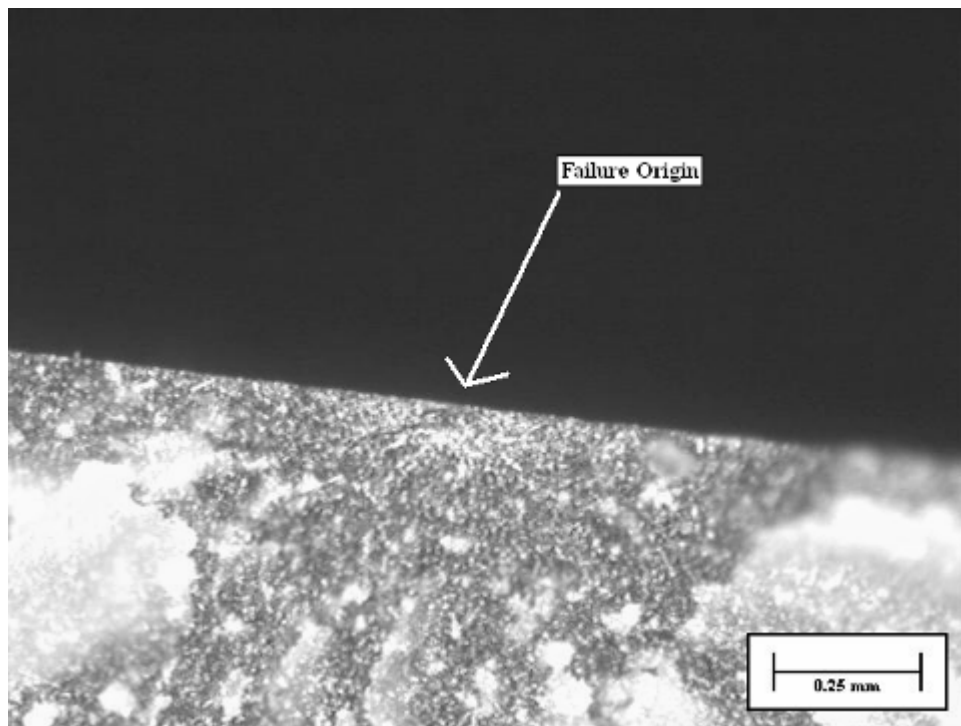


Figure D-24. ITK4-6 specimen 6.

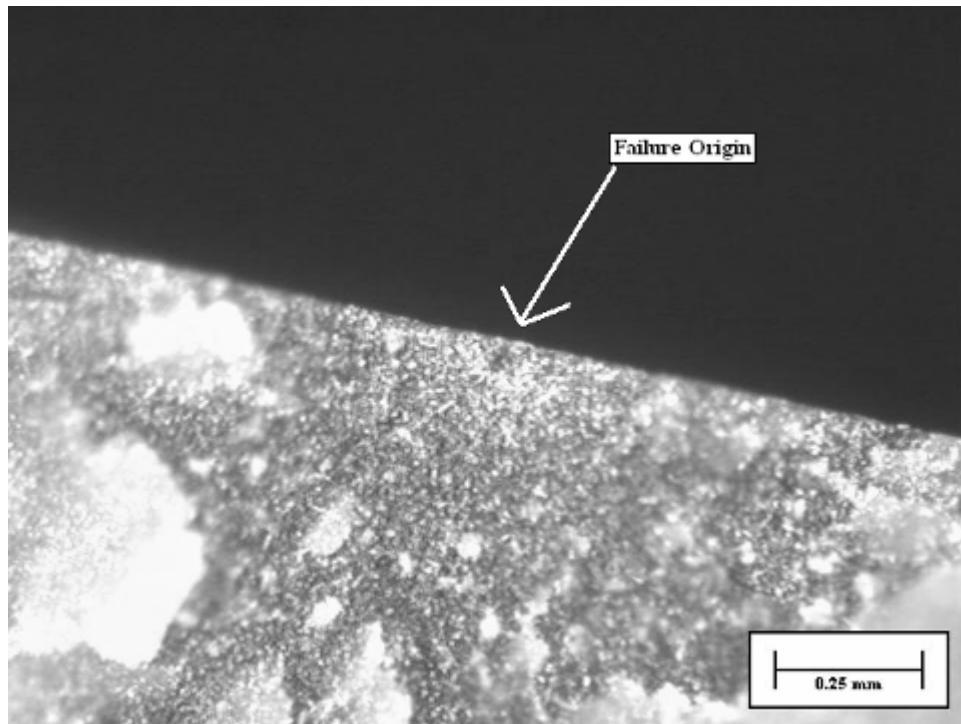


Figure D-25. ITK4-6 specimen 7.

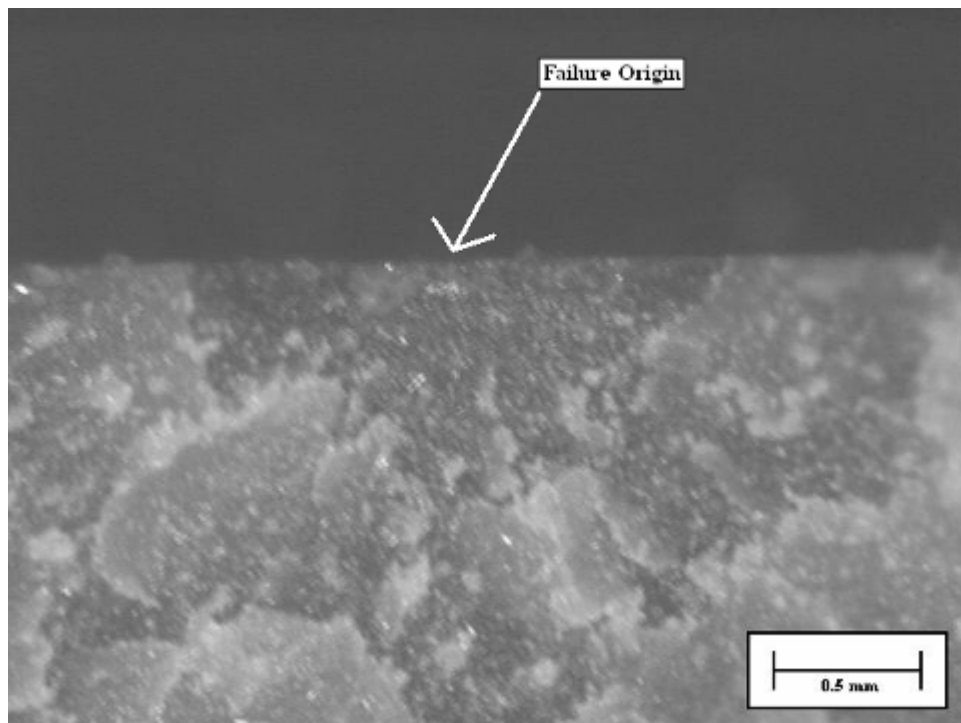


Figure D-26. ITK4-6 specimen 8.

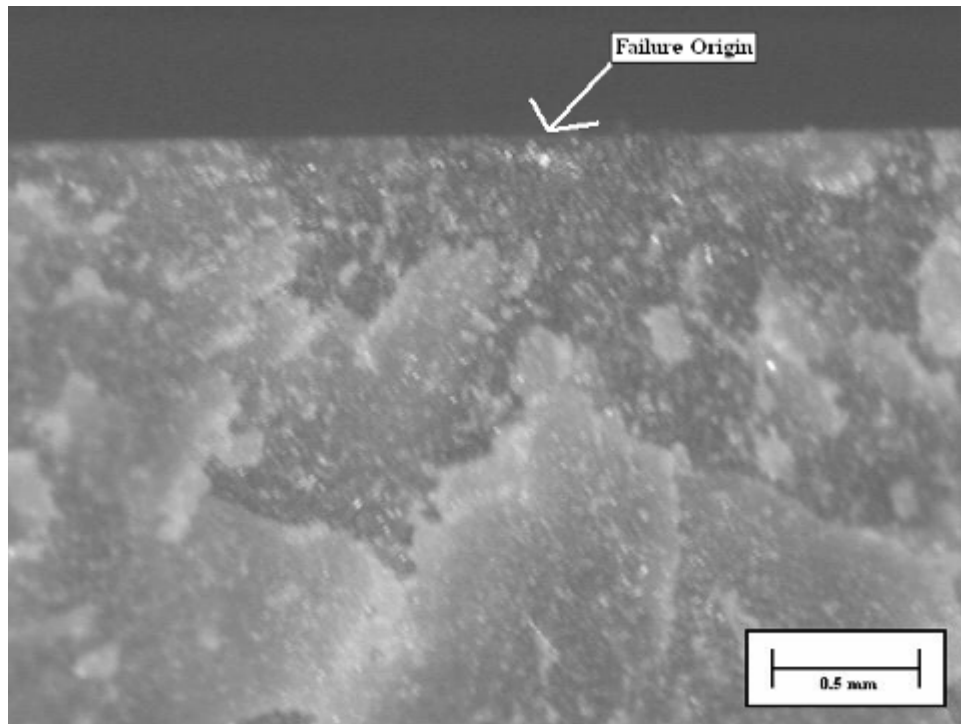


Figure D-27. ITK4-6 specimen 9.

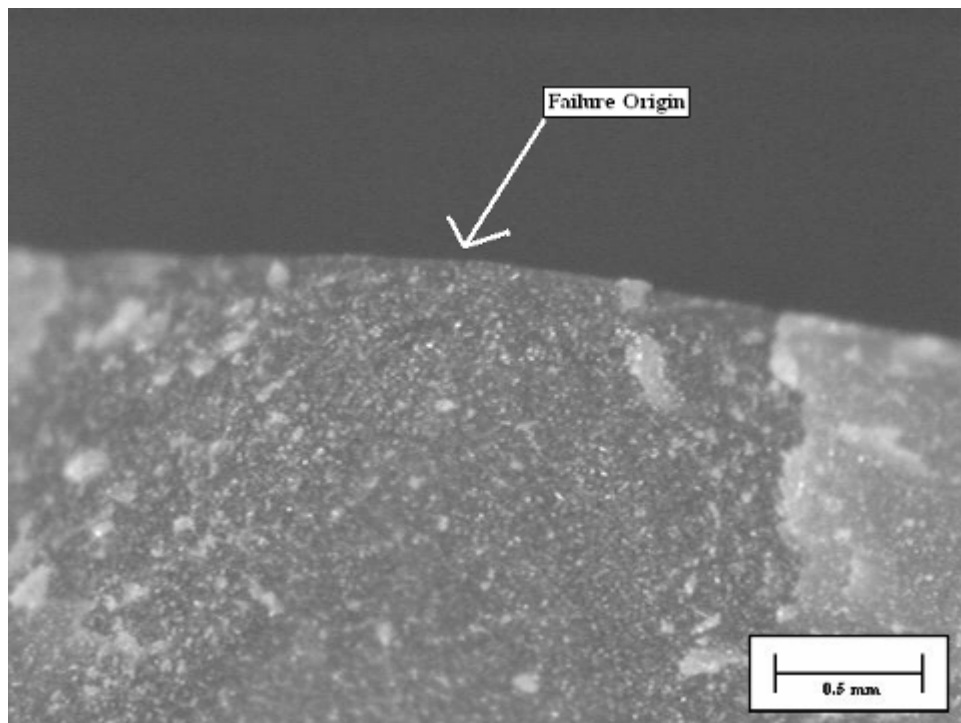


Figure D-28. ITK4-6 specimen 10.

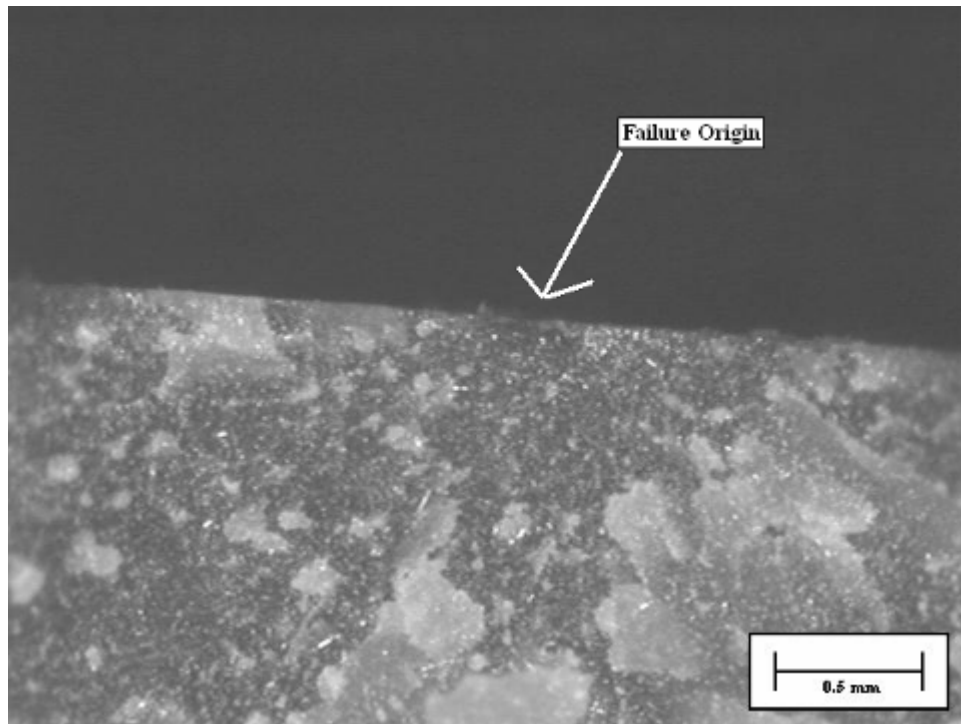


Figure D-29. ITK4-7 specimen 1.

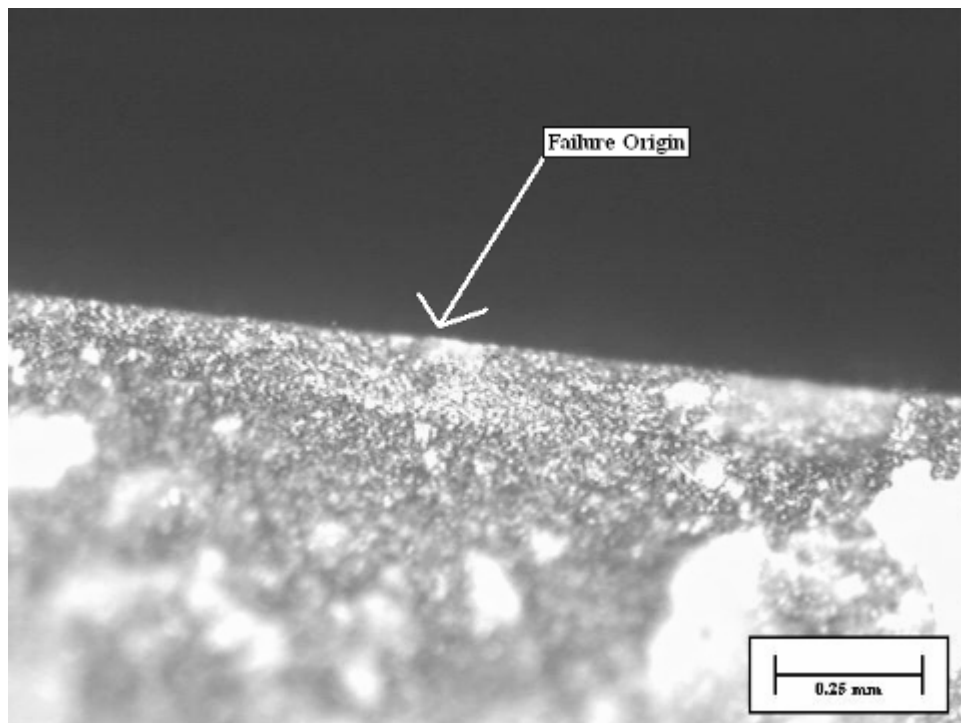


Figure D-30. ITK4-7 specimen 2.

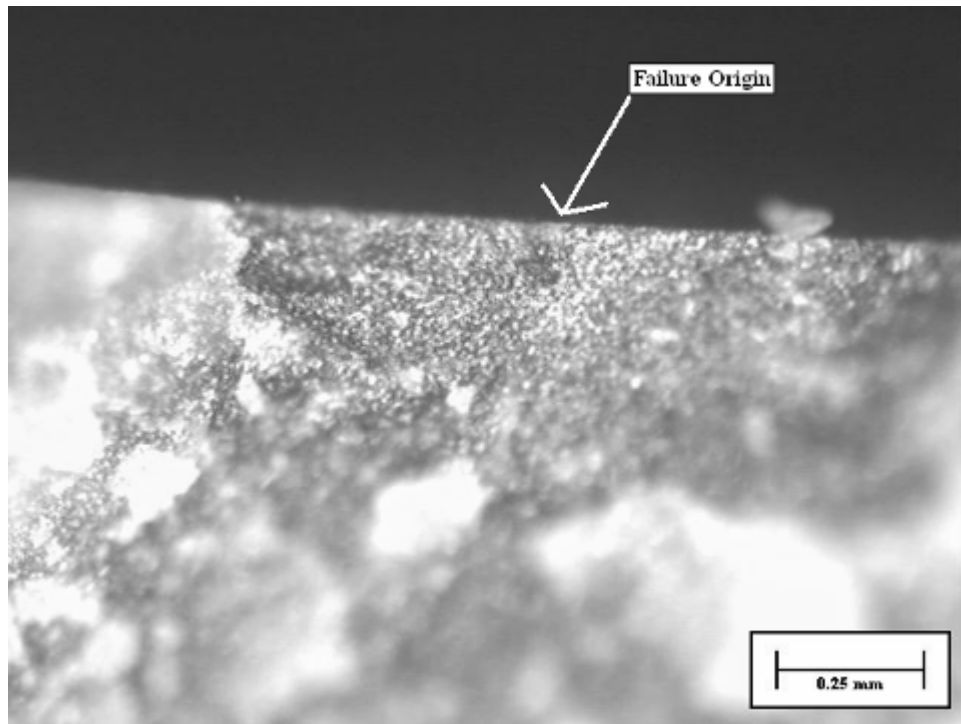


Figure D-31. ITK4-7 specimen 3.

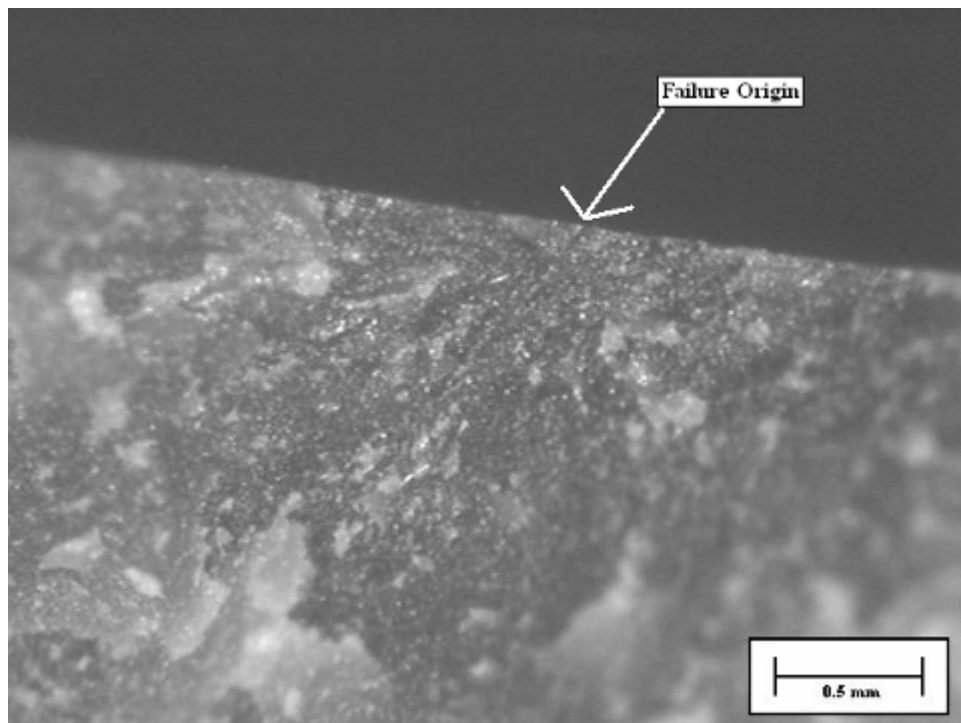


Figure D-32. ITK4-7 specimen 4.

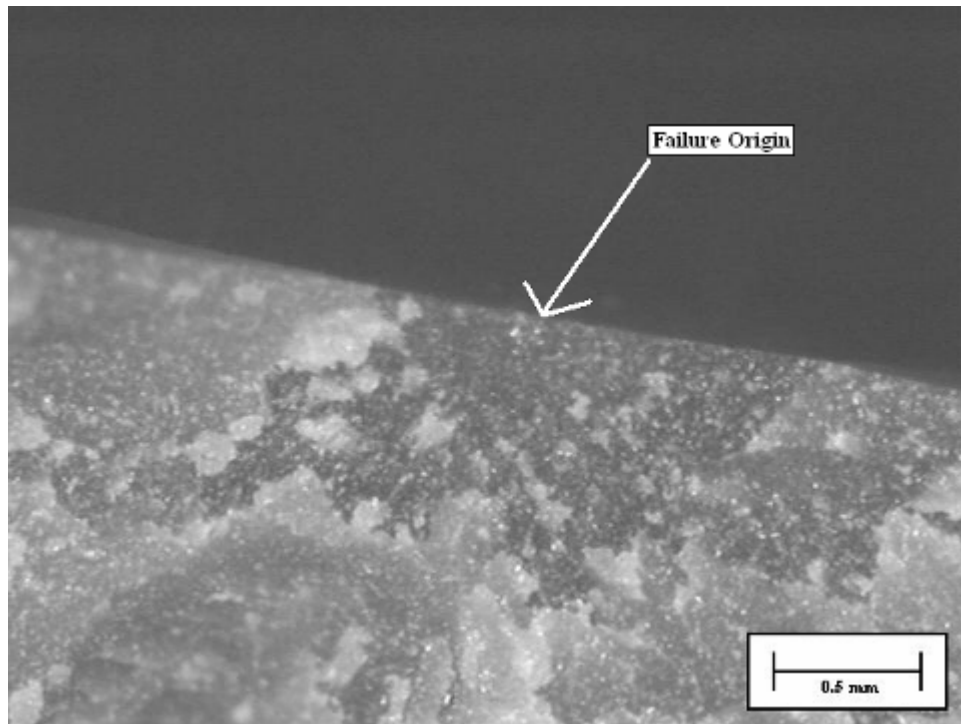


Figure D-33. ITK4-7 specimen 5.

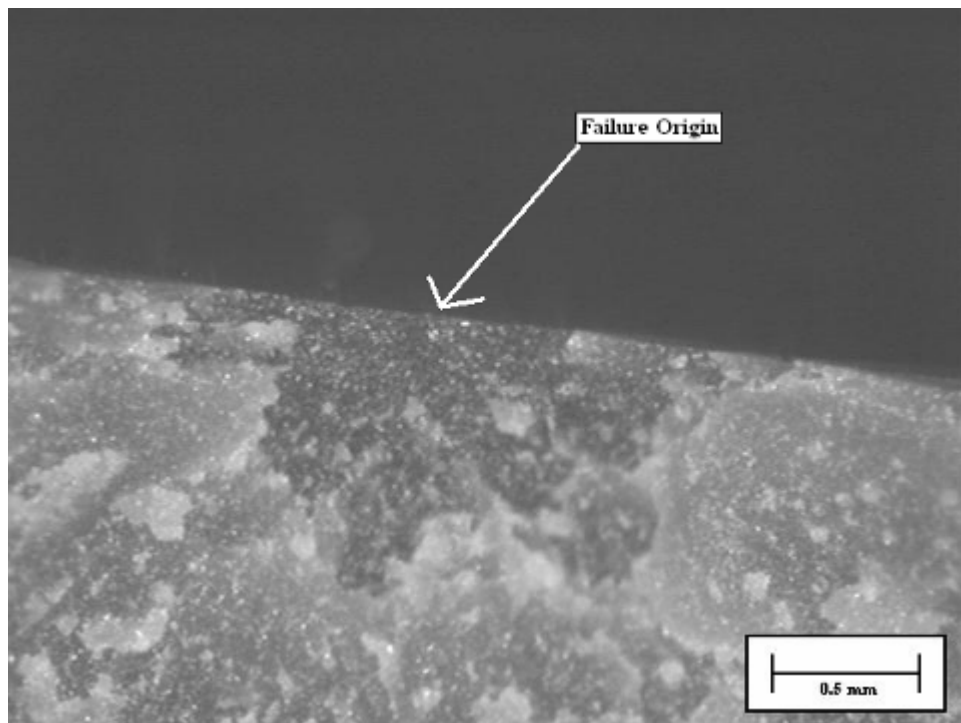


Figure D-34. ITK4-7 specimen 6.

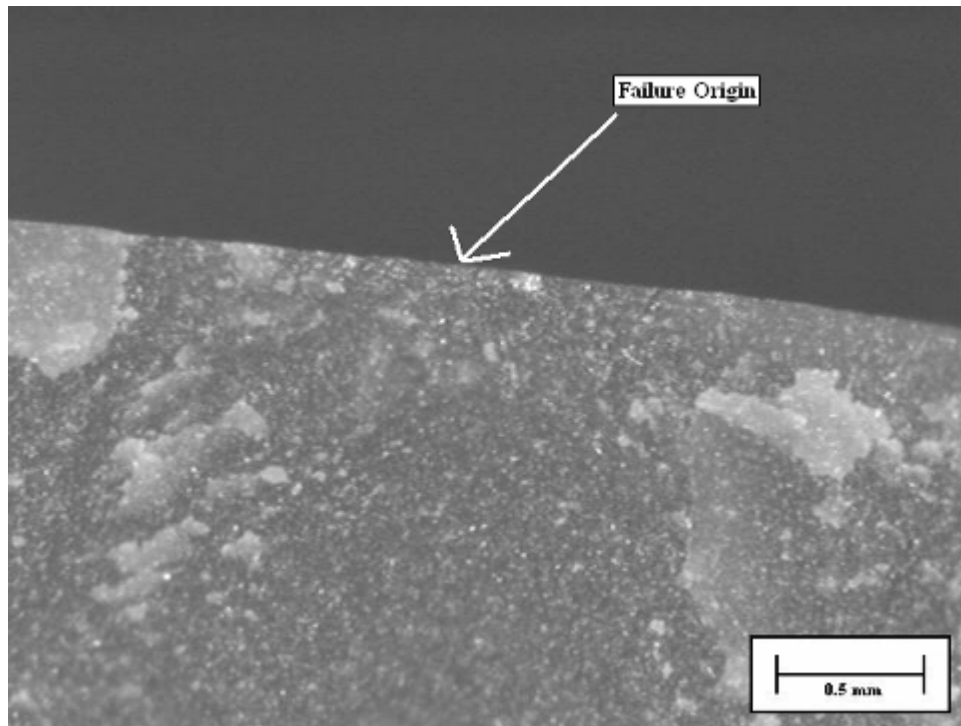


Figure D-35. ITK4-7 specimen 7.

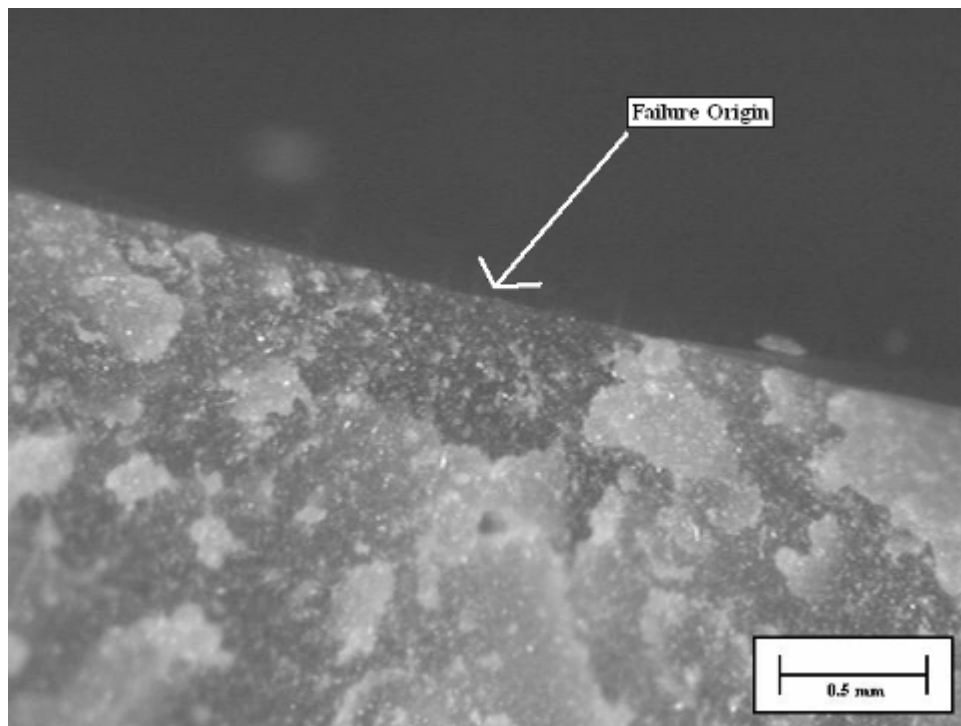


Figure D-36. ITK4-7 specimen 8.

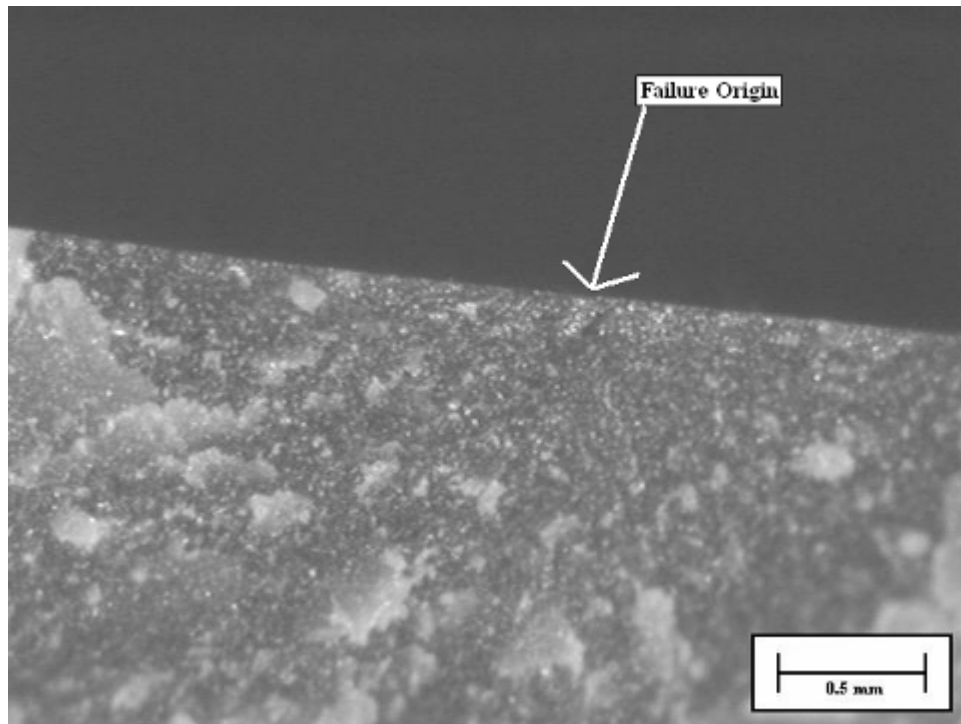


Figure D-37. ITK4-7 specimen 9.

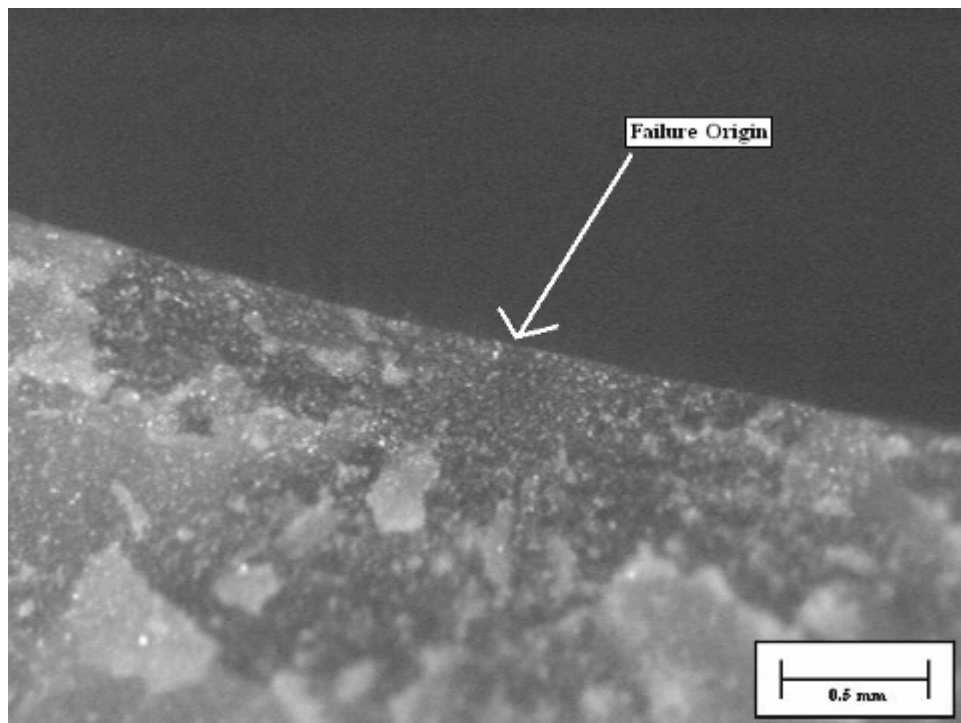


Figure D-38. ITK4-7 specimen 10.

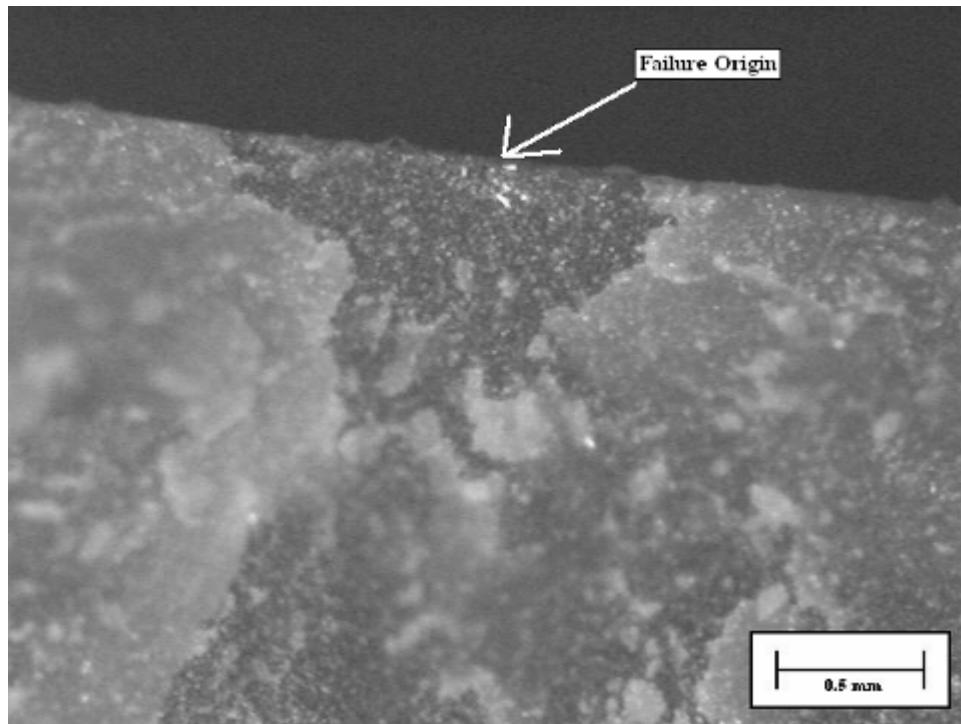


Figure D-39. ITK4-8 specimen 1.

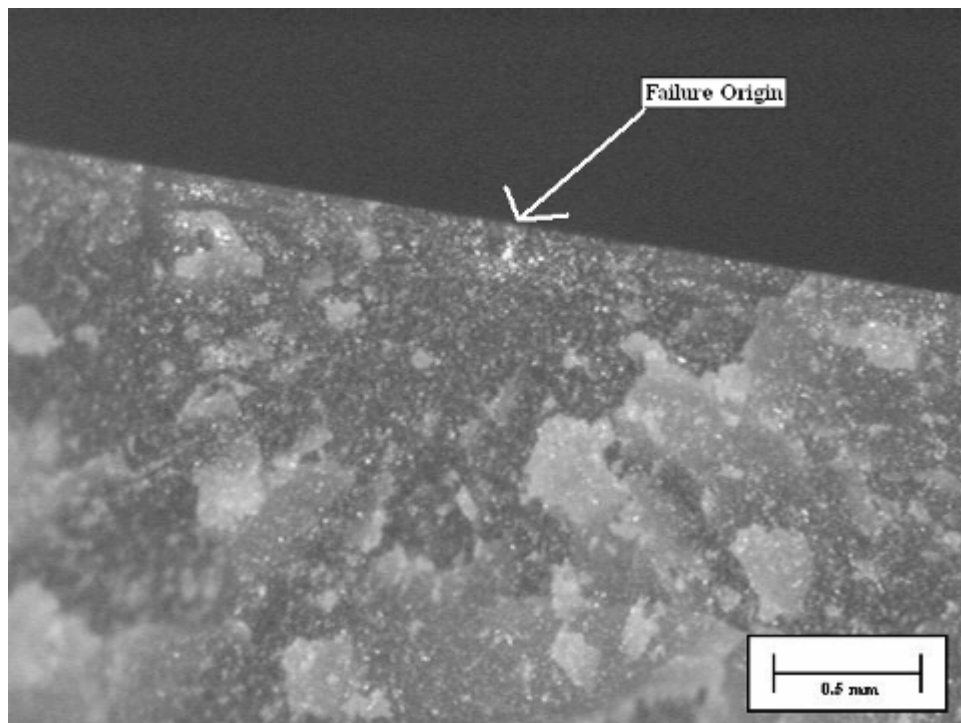


Figure D-40. ITK4-8 specimen 2.

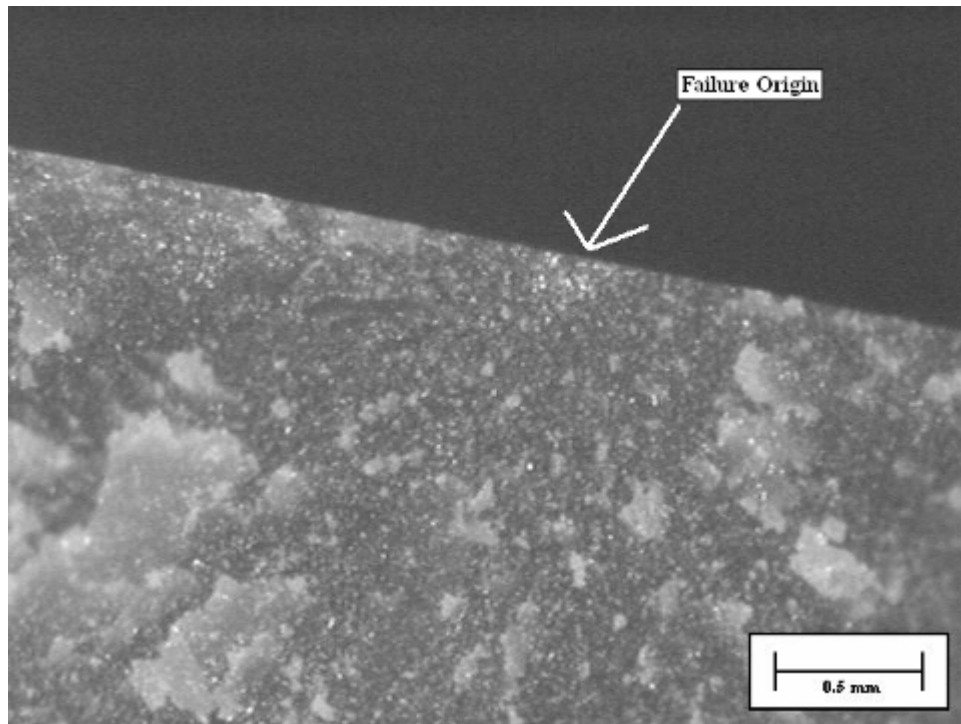


Figure D-41. ITK4-8 specimen 3.

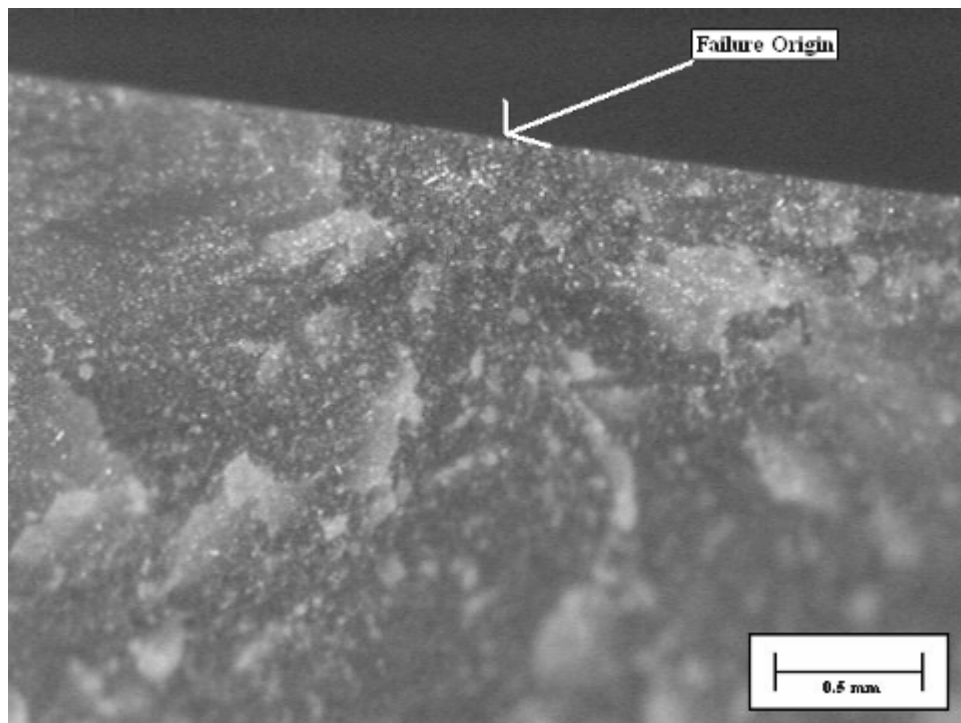


Figure D-42. ITK4-8 specimen 4.

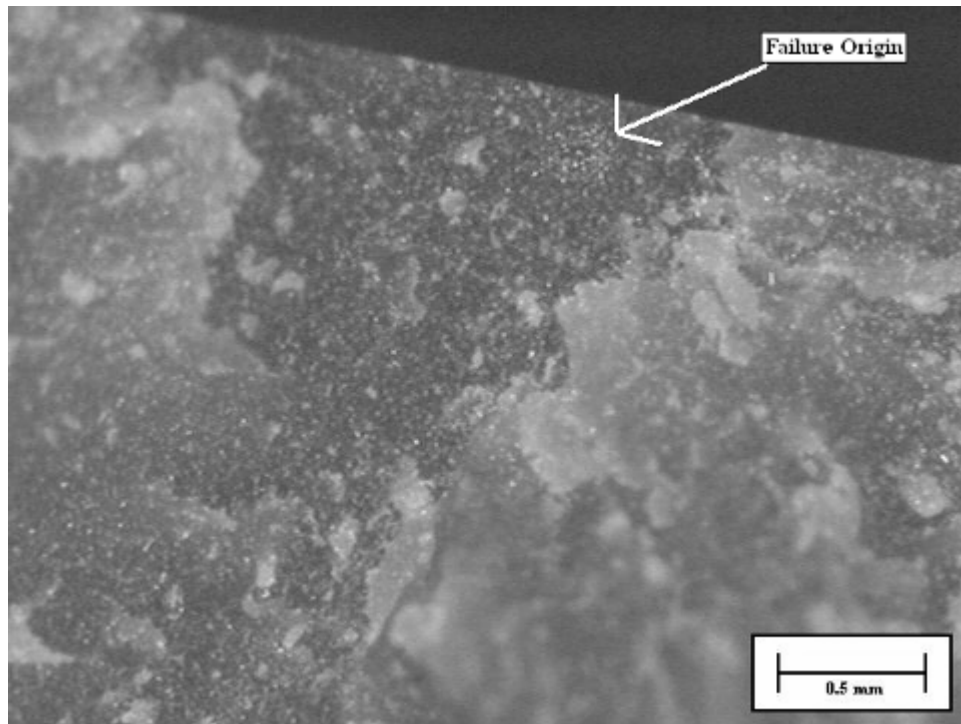


Figure D-43. ITK4-8 specimen 5.

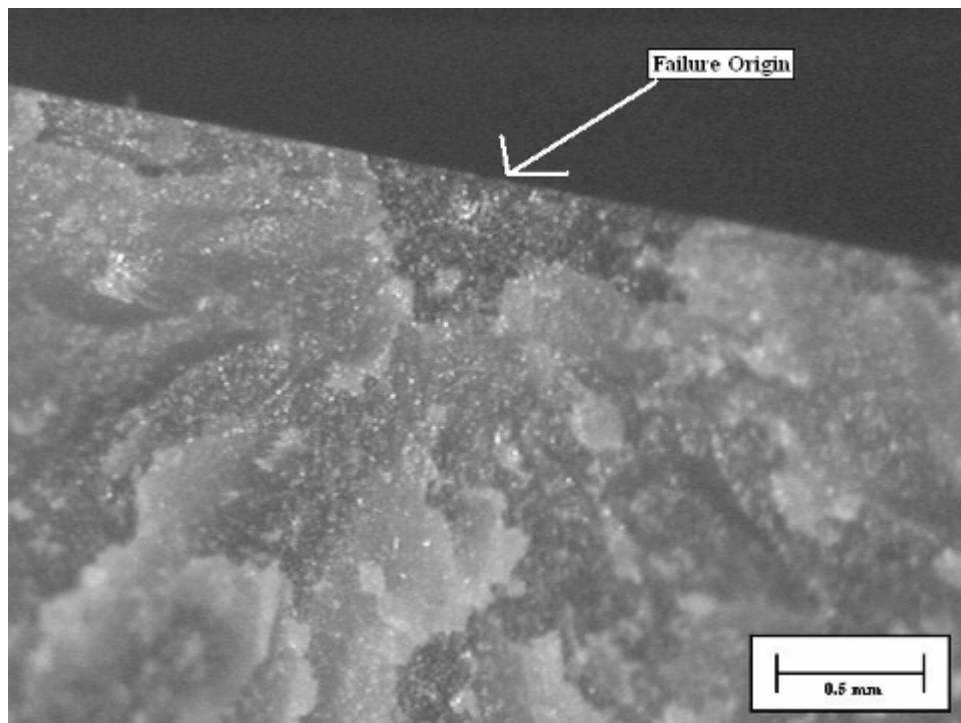


Figure D-44. ITK4-8 specimen 6.

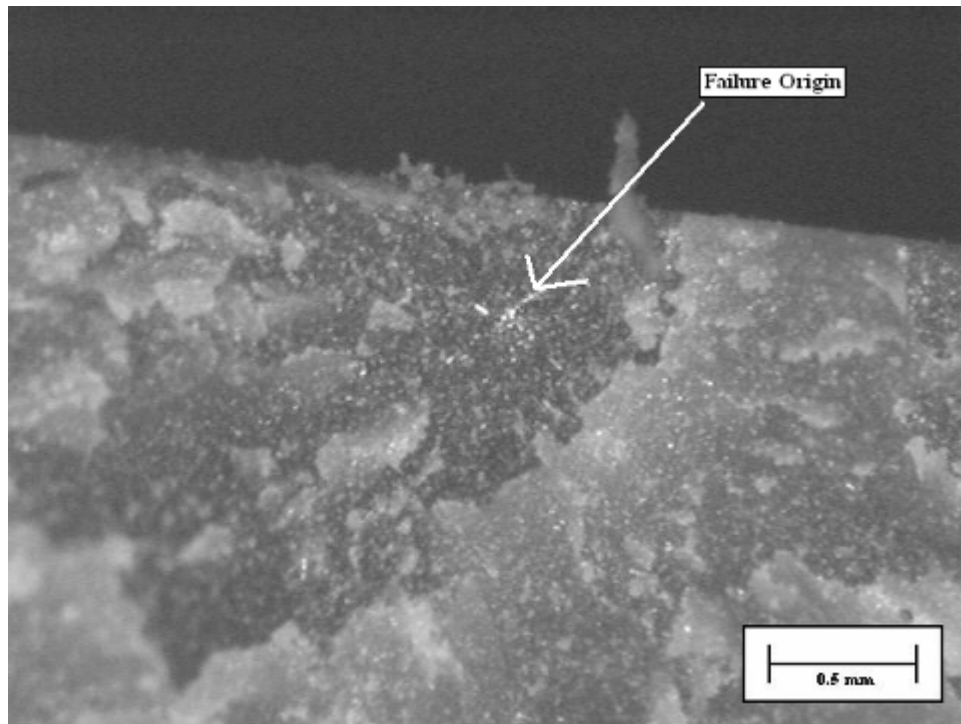


Figure D-45. ITK4-8 specimen 7.

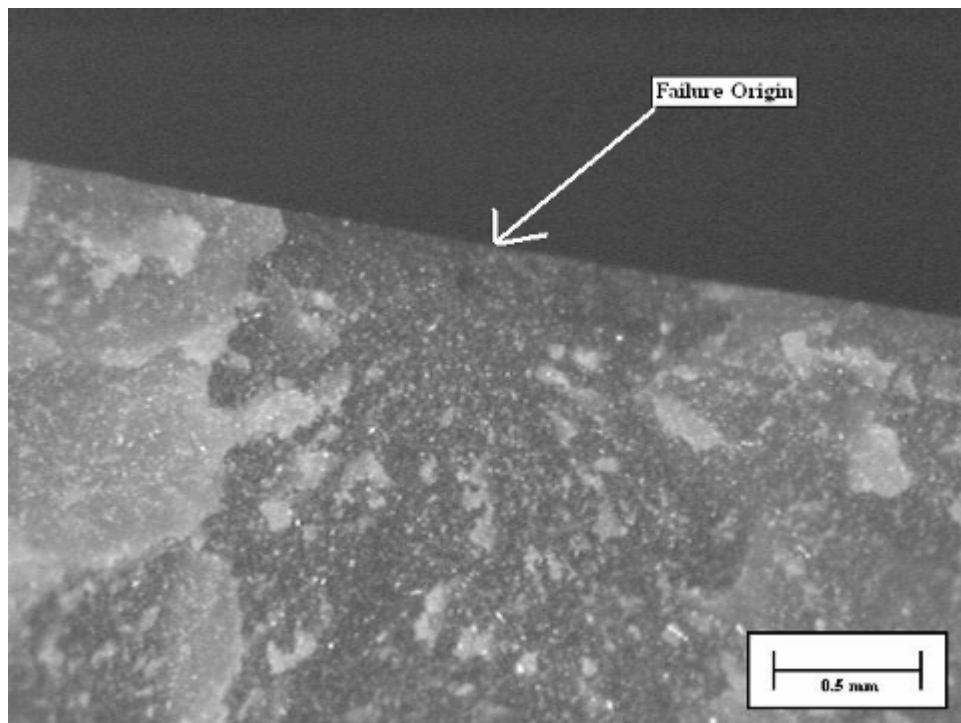


Figure D-46. ITK4-8 specimen 8.

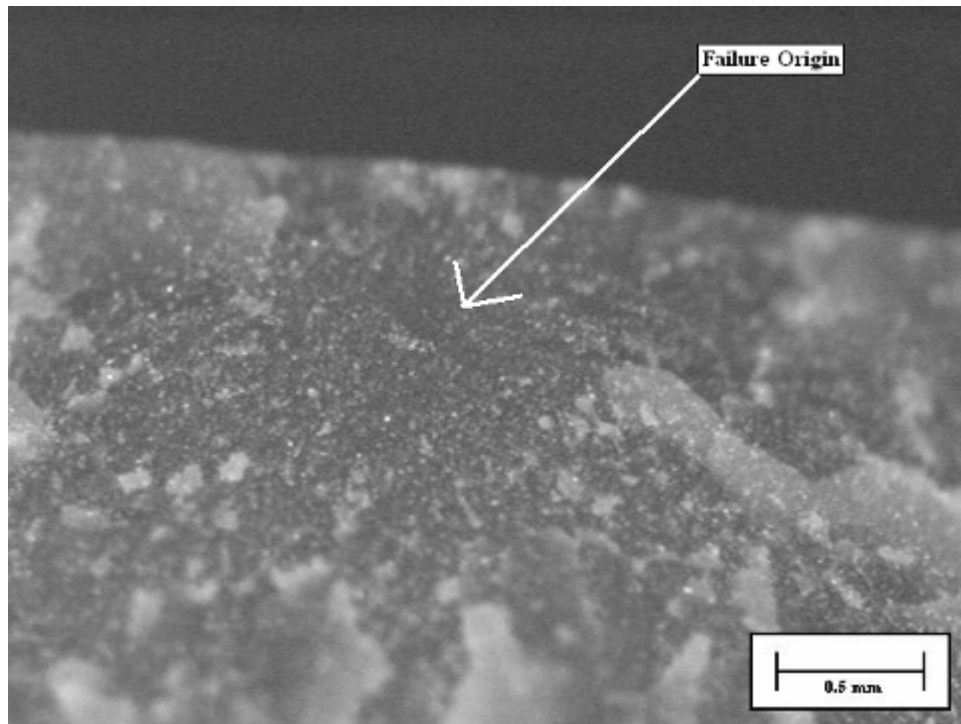


Figure D-47. ITK4-8 specimen 9.

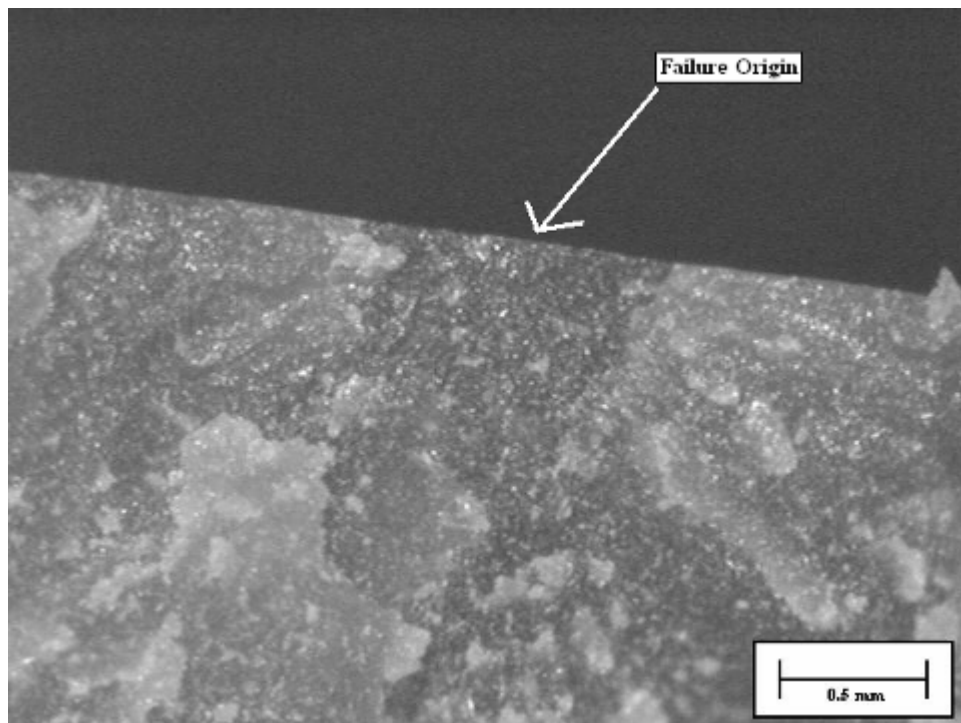


Figure D-48. ITK4-8 specimen 10.

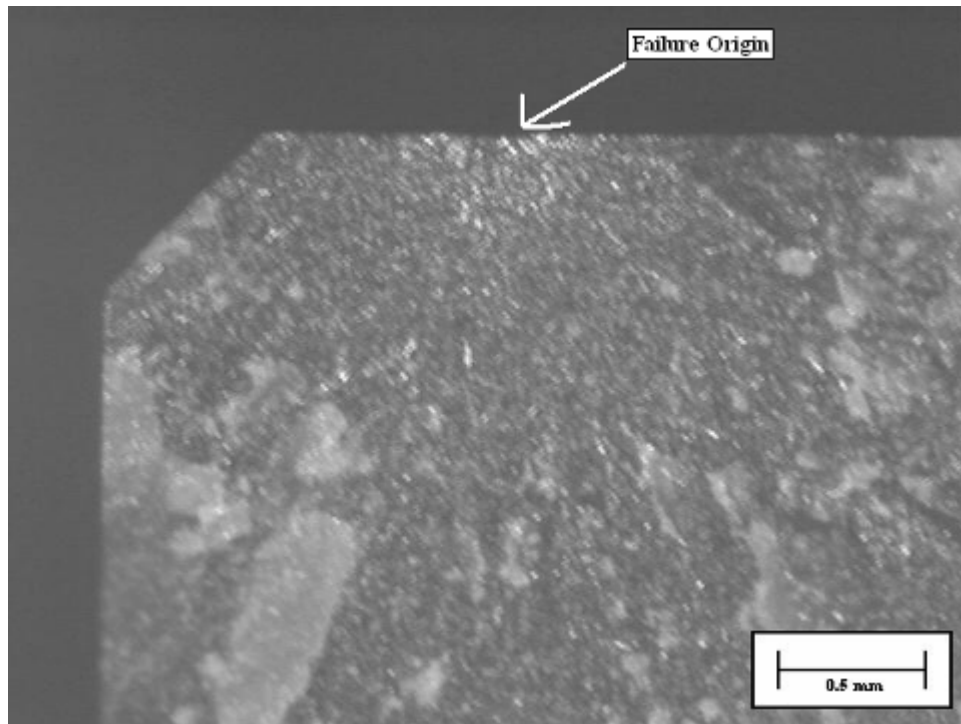


Figure D-49. ITK4-14 specimen 1.

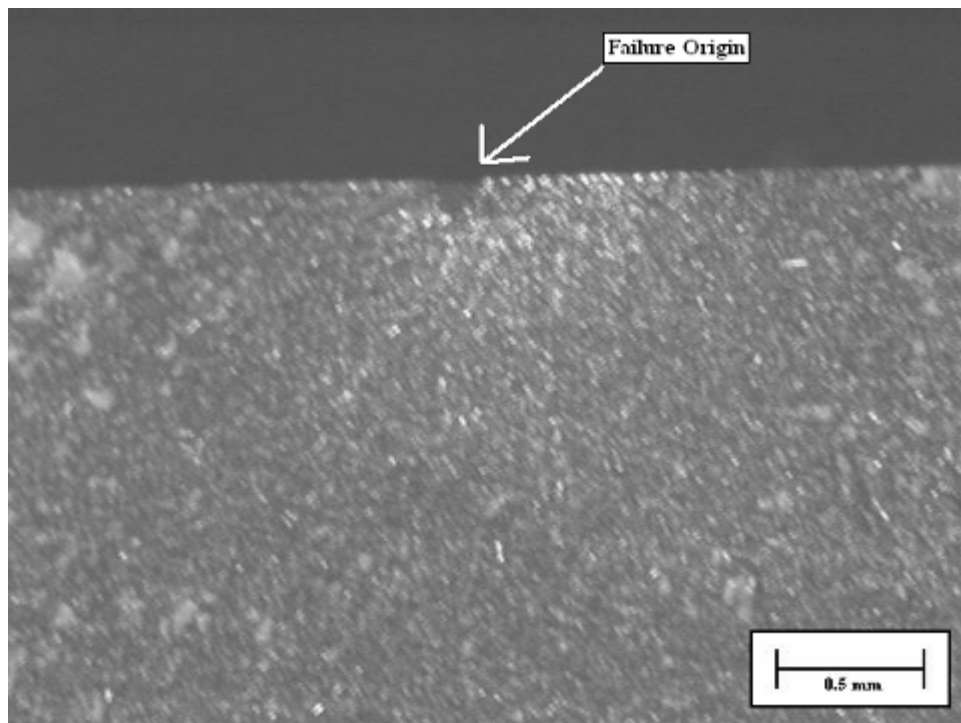


Figure D-50. ITK4-14 specimen 2.

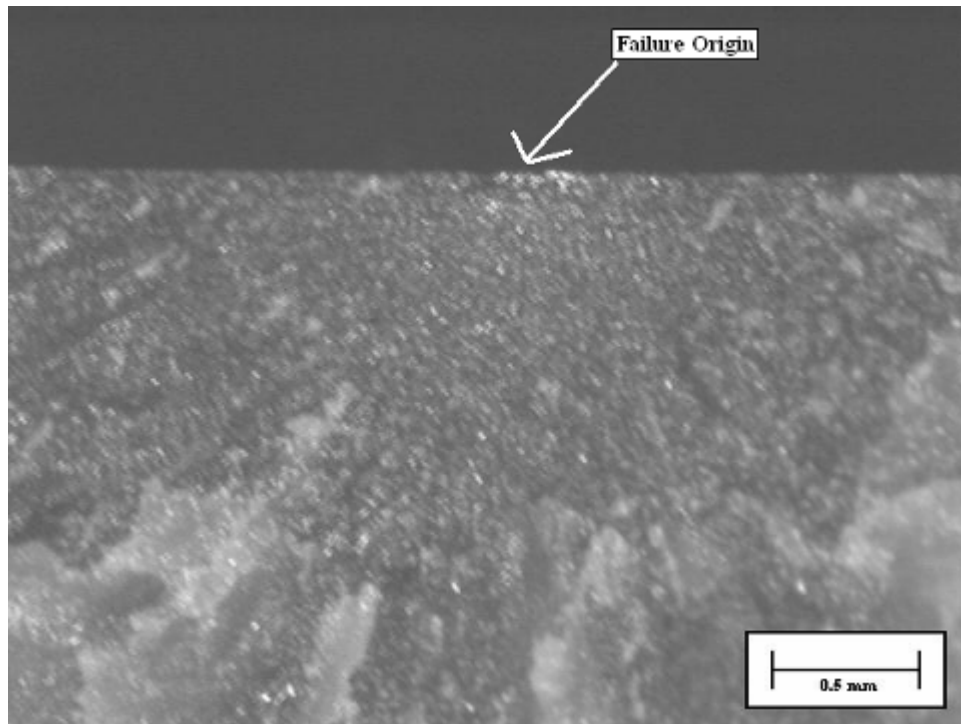


Figure D-51. ITK4-14 specimen 4.

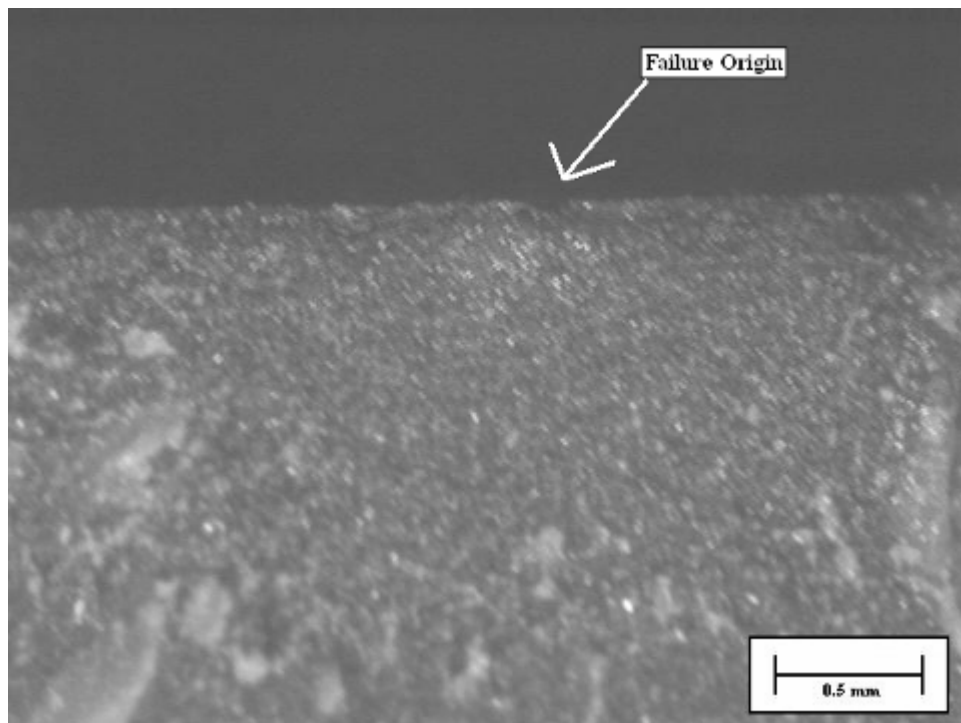


Figure D-52. ITK4-14 specimen 5.

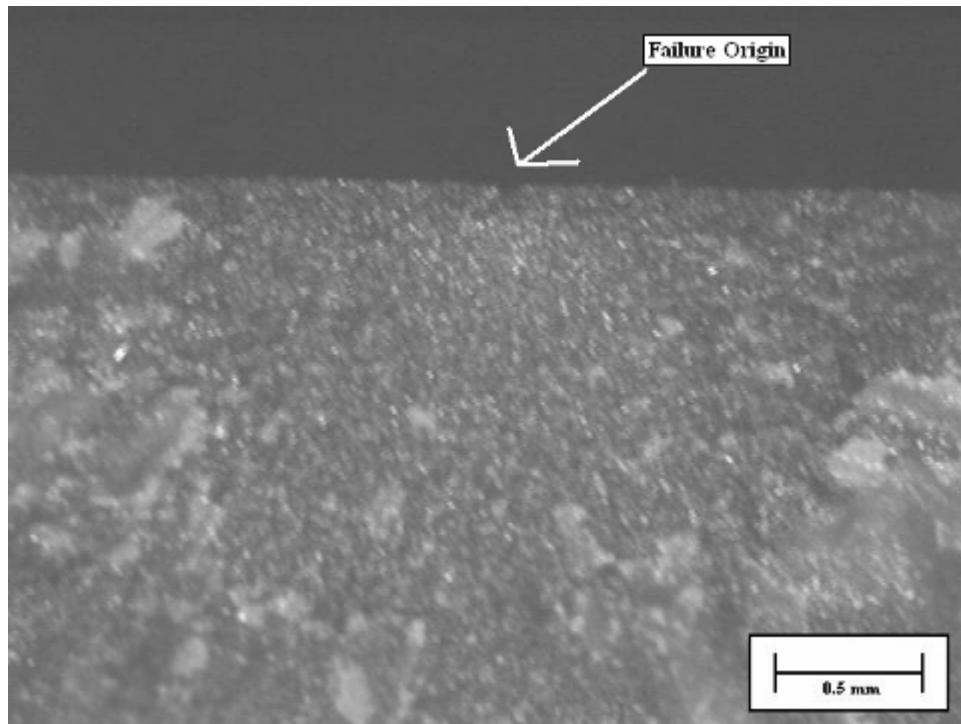


Figure D-53. ITK4-14 specimen 6.

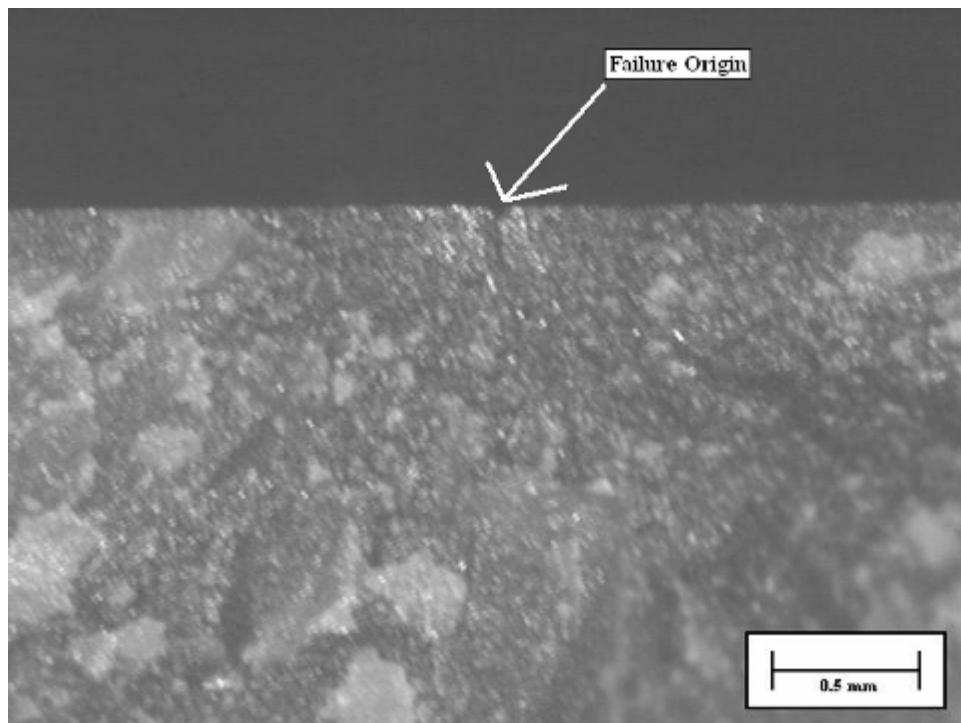


Figure D-54. ITK4-14 specimen 7.

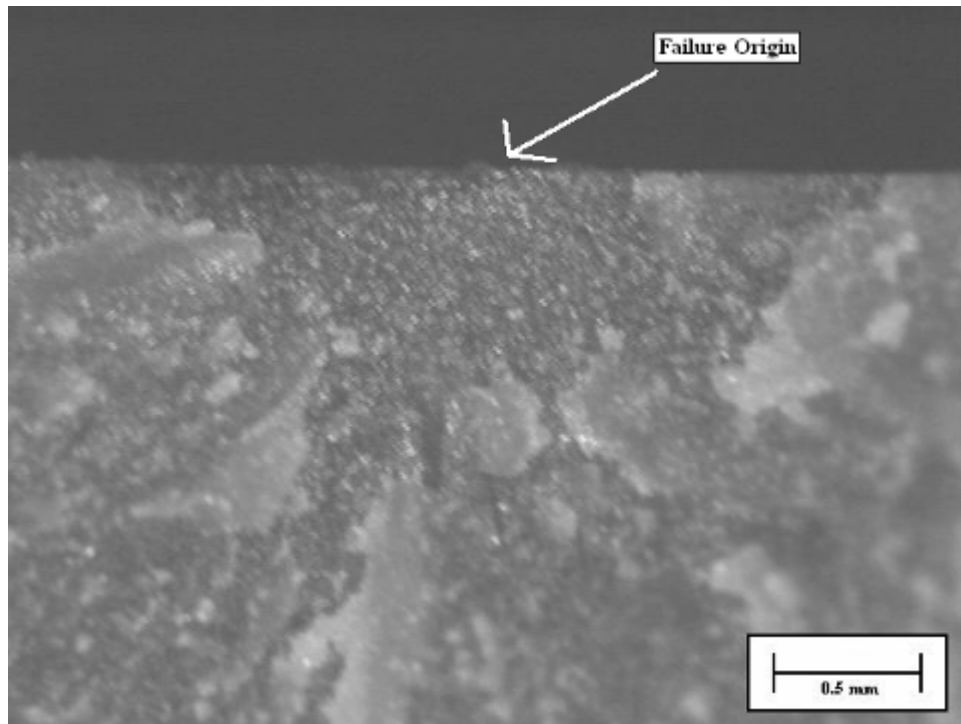


Figure D-55. ITK4-14 specimen 8.

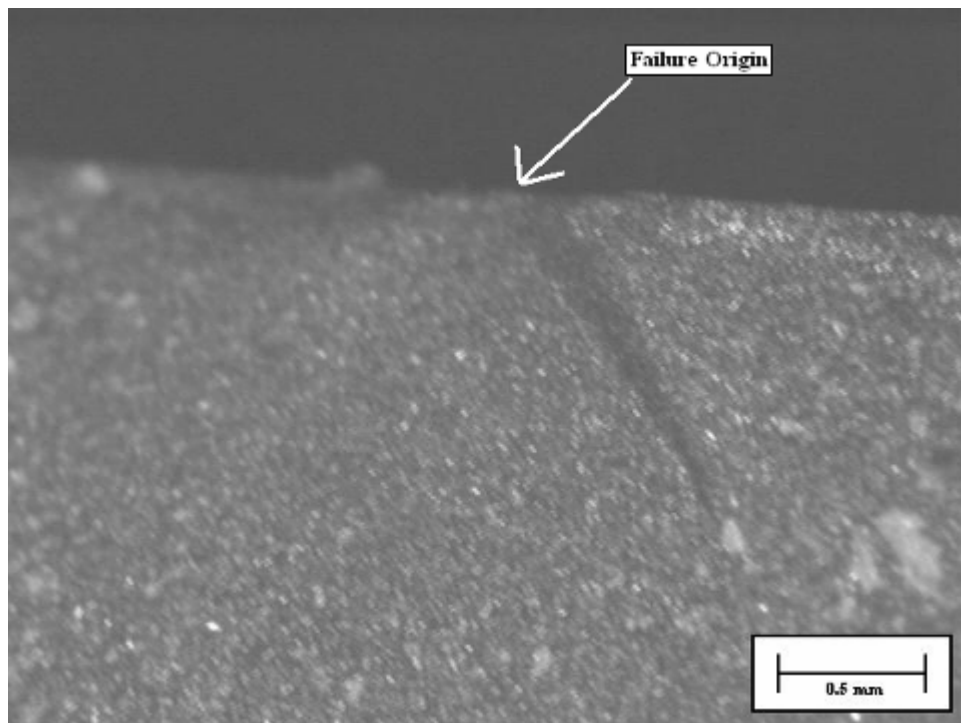


Figure D-56. ITK4-14 specimen 9.

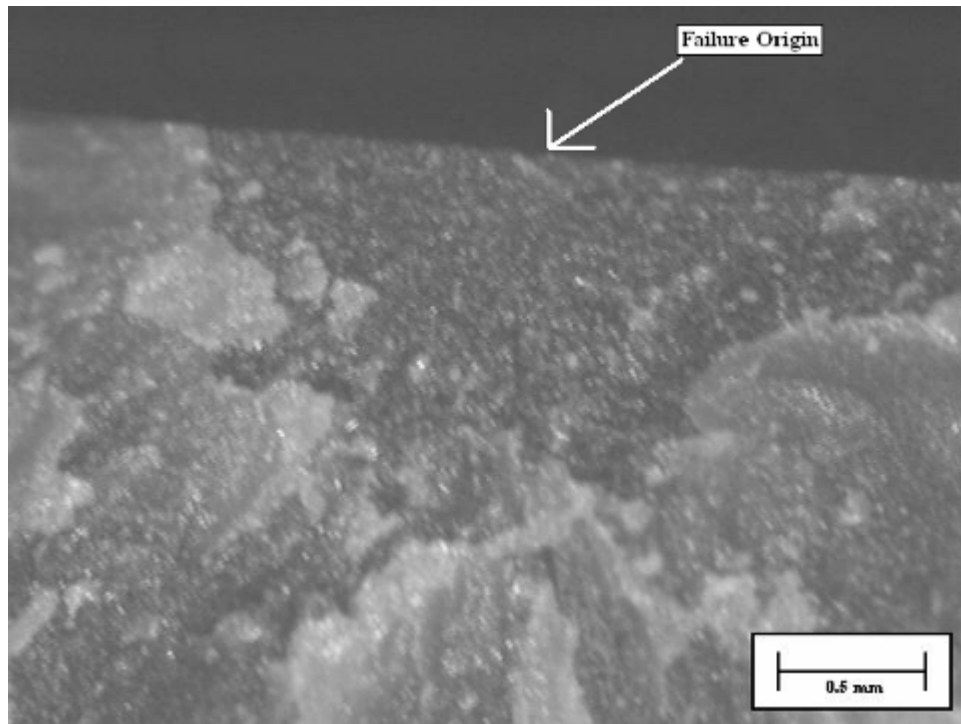


Figure D-57. ITK4-14 specimen 10.

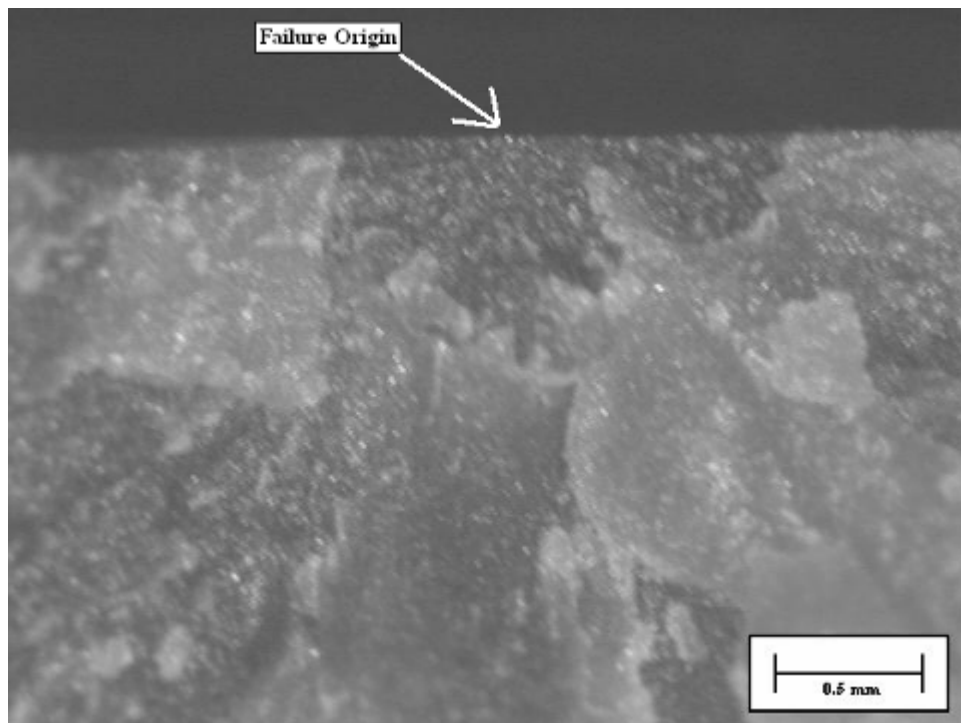


Figure D-58. ITK4-14 specimen 11.

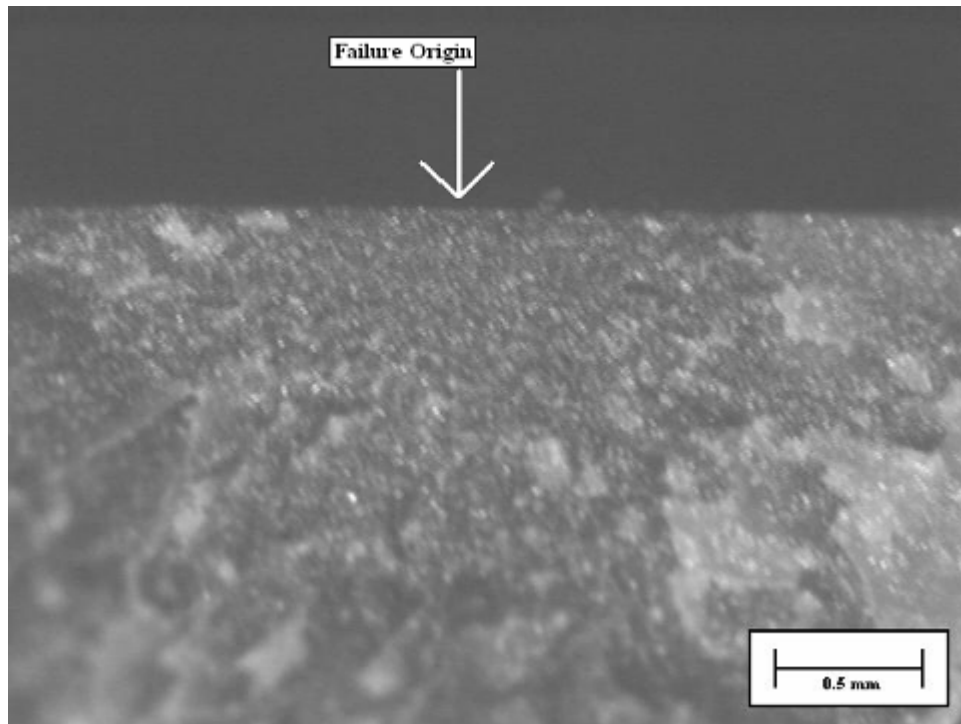


Figure D-59. ITK4-14 specimen 12.

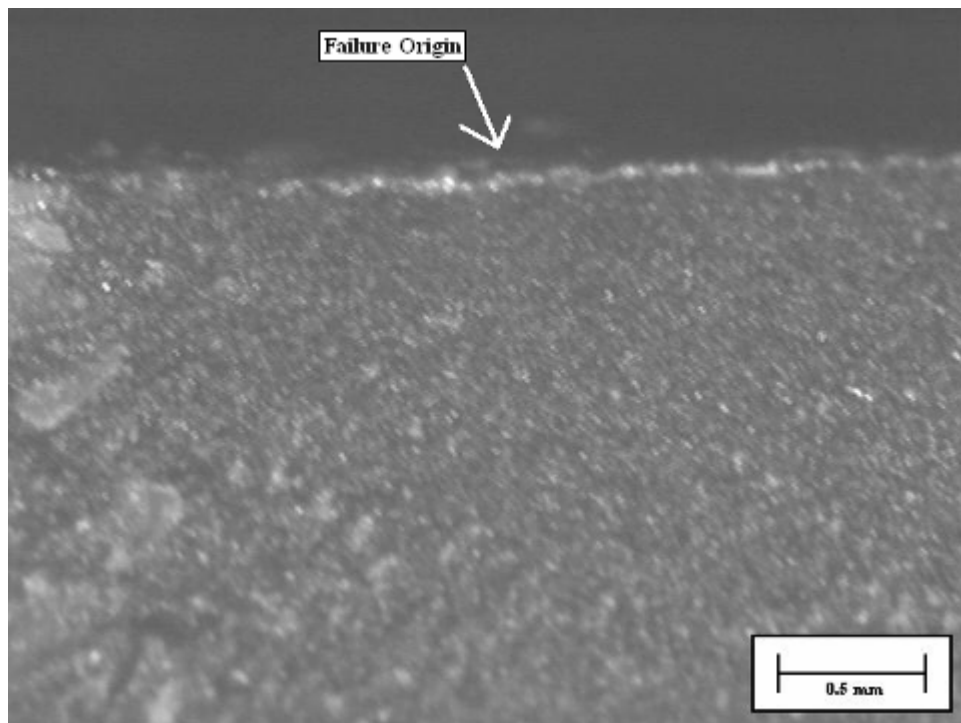


Figure D-60. ITK4-14 specimen 13.

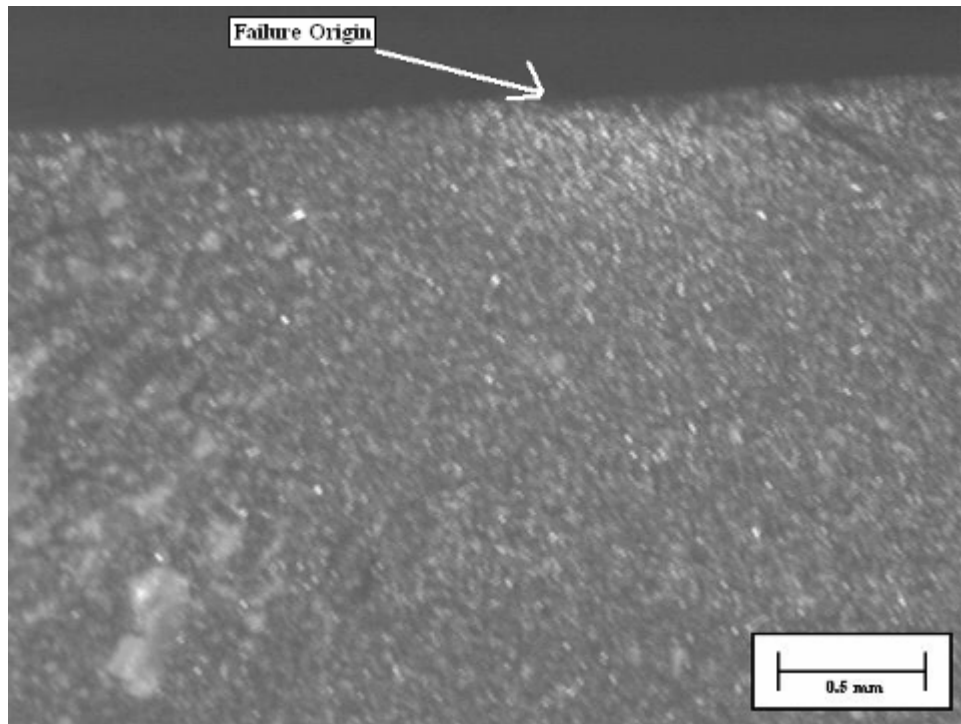


Figure D-61. ITK4-14 specimen 14.

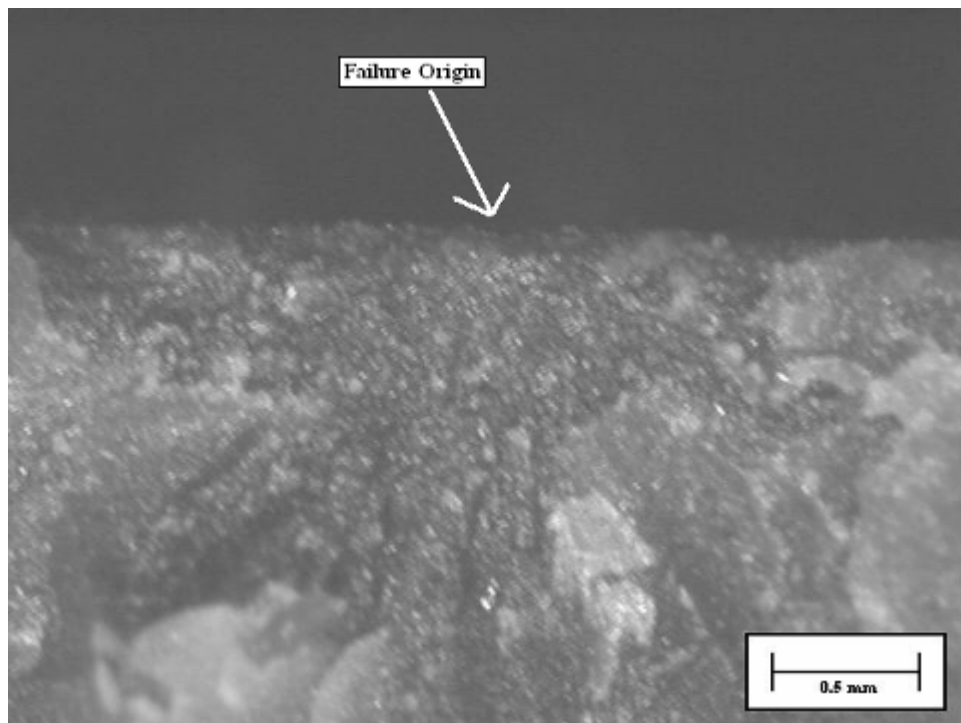


Figure D-62. ITK4-14 specimen 15.

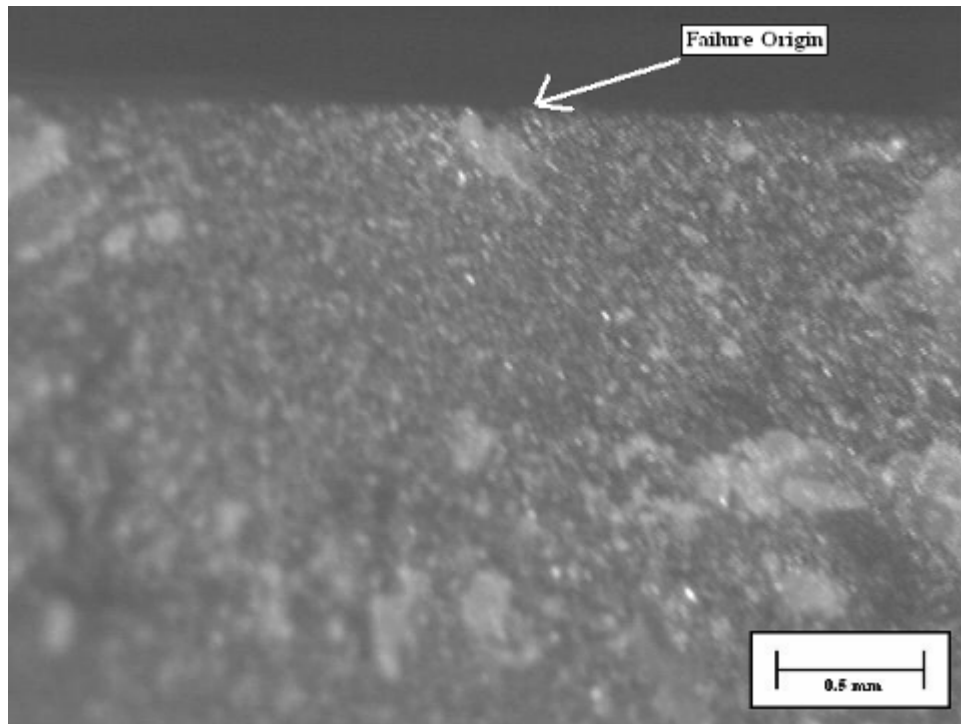


Figure D-63. ITK4-14 specimen 16.

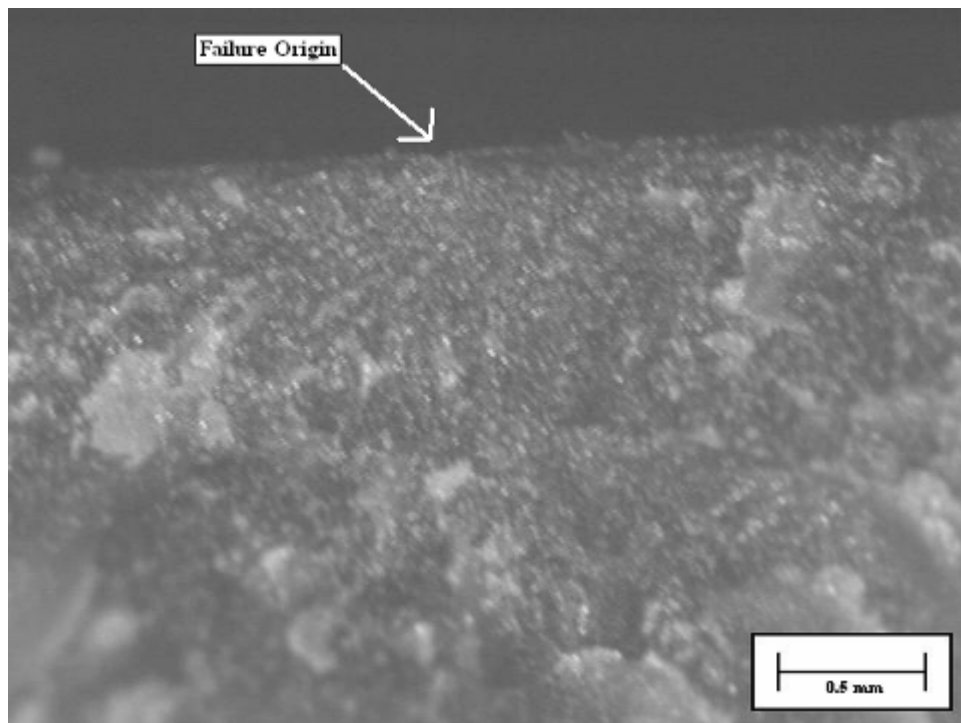


Figure D-64. ITK4-14 specimen 17.

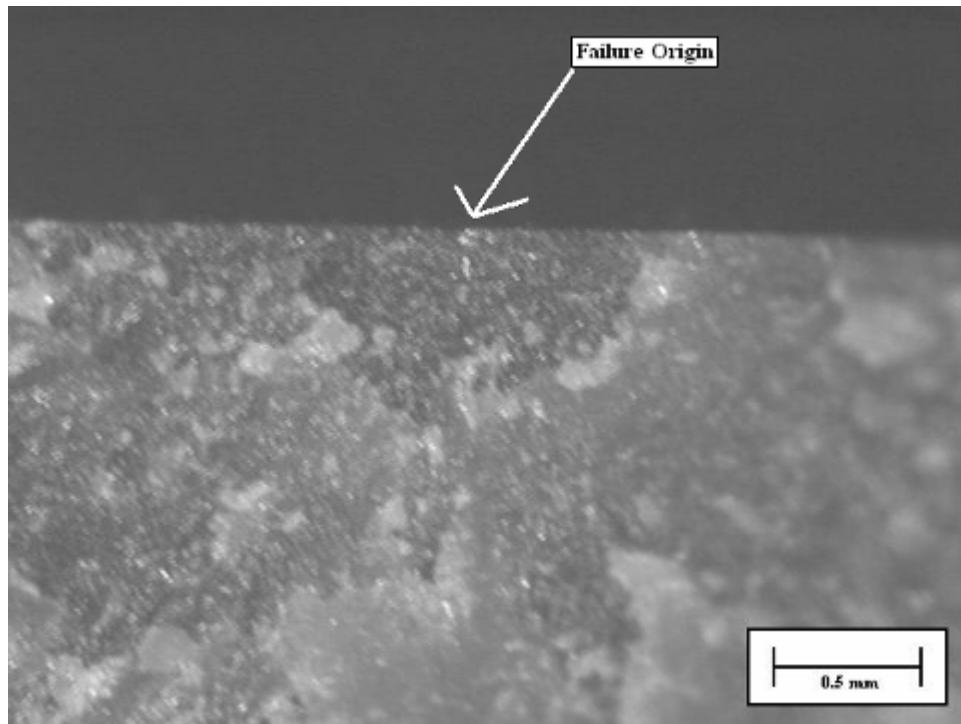


Figure D-65. ITK4-14 specimen 18.

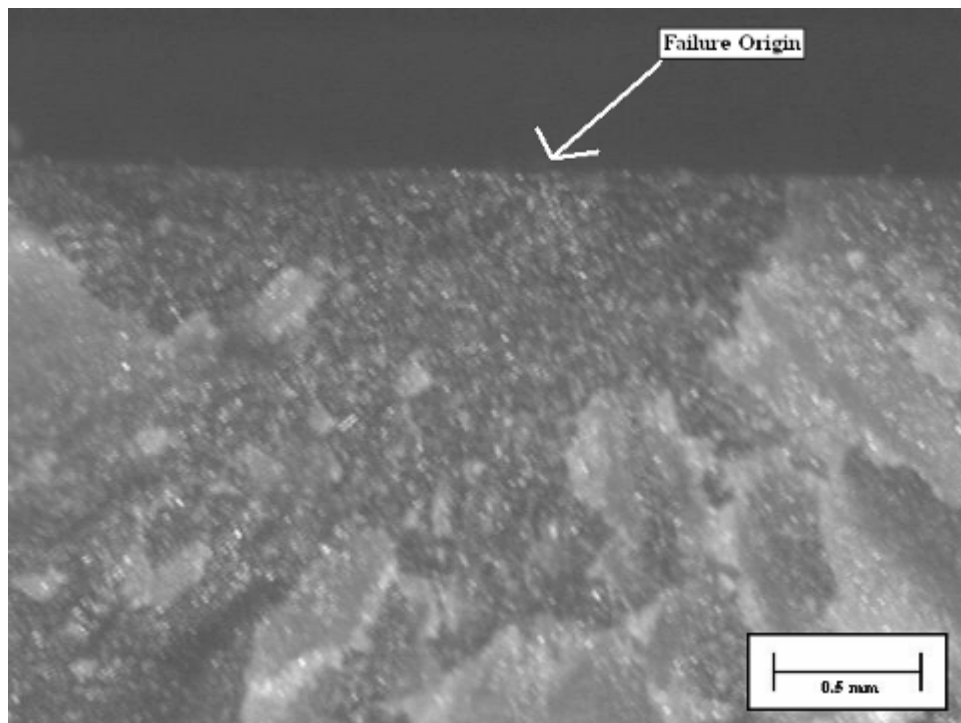


Figure D-66. ITK4-14 specimen 19.

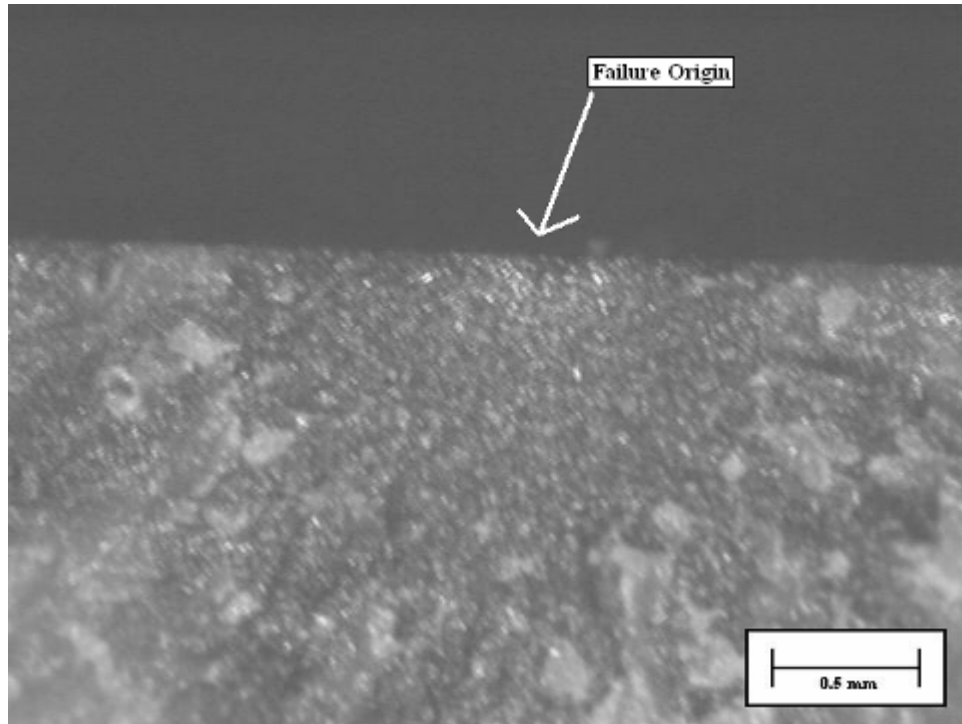


Figure D-67. ITK4-14 specimen 20.

NO. OF
COPIES ORGANIZATION

1 DEFENSE TECHNICAL
(PDF INFORMATION CTR
ONLY) DTIC OCA
8725 JOHN J KINGMAN RD
STE 0944
FORT BELVOIR VA 22060-6218

1 US ARMY RSRCH DEV &
ENGRG CMD
SYSTEMS OF SYSTEMS
INTEGRATION
AMSRD SS T
6000 6TH ST STE 100
FORT BELVOIR VA 22060-5608

1 INST FOR ADVNCD TCHNLGY
THE UNIV OF TEXAS
AT AUSTIN
3925 W BRAKER LN
AUSTIN TX 78759-5316

1 DIRECTOR
US ARMY RESEARCH LAB
IMNE ALC IMS
2800 POWDER MILL RD
ADELPHI MD 20783-1197

3 DIRECTOR
US ARMY RESEARCH LAB
AMSRD ARL CI OK TL
2800 POWDER MILL RD
ADELPHI MD 20783-1197

ABERDEEN PROVING GROUND

1 DIR USARL
AMSRD ARL CI OK TP (BLDG 4600)

NO. OF
COPIES ORGANIZATION

1 DIRECTOR
US ARMY RESEARCH LAB
AMSRD ARL SE DE
R ATKINSON
2800 POWDER MILL RD
ADELPHI MD 20783-1197

5 DIRECTOR
US ARMY RESEARCH LAB
AMSRD ARL WM MB
A ABRAHAMIAN
M BERMAN
M CHOWDHURY
T LI
E SZYMANSKI
2800 POWDER MILL RD
ADELPHI MD 20783-1197

1 COMMANDER
US ARMY MATERIEL CMD
AMXMI INT
9301 CHAPEK RD
FORT BELVOIR VA 22060-5527

2 PM MAS
SFAE AMO MAS MC
PICATINNY ARSENAL NJ
07806-5000

1 COMMANDER
US ARMY ARDEC
AMSTA AR TD
PICATINNY ARSENAL NJ
07806-5000

1 COMMANDER
US ARMY ARDEC
AMSTA AR CCH P
J LUTZ
PICATINNY ARSENAL NJ
07806-5000

1 DEPARTMENT OF THE ARMY
RDECOM ARDEC
AMSRD AAR EMO F
PICATINNY ARSENAL NJ
07806-5000

NO. OF
COPIES ORGANIZATION

13 COMMANDER
US ARMY ARDEC
AMSTA AR CCH A
F ALTAMURA
M NICOLICH
M PALATHINGUL
D VO
R HOWELL
A VELLA
M YOUNG
L MANOLE
S MUSALLI
R CARR
M LUCIANO
E LOGSDEN
T LOUZEIRO
PICATINNY ARSENAL NJ
07806-5000

1 COMMANDER
US ARMY ARDEC
AMSTA AR FSF T
C LIVECCHIA
PICATINNY ARSENAL NJ
07806-5000

1 COMMANDER
US ARMY ARDEC
AMSTA AR M
D DEMELLA
PICATINNY ARSENAL NJ
07806-5000

2 COMMANDER
US ARMY ARDEC
AMSTA AR CCH C
H CHANIN
S CHICO
PICATINNY ARSENAL NJ
07806-5000

1 COMMANDER
US ARMY ARDEC
AMSTA AR QAC T
D RIGOGLIOSO
PICATINNY ARSENAL NJ
07806-5000

<u>NO. OF COPIES</u>	<u>ORGANIZATION</u>
1	COMMANDER RDECOM ARDEC AMSRD AAR EMO F BLDG 1 PICATINNY ARSENAL NJ 07806-5000
9	COMMANDER US ARMY ARDEC AMSTA AR CCH B P DONADIA F DONLON P VALENTI C KNUTSON G EUSTICE K HENRY J MCNABOC R SAYER F CHANG PICATINNY ARSENAL NJ 07806-5000
1	PM ARMS SFAE GCSS ARMS BLDG 171 PICATINNY ARSENAL NJ 07806-5000
1	COMMANDER US ARMY ARDEC AMSTA AR WEA J BRESCIA PICATINNY ARSENAL NJ 07806-5000
1	PM MAS SFAE AMO MAS PICATINNY ARSENAL NJ 07806-5000
1	PM MAS SFAE AMO MAS CHIEF ENGINEER PICATINNY ARSENAL NJ 07806-5000
1	PM MAS SFAE AMO MAS PS PICATINNY ARSENAL NJ 07806-5000

<u>NO. OF COPIES</u>	<u>ORGANIZATION</u>
2	PM MAS SFAE AMO MAS LC PICATINNY ARSENAL NJ 07806-5000
1	COMMANDER US ARMY TACOM AMSTA SF WARREN MI 48397-5000
1	COMMANDER US ARMY TACOM PM COMBAT SYSTEMS SFAE GCS CS 6501 ELEVEN MILE RD WARREN MI 48397-5000
1	DIRECTOR AIR FORCE RESEARCH LAB MLLMD D MIRACLE 2230 TENTH ST WRIGHT PATTERSON AFB OH 45433-7817
1	OFC OF NAVAL RESEARCH J CHRISTODOULOU ONR CODE 332 800 N QUINCY ST ARLINGTON VA 22217-5600
1	COMMANDER US ARMY TACOM PM SURVIVABLE SYSTEMS SFAE GCSS W GSI H M RYZYI 6501 ELEVEN MILE RD WARREN MI 48397-5000
1	COMMANDER US ARMY TACOM CHIEF ABRAMS TESTING SFAE GCSS W AB QT T KRASKIEWICZ 6501 ELEVEN MILE RD WARREN MI 48397-5000
1	COMMANDER WATERVLIET ARSENAL SMCWV QAE Q B VANINA BLDG 44 WATERVLIET NY 12189-4050

NO. OF
COPIES ORGANIZATION

2 SFSJM CDL
HQ US ARMY JNT MUNITIONS CMND
AMSIO SMT
R CRAWFORD
W HARRIS
1 ROCK ISLAND ARSENAL
ROCK ISLAND IL 61299-6000

2 COMMANDER
US ARMY AMCOM
AVIATION APPLIED TECH DIR
J SCHUCK
FORT EUSTIS VA 23604-5577

1 NSWC
DAHLGREN DIV CODE G06
DAHLGREN VA 22448

2 US ARMY CORPS OF ENGR
CERD C
T LIU
CEW ET
T TAN
20 MASSACHUSETTS AVE NW
WASHINGTON DC 20314

1 US ARMY COLD REGIONS
RSCH & ENGRNG LAB
P DUTTA
72 LYME RD
HANOVER NH 03755

1 US ARMY TARDEC
AMSRD TAR R
D TEMPLETON
6501 E 11 MILE RD MS 263
WARREN MI 48397-5000

1 USA SBCCOM PM SOLDIER SPT
AMSSB PM RSS A
J CONNORS
KANSAS ST
NATICK MA 01760-5057

2 USA SBCCOM
MATERIAL SCIENCE TEAM
AMSSB RSS
J HERBERT
M SENNETT
KANSAS ST
NATICK MA 01760-5057

NO. OF
COPIES ORGANIZATION

8 COMMANDER
US ARMY TACOM
AMSTA TR R
R MCCLELLAND
D THOMAS
J BENNETT
D HANSEN
AMSTA TR D
D OSTBERG
L HINOJOSA
B RAJU
AMSTA CS SF
G MARSH
WARREN MI 48397-5000

14 BENET LABS
AMSTA AR CCB
R FISCELLA
M SOJA
E KATHE
M SCAVULO
G SPENCER
P WHEELER
S KRUPSKI
J VASILAKIS
G FRIAR
R HASENBEIN
AMSTA CCB R
S SOPOK
E HYLAND
D CRAYON
R DILLON
WATERVLIET NY 12189-4050

1 NSWC
TECH LIBRARY CODE B60
17320 DAHLGREN RD
DAHLGREN VA 22448

1 NSWC
CRANE DIVISION
M JOHNSON CODE 20H4
LOUISVILLE KY 40214-5245

2 NSWC
U SORATHIA
C WILLIAMS CODE 6551
9500 MACARTHUR BLVD
WEST BETHESDA MD 20817

NO. OF
COPIES ORGANIZATION

2 COMMANDER
NSWC
CARDEROCK DIVISION
R PETERSON CODE 2020
M CRITCHFIELD CODE 1730
BETHESDA MD 20084

7 DIRECTOR
US ARMY NGIC
D LEITER MS 404
M HOLTUS MS 301
M WOLFE MS 307
S MINGLEDORF MS 504
J GASTON MS 301
W GSTATTENBAUER MS 304
J CRIDER MS 306
2055 BOULDERS RD
CHARLOTTESVILLE VA
22911-8318

1 NAVAL SEA SYSTEMS CMD
D LIESE
1333 ISAAC HULL AVE SE 1100
WASHINGTON DC 20376-1100

1 AFRL MLBC
2941 P ST RM 136
WRIGHT PATTERSON AFB OH
45433-7750

1 DIRECTOR
LOS ALAMOS NATL LAB
F L ADDESSIO T 3 MS 5000
PO BOX 1633
LOS ALAMOS NM 87545

1 NSWC
CARDEROCK DIVISION
R CRANE CODE 6553
9500 MACARTHUR BLVD
WEST BETHESDA MD 20817-5700

1 AFRL MLMP
R THOMSON
2977 HOBSON WAY
BLDG 653 RM 215
WRIGHT PATTERSON AFB OH
45433-7739

NO. OF
COPIES ORGANIZATION

7 US ARMY RESEARCH OFC
A CROWSON
H EVERITT
J PRATER
G ANDERSON
D STEPP
D KISEROW
D SKATRUD
PO BOX 12211
RESEARCH TRIANGLE PARK NC
27709-2211

7 US ARMY SBCCOM
SOLDIER SYSTEMS CENTER
BALLISTICS TEAM
J WARD
W ZUKAS
P CUNNIFF
J SONG
MARINE CORPS TEAM
J MACKIEWICZ
AMSSB RCP SS
W NYKVIST
S BEAUDOIN
KANSAS ST
NATICK MA 01760-5019

8 NSWC
J FRANCIS CODE G30
D WILSON CODE G32
R D COOPER CODE G32
J FRAYSSE CODE G33
E ROWE CODE G33
T DURAN CODE G33
L DE SIMONE CODE G33
R HUBBARD CODE G33
DAHLGREN VA 22448

2 AFRL MLMP
F ABRAMS
J BROWN
2977 HOBSON WAY
BLDG 653 RM 215
WRIGHT PATTERSON AFB OH
45433-7739

1 DIRECTOR
LLNL
S DETERESA
PO BOX 808
LIVERMORE CA 94550

NO. OF
COPIES ORGANIZATION

1 DIRECTOR
LLNL
F MAGNESS L-125
PO BOX 808
LIVERMORE CA 94550

1 DIRECTOR
LLNL
M FINGER L-020
PO BOX 808
LIVERMORE CA 94550

1 DIRECTOR
LLNL
M MURPHY L-099
PO BOX 808
LIVERMORE CA 94550

1 AFRL MLS OL
L COULTER
5851 F AVE
BLDG 849 RM AD1A
HILL AFB UT 84056-5713

1 OSD
JOINT CCD TEST FORCE
OSD JCCD
R WILLIAMS
3909 HALLS FERRY RD
VICKSBURG MS 29180-6199

2 DARPA
S WAX
L CHRISTODOULOU
3701 N FAIRFAX DR
ARLINGTON VA 22203-1714

1 OAK RIDGE NATL LAB
R M DAVIS
PO BOX 2008
OAK RIDGE TN 37831-6195

1 OAK RIDGE NATL LAB
C EBERLE MS 8048
PO BOX 2008
OAK RIDGE TN 37831

4 NIST
M VANLANDINGHAM MS 8621
J CHIN MS 8621
J MARTIN MS 8621
D DUTHINH MS 8611
100 BUREAU DR
GAITHERSBURG MD 20899

NO. OF
COPIES ORGANIZATION

1 OAK RIDGE NATL LAB
C D WARREN MS 8039
PO BOX 2008
OAK RIDGE TN 37831

3 DIRECTOR
SANDIA NATL LABS
APPLIED MECHS DEPT
MS 9042
J HANDROCK
Y R KAN
J LAUFFER
PO BOX 969
LIVERMORE CA 94551-0969

1 HYDROGEOLOGIC INC
SERDP ESTCP SPT OFC
S WALSH
1155 HERNDON PKWY STE 900
HERNDON VA 20170

3 NASA LANGLEY RESEARCH CTR
AMSRD ARL VT
W ELBER MS 266
F BARTLETT JR MS 266
G FARLEY MS 266
HAMPTON VA 23681-0001

1 FHWA
E MUNLEY
6300 GEORGETOWN PIKE
MCLEAN VA 22101

1 USDOT FEDERAL RAILROAD
M FATEH RDV 31
WASHINGTON DC 20590

3 CYTEC FIBERITE
R DUNNE
D KOHLI
R MAYHEW
1300 REVOLUTION ST
HAVRE DE GRACE MD 21078

1 DIRECTOR
NGIC
IANG TMT
2055 BOULDERS RD
CHARLOTTESVILLE VA
22911-8318

NO. OF
COPIES ORGANIZATION

1	3TEX CORP A BOGDANOVICH 109 MACKENAN DR CARY NC 27511
1	DIRECTOR DEFENSE INTLLGNC AGNCY TA 5 K CRELLING WASHINGTON DC 20310
1	COMPOSITE MATERIALS INC D SHORTT 19105 63 AVE NE PO BOX 25 ARLINGTON WA 98223
1	JPS GLASS L CARTER PO BOX 260 SLATER RD SLATER SC 29683
1	COMPOSITE MATERIALS INC R HOLLAND 11 JEWEL CT ORINDA CA 94563
1	SIMULA R HUYETT 10016 S 51ST ST PHOENIX AZ 85044
2	PROTECTION MATERIALS INC M MILLER F CRILLEY 14000 NW 58 CT MIAMI LAKES FL 33014
2	FOSTER MILLER M ROYLANCE W ZUKAS 195 BEAR HILL RD WALTHAM MA 02354-1196
1	ROM DEVELOPMENT CORP R O MEARA 136 SWINEBURNE ROW BRICK MARKET PLACE NEWPORT RI 02840

NO. OF
COPIES ORGANIZATION

1	TEXTRON SYSTEMS M TREASURE 1449 MIDDLESEX ST LOWELL MA 01851
1	O GARA HESS & EISENHARDT M GILLESPIE 9113 LESAINTE DR FAIRFIELD OH 45014
1	CONNEAUGHT INDUSTRIES INC J SANTOS PO BOX 1425 COVENTRY RI 02816
1	ARMTEC DEFENSE PRODUCTS S DYER 85 901 AVE 53 PO BOX 848 COACHELLA CA 92236
3	PACIFIC NORTHWEST LAB M SMITH G VAN ARSDALE R SHIPPELL PO BOX 999 RICHLAND WA 99352
1	ALLIANT TECHSYSTEMS INC 4700 NATHAN LN N PLYMOUTH MN 55442-2512
1	APPLIED COMPOSITES W GRISCH 333 N SIXTH ST ST CHARLES IL 60174
1	CUSTOM ANALYTICAL ENG SYS INC A ALEXANDER 13000 TENSOR LANE NE FLINTSTONE MD 21530
1	AAI CORP DR N B MCNELLIS PO BOX 126 HUNT VALLEY MD 21030-0126
1	PROJECTILE TECHNOLOGY INC 515 GILES ST HAVRE DE GRACE MD 21078

NO. OF
COPIES ORGANIZATION

1 PRATT & WHITNEY
C WATSON
400 MAIN ST MS 114 37
EAST HARTFORD CT 06108

3 ALLIANT TECHSYSTEMS INC
J CONDON
E LYNAM
J GERHARD
WV01 16 STATE RT 956
PO BOX 210
ROCKET CENTER WV
26726-0210

5 NORTHROP GRUMMAN
B IRWIN
K EVANS
D EWART
A SHREKENHAMER
J MCGLYNN
BLDG 160 DEPT 3700
1100 W HOLLYVALE ST
AZUSA CA 91701

1 BRIGS COMPANY
J BACKOFEN
2668 PETERBOROUGH ST
HERNDON VA 22071-2443

1 ZERNOW TECHNICAL SERVICES
L ZERNOW
425 W BONITA AVE STE 208
SAN DIMAS CA 91773

2 GENERAL DYNAMICS OTS
FLINCHBAUGH DIV
K LINDE
T LYNCH
PO BOX 127
RED LION PA 17356

1 GKN WESTLAND AEROSPACE
D OLDS
450 MURDOCK AVE
MERIDEN CT 06450-8324

1 AEROSPACE CORP
G HAWKINS M4 945
2350 E EL SEGUNDO BLVD
EL SEGUNDO CA 90245

NO. OF
COPIES ORGANIZATION

2 UDLP
G THOMAS
M MACLEAN
PO BOX 58123
SANTA CLARA CA 95052

2 UDLP
R BRYNSVOLD
P JANKE MS 170
4800 E RIVER RD
MINNEAPOLIS MN 55421-1498

1 GDLS DIVISION
D BARTLE
PO BOX 1901
WARREN MI 48090

1 GDLS
M PASIK
PO BOX 2074
WARREN MI 48090-2074

1 GDLS
MUSKEGON OPER
M SOIMAR
76 GETTY ST
MUSKEGON MI 49442

5 INST FOR ADVANCED
TECH
H FAIR
I MCNAB
P SULLIVAN
S BLESS
C PERSAD
3925 W BRAKER LN
AUSTIN TX 78759-5316

1 ARROW TECH ASSOC
1233 SHELBURNE RD STE D8
SOUTH BURLINGTON VT
05403-7700

1 R EICHELBERGER
CONSULTANT
409 W CATHERINE ST
BEL AIR MD 21014-3613

1 SAIC
G CHRYSSOMALLIS
8500 NORMANDALE LAKE BLVD
SUITE 1610
BLOOMINGTON MN 55437-3828

NO. OF
COPIES ORGANIZATION

1 UCLA MANE DEPT ENGR IV
H T HAHN
LOS ANGELES CA 90024-1597

1 IIT RESEARCH CTR
D ROSE
201 MILL ST
ROME NY 13440-6916

1 MICHIGAN ST UNIV
MSM DEPT
R AVERILL
3515 EB
EAST LANSING MI 48824-1226

1 PENN STATE UNIV
R S ENGEL
245 HAMMOND BLDG
UNIVERSITY PARK PA 16801

1 PENN STATE UNIV
C BAKIS
212 EARTH ENGR
SCIENCES BLDG
UNIVERSITY PARK PA 16802

1 PURDUE UNIV
SCHOOL OF AERO & ASTRO
C T SUN
W LAFAYETTE IN 47907-1282

1 UNIV OF MAINE
ADV STR & COMP LAB
R LOPEZ ANIDO
5793 AEWB BLDG
ORONO ME 04469-5793

1 JOHNS HOPKINS UNIV
APPLIED PHYSICS LAB
P WIENHOLD
11100 JOHNS HOPKINS RD
LAUREL MD 20723-6099

1 UNIV OF DAYTON
J M WHITNEY
COLLEGE PARK AVE
DAYTON OH 45469-0240

NO. OF
COPIES ORGANIZATION

5 UNIV OF DELAWARE
CTR FOR COMPOSITE MTRLs
J GILLESPIE
M SANTARE
S YARLAGADDA
S ADVANI
D HEIDER
201 SPENCER LAB
NEWARK DE 19716

1 MISSISSIPPI STATE UNIV
DEPT OF AEROSPACE ENGRG
A J VIZZINI
MISSISSIPPI STATE MS 39762

1 DREXEL UNIV
A S D WANG
3141 CHESTNUT ST
PHILADELPHIA PA 19104

1 DEPT OF MTRLs
SCIENCE & ENGRG
UNIV OF ILLINOIS
AT URBANA CHAMPAIGN
J ECONOMY
1304 W GREEN ST 115B
URBANA IL 61801

3 UNIV OF TEXAS AT AUSTIN
CTR FOR ELECTROMECHANICS
J PRICE
A WALLS
J KITZMILLER
10100 BURNET RD
AUSTIN TX 78758-4497

1 SOUTHWEST RESEARCH INST
ENGR & MATL SCIENCES DIV
J RIEGEL
6220 CULEBRA RD
PO DRAWER 28510
SAN ANTONIO TX 78228-0510

3 DIRECTOR
US ARMY RESEARCH LAB
AMSRD ARL WM MB
A FRYDMAN
2800 POWDER MILL RD
ADELPHI MD 20783-1197

NO. OF
COPIES ORGANIZATION

1 DEPARTMENT HEAD
US MILITARY ACADEMY
K NYGREN
CIVIL & MECH ENGRG DEPT
WEST POINT NY 10996-1792

1 DIRECTOR
US MILITARY ACADEMY
D BOETTNER
MECH ENGRG DIV
WEST POINT NY 10996-1792

1 COMMANDER
US ARMY ARDEC
AMSTA AR FSA
A WARNASH
BLDG 1
PICATINNY ARSENAL NJ
07806-5000

1 COMMANDER
US ARMY ARDEC
AMSTA AR FSA
B MACHAK
BLDG 1
PICATINNY ARSENAL NJ
07806-5000

1 COMMANDER
US ARMY ARDEC
AMSTA AR FSA
M CHIEFA
BLDG 1
PICATINNY ARSENAL NJ
07806-5000

1 COMMANDER
US ARMY ARDEC
AMSTA AR FSP G
M SCHIKSNIS
BLDG 1
PICATINNY ARSENAL NJ
07806-5000

1 COMMANDER
US ARMY ARDEC
AMSTA AR FSP G
D CARLUCCI
BLDG 1
PICATINNY ARSENAL NJ
07806-5000

NO. OF
COPIES ORGANIZATION

ABERDEEN PROVING GROUND

1 US ARMY ATC
CSTE DTC AT AD I
W C FRAZER
400 COLLERAN RD
APG MD 21005-5059

49 DIR USARL
AMSRD ARL CI
AMSRD ARL O AP EG
M ADAMSON
AMSRD ARL SL BM
D BELY
AMSRD ARL WM
J SMITH
AMSRD ARL WM B
CHIEF
T KOGLER
AMSRD ARL WM BA
D LYON
AMSRD ARL WM BC
J NEWILL
P PLOSTINS
AMSRD ARL WM BD
P CONROY
B FORCH
M LEADORE
C LEVERITT
R LIEB
R PESCE-RODRIGUEZ
B RICE
A ZIELINSKI
AMSRD ARL WM BF
S WILKERSON
AMSRD ARL WM M
J MCCAULEY
S MCKNIGHT
AMSRD ARL WM MA
CHIEF
L GHIORSE
E WETZEL
AMSRD ARL WM MB
J BROWN
L BURTON
R CARTER
K CHO
W DE ROSSET
R EMERSON
D GRAY
R KASTE
L KECSKES
D SNOHA
J SOUTH

NO. OF
COPIES ORGANIZATION

J SWAB (10 CPS)
J TZENG
AMSRD ARL WM MC
CHIEF
E CHIN
J LASALVIA
J MONTGOMERY

NO. OF
COPIES ORGANIZATION

1 NIST
G QUINN MS 8521
100 BUREAU DR
GAITHERSBURG MD 20899

1 PENN STATE UNIV
A SEGALL
212 EARTH ENGR
SCIENCES BLDG
UNIVERSITY PARK PA 16802

1 GATEWAY MATERIALS TECH INC
S GONCZY
221 S EMERSON
MOUNT PROSPECT IL 60056

1 GENERAL ELECTRIC COMPANY
C JOHNSON
BLDG K 1 RM MB 161
PO BOX 8
SCHENECTADY NY 1230

3 NASA GLENN RSRCH CTR
J SALEM
N NEMETH
J GYEKENYESI
LIFE PREDICTION BR MS 49 7
21000 BROOKPARK RD
CLEVELAND OH 44135

1 LLNL DEFENSE TECHNOLOGIES
ADVANCED ENGRNG ANLYS
R RIDDLE
PO BOX 808 L 125
LIVERMORE CA 94551

1 ADVNCD MATERIALS TECH CTR
D PYSHER
BLDG 201 4 N 01
ST PAUL MN 55144-1000

2 CERADYNE INC
K MOELLER
J SHIH
3169 REDHILL DR
COSTA MESA CA 92626

3 COORSTEK
H LOPEZ
T HAEN
J SCHIENLE
16000 TABLE MOUNTAIN PKY
GOLDEN CO 80403-1640

NO. OF
COPIES ORGANIZATION

1 UNIV OF WISCONSIN
PLATTEVILLE
COLLEGE OF ENGRG MATH SCI
O JADAAN
150 OTTENSAN HALL
PLATTEVILLE WI 53818

1 SAINT GOBAIN ABRASIVES
K BREDER
ONE BOND ST
PO BOX 15008
WORCESTER MA 01615

5 PENN STATE UNIV
J HELLMANN
124 STEIDLE BLDG
UNIVERSITY PARK PA 16802

1 UNIV OF DETROIT MERCY
M JENKINS
4001 W MCNICHOLS RD
PO BOX 19900
DETROIT MI 48219-0900

1 COORSTEK
B SEEGMILLER
600 9TH ST
GOLDEN CO 80401

1 KENNAMETAL INC
R YECKLEY
1600 TECHNOLOGY WAY
LATROBE PA 15650

1 KENNAMETAL ENGINEERED
PRODUCTS GROUP
W HUSTON
2879 AERO PARK DR
TRAVERSE CITY MI 49686

1 SAINT-GOBAIN ADVNCD CERAMICS
J RUPPEL
23 ACHESON DR
NIAGARA FALLS NY 14303

3 A WOODRUFF
182 WALTON DR
MORRISVILLE PA 19067

1 OAK RIDGE NATIONAL LAB
A WERESZCZAK
1 BETHEL VALLEY RD
BLDG 4515 RM 256
PO BOX 2008 MS 6068
OAK RIDGE TN 37831-6068

INTENTIONALLY LEFT BLANK.